COLOUR RECEPTORS, AND THEIR SYNAPTIC CONNEXIONS, IN THE RETINA OF A CYPRINID FISH

By J. H. SCHOLES†
The Laboratory of Experimental Psychology, University of Sussex, Brighton

(*Communicated by B. B. Boycott, F.R.S. – Received* 8 *April* 1974)

[Plates 1–11]

CONTENTS

† Present address: The Medical Research Council Cell Biophysics Unit, University of London, King's College, 26–29 Drury Lane, London W.C. 2.

Morphologically speaking, there are five kinds of cone cells in the retina of the rudd (*Scardinius erythrophthalmus*). But two of them, the *principal* elements of the double cones and the *free principal* cones, are probably functionally equivalent, while another, sparse, population of small (*oblique*) cones (which disappear in older fish), is unlikely to make a significant contribution to visual spectral sensitivity. Thus, *principal* and *accessory cones* (usually paired with one another), and *single* cones seem to be the three receptors which underlie the fish's trichromacy.

Photographic densitometry of individual cone cells was used to provide evidence that accessory cones contain a green-absorbing photopigment and the single cones a blue one. Other arguments are given in support of those identifications, and they also strongly suggest that principal cones contain the red-absorbing pigment.

Golgi-impregnated bipolar cells were examined electron-microscopically to determine the specific patterns of synaptic connexion they make with these different, anatomically identifiable, colour cones and with the retinal rods. Three principal arrangements were distinguished (see figure 69, page 100).

(1) *Rod bipolar* cells comprise two distinct morphological types, both of which connect exclusively to principal (red) cones as well as to the rods within the outlines of their dendritic fields.

(2) *Selective cone bipolar* cells, more delicate neurons with considerably wider dendritic fields, connect (according to type) to one or other of the different colour cone populations. Examples analysed were specific for the accessory (green) or for the single (blue) cones; no bipolar cells were found connected only to red cones.

(3) *Mixed cone bipolars* have the smallest dendritic fields, and connect to combinations of cones (for example, red and green, or green and blue, but not red and blue). They also have synaptic input (usually relatively sparse) from the rods. Cells were encountered connecting to all three cone types, but they were only partially analysed, and are not described at length.

The light microscopic morphology of these bipolar cell types consistently reflects the detailed pattern of connexion each makes with the different receptor populations (just as the morphology of the cones reflects the spectral properties of their photopigment). But while their synaptic connectivity is generally highly specific for cone type, they do occasionally make anomalous connexions with the 'wrong' receptors.

There is a high degree of divergence (page 85) at the receptor-bipolar synapses, and the different kinds of cones each characteristically connect to different numbers of bipolar cells. Principal (red) cones, which are the most numerous, individually connect to more bipolars than cones of other types, whose characteristic synaptic divergence is likewise related to the frequency with which they occur in the retina. However, rods, which are much more numerous than cones, do not conform with this generalization.

The selectivity with which the synaptic terminals of the different cones are connected together by their invaginating basal processes was also examined. These processes link neighbouring synaptic terminals of differently coloured cones: specifically, principal (red) cone basal processes invaginate accessory (green) cone pedicles, and vice versa. Single (blue) cone basal processes connect only to accessory cone pedicles, but that synaptic relation is not reciprocated.

These synapses between the cones have important bearing upon interpretation of the bipolar cell connectivity patterns. In their light, the interaction between colour channels which the convergence of different cones onto the *mixed cone bipolar* dendrites mediates, seems to re-iterate a process already undertaken more peripherally. Likewise, whereas the anatomy of the *selective cone bipolars* appears designed to convey activity from the individual cone populations, the responses of the receptors they sample must already be influenced by activity in other colour channels.

INTRODUCTION

In primates and Man, three photolabile pigments with different absorption spectra capture light imaged onto the retina (Marks, Dobelle & MacNichol 1964; Brown & Wald 1964). They are segregated into different populations of cone cells, and the analysis they effect, mapping wavelength distribution into excitation of separate receptor channels, forms the basis upon which subsequent neural interactions in the visual pathway establish the central representation of hue. The nature of these interactions remains largely inferred from the responses of single cells to coloured stimuli, and it would clearly be profitable to establish something of their structural basis.

No morphological clues to the chromatic identities of the different cones have yet been recognized in human and monkey eyes. They are only distinguishable by the spectra of the labile pigments they contain, and this is one reason why elucidation of the neural connexions of the three colour channels in the retina has not been susceptible to the techniques of anatomy, and remained a concern only of physiology. The purpose of the present work is to approach just this problem, by means of anatomical methods and by taking advantage of one of the many lower vertebrate eyes where the different colour cones can be distinguished from one another by conventional light microscopy alone.

There is no lack of evidence that many of the important neural processes underlying colour vision are carried out retinally in certain vertebrate species. For example, it has been argued

(Daw 1967) that the double opponent ganglion cells in the fish retina may be the basis of the colour constancy mechanisms that these creatures, like man, are known to possess (Burkamp 1923).

In non-mammalian vertebrates, opponent colour interactions not only dominate the responses of the ganglion cells, but also appear at the most peripheral synaptic station of the retina. Both colour-coded bipolar cell receptive fields (Kaneko 1971) and individual cones (Baylor & Hodgkin 1973) have antagonistic surround mechanisms mediated by horizontal cells and driven by different colour receptors. The exact neuronal connexions underlying these processes, however, are not known, and it remains an enigma that, while the spectral sensitivity curves of the three cone mechanisms appear to be distorted at an early stage in the visual pathway by such antagonism between the colour channels, they may nevertheless, both in man (Stiles 1959) and fish (Muntz & Northmore 1971*a*), under certain circumstances, be retrieved unchanged from psychophysical measures of sensory performance.

This paper describes the morphology of the receptors and some of the bipolar cells in the retina of a cyprinid fish (*Scardinius erythrophthalmus*, the rudd). Evidence is given for the chromatic identities of the different kinds of cone cells, and identified Golgi-impregnated bipolars are examined by electron microscopy (Stell 1965, 1972) to determine the patterns of colour cones and rods to which they connect. The colour coding of a possible direct synaptic pathway between the cones is described. Evidently, while some bipolars connect to receptors of uniform spectral sensitivity, another population synapses with combinations of (opponent) colour cones. The different colour channels interact peripherally not only through this convergence onto common bipolar cells, but possibly also by synaptic connexions which link neighbouring cones of opponent colour sensitivity. Horizontal cells, the other neurons involved in the synapses in the outer plexiform layer, did not stain adequately in the Golgi impregnations, so their patterns of connectivity remain to be determined.

The rudd is closely related to the goldfish and the carp, of whose retinal physiology a lot is known. Aspects of the rudd's behavioural colour discrimination performance are rather well understood (Muntz & Northmore 1970, 1971*a*) and it possesses a trichromacy broadly similar to that of the goldfish (Marks 1965; Yager 1967). In principle, therefore, an opportunity arises to relate the anatomical findings both to physiological and behavioural measures of colour vision. Seeking generality in them, one may also justifiably stress the extent to which the known properties of colour vision in fish resemble those in man.

Some fish are trichromatic (see, for example, Yager 1967; Muntz & Northmore 1970) and the colour confusions they make suggest an extraspectral purple in their colour space (Hamburger 1926). Simultaneous colour contrast and constancy (Burkamp 1923) effects can be detected in their discrimination performance. Their three colour mechanisms determine visual behaviour independently at threshold (Muntz & Northmore 1970), and the adaptational sensitivity of each is determined by its history of light capture alone (Muntz & Northmore 1971*a*). In each of these respects, fish vision resembles that in man; nevertheless, it is important to voice caution about interpreting the peripheral organization of mammalian retinal colour channels in the light of these common features of visual performance. The special relation of central area midget bipolar cells with single cones (Polyak 1941; Boycott & Dowling 1969) suggests that activity in the colour channels may remain segregated during transmission between the two synaptic layers of the primate retina, rather than chromatically interact, as it does (Naka & Rushton 1966*a*, *b*, *c*; Kaneko 1971; Baylor & Hodgkin 1973; Fuortes, Schwarz &

Simon 1973) in the outer plexiform layer of lower vertebrates. There is no evidence that the horizontal cells are as elaborately organized with respect to colour in primates as they are in fish, nor, in their bipolar population (Boycott & Dowling 1969), is there anything approaching the extreme degree of morphological variety that Cajal (1892) recognized among these cells in reptiles and amphibians. There is no indication of structures of the sort that will be shown to link cones of *unlike* colours in the fish.

It is possible, then, that the functional organization of the outer plexiform layer in primates is different in principle to that in the lower vertebrates, even though it involves the same three basic cell populations. If so, the implication is that visual processes concerned with colour in primates and non-mammalian vertebrates, remarkable more for their similarities than for their differences, are mediated by radically different neuronal architecture. If not, *functional* differentiation among the more peripheral retinal neurons in primates must be concealed by their relative *morphological* homogeneity.

MATERIALS AND METHODS

The fish (*Scardinius erythrophthalmus*, Cyprinidae) were caught in local streams and lakes, and maintained in the laboratory. The retinae were stripped from dark adapted (4–12 h) eyes of young specimens, and light adapted in a moist chamber for a few minutes to contract their cone myoids and aline these receptors close to the external limiting membrane. For conventional light and electron microscopy, they were prefixed in chilled, phosphate-buffered (pH 7.4), glutaraldehyde for up to $1\frac{1}{2}$ h, and post-fixed in osmium tetroxide for around the same time. Sections were cut from Epoxy resin embedded material, and examined by phase contrast without staining in the light microscope, or stained with lead and uranium salts for the electron microscope.

Retinae intended for Golgi-impregnation were flattened onto filter paper tags during fixation and dehydration, so that local orientation of the tissue could accurately be established. They were prefixed in buffered gluraldehyde as for conventional microscopy, osmicated for up to 20 min, and taken through as many cycles of a slightly modified Golgi-rapid procedure as was deemed necessary. This usually involved overnight immersion in potassium dichromate (1–10 %) at 30–40 °C, then, after thorough washing, soaking in silver nitrate (1 %) at the same temperature for 2 or 3 h. Retinae that stained well were hand sliced in the vertical plane before complete polymerization of their Epoxy embedment. Individual cells were cut from these slices in small cubes that contained also the region of the receptor layer they were connected to, and remounted for thinner sectioning for light and electron microscopy. The e.m. sections were not further stained, since there was adequate contrast in the tissue background of the Golgi material and it was helpful to avoid contamination confusing silver deposits in the cell processes of interest.

For a general discussion of the methodology and potential of electron microscopy of Golgi-impregnations, the reader is recommended to Stell's (1972) careful review of vertebrate retinal organization.

RESULTS

1. Receptor morphology

(*a*) *Introduction*

In all of the vertebrate groups other than the mammals, there are several populations of quite distinct retinal receptors. In duplex retinae, the major distinction is between rods and cones, but in addition the cone population may be further subdivided into as many as five morphological types. They are distinguished by such characteristics as size, position in retinal depth, and pairing with other elements (double cones): these light microscopical features are also matched by differences in ultrastructure (see, for example, Nilsson 1964*a*; Morris & Storey 1967). The distinction between *double* and *single* cone populations is clear cut in representative species from all the vertebrate groups outside the mammals, and despite considerable variation in detail, there are other basic features of the organization of these cones, such as their mosaic layout and relative sizes, which are, broadly speaking, common to all.

There is now a lot of evidence that such purely anatomical differences between cones reflect, in the animals which possess some sort of colour vision, the chromatic identities of the receptors. For example, distinct cones in reptiles and birds contain particular coloured oil droplets and visual pigments (Liebman & Granda 1971; King-Smith 1969), and it has been the general experience of microspectrophotometry that different photolabile pigments are found in characteristic receptor types (Marks 1965; Liebman 1972). However, the matter is not entirely simple, for in one case the same (red-absorbing) pigment is found in two morphologically quite dissimilar cones (Liebman & Entine 1968), and there is certainly no ground for confidence that similar cones in different species will possess the same pigments. The rudd retina is unexceptional in possessing differentiated cone populations; however, unlike that of many other fish, it does not have a geometrically regular mosaic arrangement of the receptors, which means that some care must be observed in attributing identities to particular elements in the light and electron microscope.

There are three main reasons for describing the structure of the retinal receptors in some detail here. First of all, since the concern is to establish the patterns of their synaptic connectivity in the outer plexiform layer, it is important to specify those of the morphological characteristics of the cones which enable their reliable identification in histological preparations, and to be quite clear as to which of them correspond to the receptors identified in other Cyprinid eyes (for example, Marks 1965; Tomita *et al.* 1967; Engström 1960) more commonly used in studies of spectral sensitivity and retinal anatomy. Secondly, the way in which the sizes and the numerical populations of the cone classes vary in the retina must have important implications for the effectiveness with which the three colour mechanisms participate in visual function. Finally, the different cone types are arranged in a particular way with respect to the chromatic properties of the lens of the eye, and it cannot but be informative to determine the consistency of this arrangement with the chromatic identities which will be attributed to the cones in the next section of this paper (§2, page 75).

(*b*) *Observations*

(i) *Receptor nomenclature*

The rudd retina contains rods and five morphologically distinct kinds of cone cells. Each of the cone types has been recognized by earlier light microscopists (see, for example, Engström 1960) though usually not all of them are represented in any particular fish retina. Two of them comprise the paired elements of (unequal) double cones, customarily referred to as principal and accessory cones. The remainder are unpaired (single) cones.

Conventionally, single cones are named according to their sizes (e.g. long and short single cones; Engström 1960), or to the positions they assume relative to their neighbours in regular retinal receptor mosaics (thus, central and additional single cones; Lyall 1957*b*), but both of these systems of nomenclature are inadequate in certain respects. In some retinae, the size relations between the single cones may be reversed (compare *Lebistes*; Müller 1952) with the stem cyprinid pattern (Engström 1960), and in many, like that of the rudd, there is no regular mosaic against which the cones can firmly be identified. Furthermore the rudd is by no means unique in possessing three rather than two kinds of single cones.

Because of these ambiguities, a somewhat different single cone nomenclature (below) has been adopted for the purpose of this paper. It is intended to economize in prefixes, and refers to characters of the cones involved which suggest homologies with different receptors in this or in other retinae. But more knowledge of the photopigments and the ubiquity of these receptors is needed before definitive names may be devised for them.

principal cones
accessory cones
} paired as double cones

free principal cones
single cones (= central single (Lyall 1957*b*))
oblique cones (= additional single (Lyall 1957*b*))
} unpaired

(ii) *The retinal cone types*

The rudd retina, whose vertical organization is shown in the *camera lucida* sketch of figure 1, has a great excess of rods over cones, which varies, as does cone size and packing density between the top and bottom of the eye (Muntz & Northmore 1971*a*). While, to both light and electron microscopy, the rods are a homogeneous population, the five kinds of cones can easily be recognized in vertical sections of light adapted retinae by their sizes and positions in depth. All of them make photomechanical adaptive movements.

(1) *Double cones (principal and accessory cones)*. The principal elements of the double cones are the largest of the retinal receptors and the most distally placed of the cones. Normally, they are tightly linked to accessory cones by mutual invagination of their myoids, but the ellipsoids and outer segments of the accessories are precisely arranged in a tier some 10 μm proximal to those of the principal cones. Their nuclei are both at the same level, just distal to the external limiting membrane, and their ellipsoids, composed of specialized mitochondrial aggregations, are highly refractile.

In the aldehyde-fixed material examined here, the ultrastructure of principal and accessory cones differed clearly in just one important respect. The outer segment lamellae of the accessory cones were consistently less well preserved than those of the principals and the unpaired cones (compare figure 6 with figures 5, 7 and 8, plate 1). Their appearance (figure 6, plate 1)

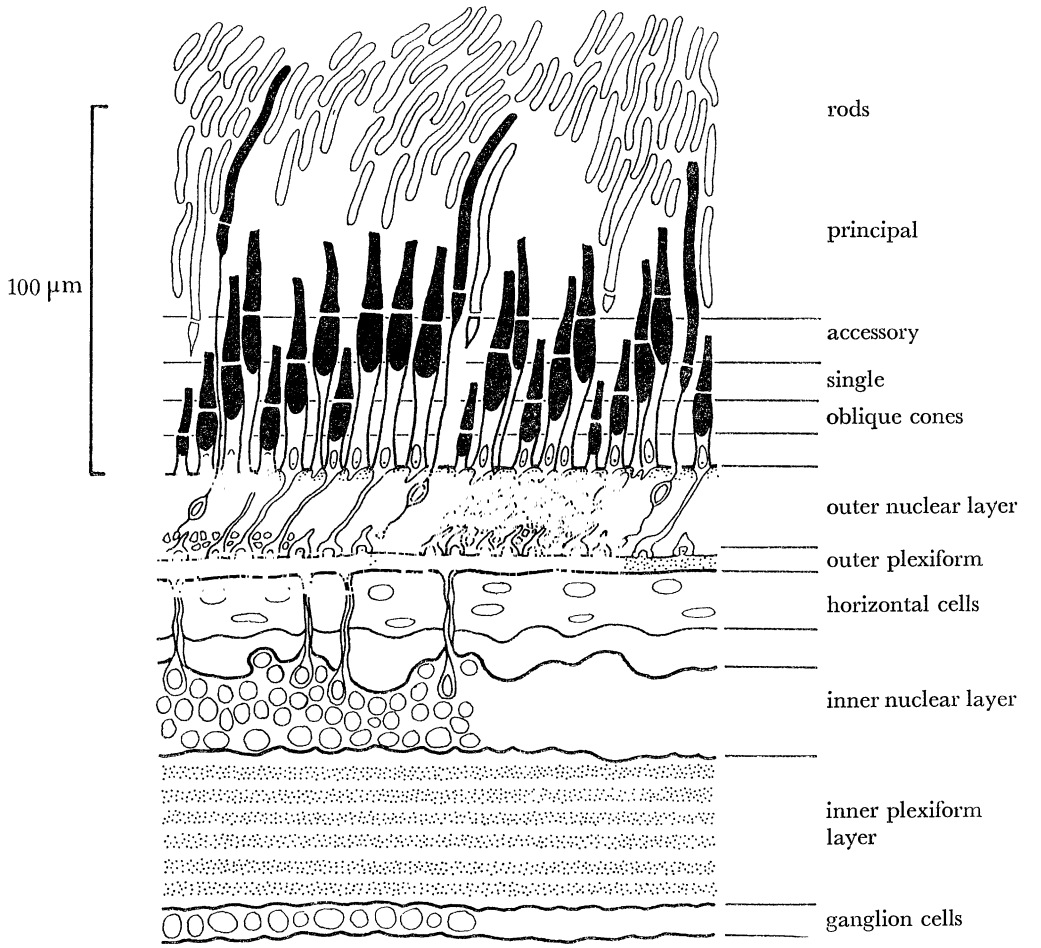

FIGURE 1. The organization of the retinal layers in the rudd, drawn semi-diagrammatically from light microscope sections. The outer and inner segments of the cones are filled black, and the horizontal lines drawn behind them, at the level of their outer and inner segment junctions show the layered arrangement of the different types in depth. Each line is labelled according to the cone species it intersects. For simplicity, not all of the retinal rods are drawn in, but the axons, perikarya, and synaptic spheres of three of them (filled) are diagrammed, and the projection of some of the cone axons through the outer nuclear layer to their pedicles is also shown. The outer and inner (which has six strata, figure 38, plate 5), plexiform layers are shown stippled and the density of perikarya in the various cellulai layers is roughly shown by the circular nuclear profiles.

suggests that structural binding between the interior membrane surfaces of the disks is less stable than in the other cones. It may well be significant that this feature of the accessory cones was shared (though less consistently) by the outer segments of the rods (see figure 2, plate 1), since microspectrophotometry of fish (Liebman 1972) and other lower vertebrate retinae (Liebman 1972; Liebman & Entine 1968) has suggested that accessory cones and rods invariably possess the same photopigment chromophore.

(2) *Free principal cones.* These large single cones were first recognized in the roach eye by Greeff (1900), who called them, attending to their size, 'great' single cones. Subsequently they have been noticed in other teleostean retinae (Lyall 1957*b*; Engström 1960), but their occurrence seems to be sporadic both in particular fish, and between species. In the rudd, they have exactly the same size and position in the depth of the retina as the conventionally paired

principal elements of the double cones (figures 11–13, plate 2), and this is the reason for calling them *free* principal cones. To name them so implies a functional identity with conventional principal cones which is hard to justify on this gross morphological level alone; however both their ultrastructure and their specific synaptic connexions with certain of the retinal bipolar cells are also identical (see page 93).

The present view is that they are the product of some anomaly in the normal cell division cycles which generate double and single cones in the retinal mosaic. They are never accompanied by free accessory cones and are unrelated to the occasional triple cones that occur. Although their occurrence is sporadic, they can make up a significant fraction of the cone population (see §(iii) and table 1).

(3) *Single cones.* The most numerous of the unpaired cones are nearly half the size of the principal elements, with their outer segments deployed in an accurate tier (figure 1) some 10–20 μm proximal to those of the accessory cones. Their outer segment lamellar ultrastructure (figures 3 and 7, plate 1) is like that of the principal cones (figures 2 and 5, plate 1), and so is their inner segment ultrastructure. Their nuclei are located above the external limiting membrane, and they differ from the other two unpaired cone types in that, irrespective of age or retinal location, they are never found to be absent from the retina. In other fish, they have variously been termed 'central single cones' (Lyall 1957) or, depending on which of the other unpaired cones were recognized, 'long' or 'short' single cones (Engström 1960). In the rudd they are intermediate in size (see figure 3, plate 1).

(4) *Oblique cones.* In the rudd, these are the smallest of the unpaired cones, arranged in a fourth layer close to the external limiting membrane. Though they occur in a rather regular lattice arrangement (cf. figure 13, plate 2), they are the least numerous of the cone types. They are only reliably found at the periphery of the retina, so it is true to say, since the retina

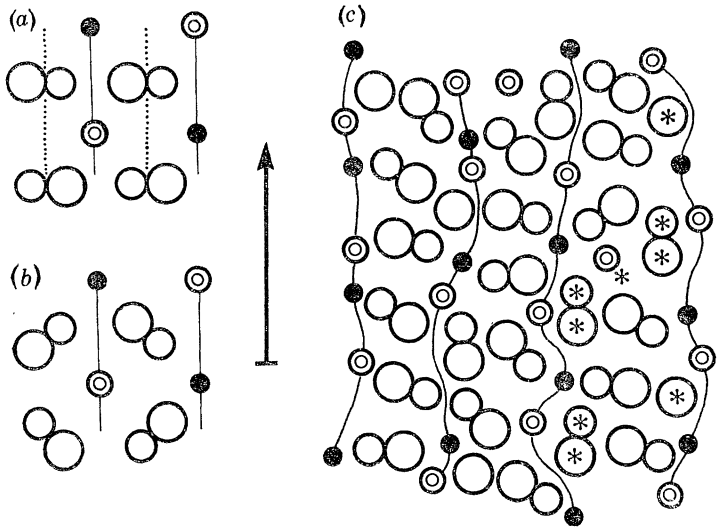

FIGURE 9. Cone mosaics. (*a*) and (*b*) are schematics of the positions of the cones in the standard mosaics found respectively in young and mature teleost retinae. Paired circles are double cones, smaller ones indicating accessory elements and larger ones, the principals. Filled circles are additional single (oblique) cones, often absent from the mature retina. Concentric circles stand for single cones, and the arrow points toward the retinal periphery. Thin lines indicate alternating rows of single cones. (*c*) Cone locations in a small area of young rudd retina. The notation is the same, except that 'free' principal cones are indicated by solitary large circles. The regular basic mosaic is disrupted by insertion of these receptors and extra double and single cones (examples asterisked).

grows concentrically by cell division at its ciliary margin, that they have only a limited time of survival after their differentiation. This curious characteristic is important, for it enables them to be identified with a species of cone well known in other fish retinae. Fürst (1904) and Lyall (1957*a*) distinguished two types of unpaired cones in the highly regular retinal mosaic of salmonid eyes. These 'central single' and 'additional single' cones have characteristic positions in the horizontal plane, relative to the double cone mosaic (cf. figure 9*b*), which seems to be their most basic distinguishing feature. Also the 'additional single cone' disappears from the retina with increasing age. So, although there is no regular lattice of double cones in the rudd against which to identify this small, third, type of unpaired cone, its disappearance from the retina with age is sufficient ground to recognize it as being the same element as the additional single cones in salmonids, and as other differently named (mittelzapfen, Müller 1952; short single cones, Engström 1960) elements in the retinae of other fish.

These small unpaired elements in the rudd are called oblique cones here (following Cajal 1892) simply to emphasize their most curious property. It is shown in a later section (page 85) that they have the 'oblique', sideways-projecting axons that Cajal showed to characterize certain of the cones in a wide variety of lower vertebrate retinae. This and their size apart, they differ from the other cones in two important respects. Their nuclei (which have the light electron density characteristic of cones) are located below the external limiting membrane among the rod perikarya (figure 4, plate 1). Also their ellipsoid mitochondria are less specialized and electron dense than those of the other cones, more resembling those of the rod inner segments (figure 4, plate 1). Although both of these properties of the oblique cones are rod-like, their outer segment lamellar structure is characteristic of cones (Laties & Liebman 1970; Cohen 1965); the disk membranes are continuous with the bounding plasma membrane of the outer segment (figure 8, plate 1).

Description of plate 1

These electron micrographs illustrate the main morphological features which differentiate the four kinds of cone cells. The cone myoids were contracted by light adaptation before fixation with glutaraldehyde and osmium, and the sections were lead stained.

Figure 2. Vertical section through the paired elements of a double cone. Always, after this fixation (methods), the outer segment lamellae of the accessory (a) cones are less well preserved than those of the principal cones (p) and of the other cone types (figures 3 and 4). The same artefact afflicts the rod (r) outer segments; in both cases it results from periodic separations of the internal surfaces of the disk membranes (cf, figure 6). The detailed ultrastructure of the ellipsoids of the principal and accessory cones differ in subtle ways, and their separation in depth is always the same in a given retinal area. For reasons of space, the double cone myoids are not shown in this picture, but appear in figures 3 and 4, so that the relative sizes of all the cones can be inferred. (Magn. × 2600.)

Figure 3. Vertical section of a single cone (s), nearby in the same retina, flanked by portions of an accessory and a principal cone. Notice that the nucleus of this receptor, and those of the adjacent principal cone and of the accessory cone to the left of figure 4 all, typically, are located above the external limiting membrane (oblique black lines). (Magn. × 2600.)

Figure 4. Vertical section of a neighbouring oblique cone (o). Compare its length with that of the other cones, and notice that its ellipsoid ultrastructure more resembles that of the rod inner segments than that of the other cones. Characteristically, oblique cone nuclei lie *below* the external limiting membrane, among the perikarya of the rods. (Magn. × 2600.)

Figures 5–8. These higher magnification pictures show the outer segment–inner segment junction in a principal, an accessory, a single and an oblique cone respectively. Accessory cone lamellae, only, are disrupted: those of the other cones resemble one another. The disks in each cone, including the oblique, are continuous with the outside. (Magn. × 21 000.)

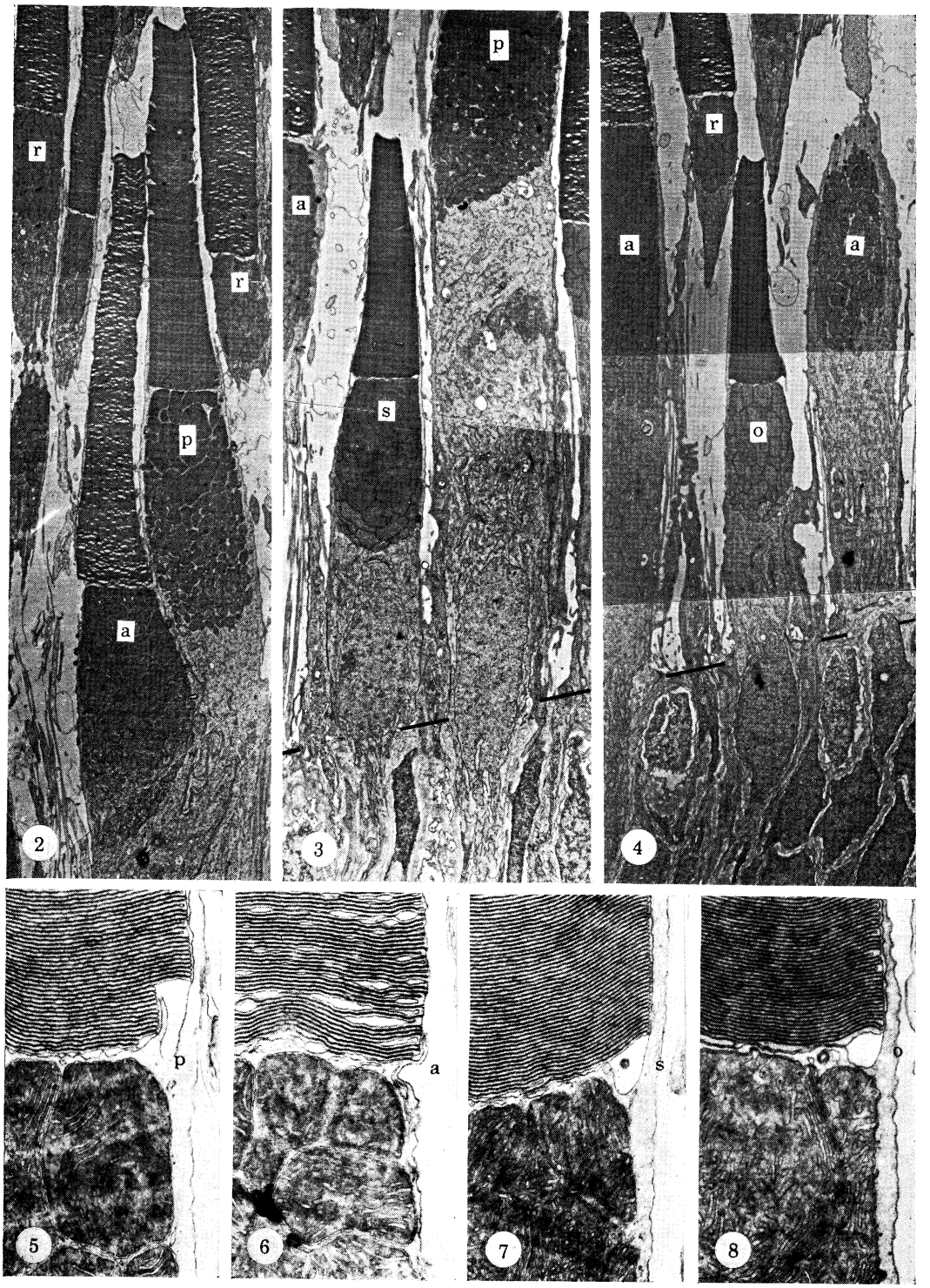

FIGURES 2–8. For description see opposite.

(Facing p. 70)

There have been speculations that the fate of additional single cones (oblique cones, here) which disappear from the retina of mature teleosts is to be 'transmuted' into rods (Fürst 1904; Lyall 1957*a*). No evidence to support this suggestion was found in the rudd retina, and certainly the relative numbers of oblique cones and rods (table 1) indicate that any such change would functionally be rather pointless, unless it were accompanied by cell division.

(iii) *Retinal mosaics and the numerical distribution of the cones*

In highly regular teleostean retinal mosaics (Müller 1952; Lyall 1957*b*; Engström 1960), cones equivalent to the free principal elements are not encountered, and there are just two double cones for each of the unpaired (central and additional single) cones. The simple pattern of the mosaic (figure 9*b*) is a reflexion of this exact ratio, whose value must, in measure, determine the effectiveness with which the colour mechanisms that reside in these cones can contribute to retinal excitation.

Throughout post-larval life, the fish retina proliferates from an annular zone of cell division around its margin (Müller 1952), and the orientation of the *axes* of the cone mosaic are determined by this radial direction of growth. Thus rows of double and single cones radiate from the central area, and from the centre to the periphery of the retina, new rows are interpolated to accommodate its continually increasing circumference (Müller 1952). In young fish, and close to the retinal margin in older ones, the mosaic takes the form shown in figure 9*a*; the two basic types of unpaired cones alternate with one another along the radial axes (continuous lines) of the lattice, with their sequence in anti-phase between adjacent rows. Double cone rows (dotted lines, figure 9*a*) alternate with those of single cones, and the orientation of the component principal and accessory elements also alternates along these rows.

Commonly, in older fish (towards the central area) the orientation of units in the mosaic changes with a 45° rotation of each of the double cones. The direction of rotation alternates along the rows, and it is an outcome of this reorganization (figure 9*b*) that the two kinds of unpaired cones become recognizable not only by their individual morphology (cf. figures 3 and 4, plate 1) but also by the positions they assume relative to the double cone lattice. Thus additional single cones always occupy a characteristic station at the intersections of the orientations of four adjacent double cones (figure 9*b*). Usually, however, as already mentioned, they disappear with ageing, leaving their station in the lattice vacant.

In the rudd retina, the layout of the receptors in the horizontal plane is irregular, though the different types remain identifiable on account of their precise distribution in the *depth* of the retina (figures 10–13, plate 2). This irregularity (cf. figure 9*c*), in fact, is the result of the insertion of 'extra' cones of different types into the regular juvenile mosaic pattern (figure 9*a*). The insertions occur haphazardly, but involve specific cone types, or combinations of them (unpublished observations). They are of functional importance because they occur sufficiently frequently to alter significantly the numerical distribution of the different cone types in the retina. If particular cones contain particular pigments, this must result in alteration of overall retinal spectral sensitivity. In this sense, it may well be that the *irregular* cone arrangement in rudd is not a degenerate condition, but one specialized best to utilize the particular spectral distribution of light reflected from objects of interest in the fish's visual world.

The most frequent insertions are of free principal cones, and less frequently, extra doubles occur which may or may not be accompanied by extra single cones. Extra oblique cones are never found, so that the spatial distribution of these receptors is more orderly than that of the

other cones (figure 13, plate 2) until they begin to disappear from the mosaic. The result is that principal cones, counting free and paired ones, are the most numerous of the rudd cones (see table 1). Both they and the accessory cones are more than twice as numerous as single cones. Because a few extra single cones are inserted into the mosaic, these elements in turn are more numerous than the full complement of obliques. The relative frequencies of the different cones vary locally, apparently haphazardly, and usually take non-integral values (table 1) so that there can be no simple repetitive mosaic pattern in their layout.

TABLE 1. RELATIVE PROPORTIONS OF THE DIFFERENT RECEPTOR TYPES IN THE REGULAR TELEOSTEAN RETINAL MOSAIC, AND IN A REPRESENTATIVE AREA OF RUDD RETINA WHERE SPATIAL ORDER IS DISRUPTED BY INSERTION OF EXTRA CONES

	principal	accessory	single	oblique	rods
basic mosaic	2	2	1	1 or 0†	—
rudd mosaic (including insertions)	3.5	2.6	1.6	1 or 0†	*ca.* 50

† Depending on age.

In summary, although in a strict anatomical sense there are five sorts of cone cells in this eye, two of them, that is the free and the paired principal cones, are likely to be functionally equivalent to one another. Furthermore, the small size and sparse distribution of the oblique cones means that they are unlikely to contribute significantly to spectral sensitivity. Therefore, the substrate for the rudd's trichromacy need only be sought among the principal, accessory and single cone populations.

(iv) *Optical considerations and the arrangement of the cones*

Does the arrangement of the cones in the retinal mosaic bear any relation to the optical quality of the retinal image? This question is important because the layering of the different cone populations (figure 1) is suggestive of a mechanism which might compensate for chromatic imperfection in the optics of the eye (Eberle 1967). In this connexion, it has to be considered whether the performance of the rudd lens at single wavelengths is sufficient that the dimensions of the cones are significant in relation to the size of the retinal image blur circle, and further, whether its axial chromatic dispersion is indeed of a magnitude at all related to the vertical distance between them. Were it so, this would presuppose a particular ordering of the photopic pigments between the morphological cone types.

(1) *Spherical aberration.* The focal length of the fish lens is very short for its dimensions, and useful image formation could only be achieved by a unique radial distribution of refractive index within its substance (Fletcher, Murphy & Young 1954), to compensate the drastic spherical aberration shown by a homogeneous lens of the same power and aperture. Pumphrey (1961) has shown qualitatively that fish lenses are indeed free of serious spherical aberration. I evaluated the lens performance in excised eyes of rudd and other cyprinids, including minnows and goldfish, by measuring, in the plane of the retina, the energy distribution profile in the blurred image of a distant monochromatic point source of light.

Freshly isolated eyes were supported on a wire loop with their corneal surfaces immersed in water, and confronted (natural, slightly dilated, pupils) with a small lamp filament and interference filter, 1 m distant on the other side of the optically flat bottom of the vessel. A small window was opened in the rear surface of the eye, and retina and pigment epithelium

cleared to expose the vitreous body. The image plane of the eye was inspected with a sharply pointed water immersion objective dipped into the vitreous (parts of the Leitz ×55 W, epi-illumination lens, n.a. 0.8), and the distribution of light in it monitored by a photomultiplier with a pinhole aperture at a conjugate plane in the microscope. Photocurrent was read as the point source was moved to different angular positions with respect to the eye, and its linear range was checked.

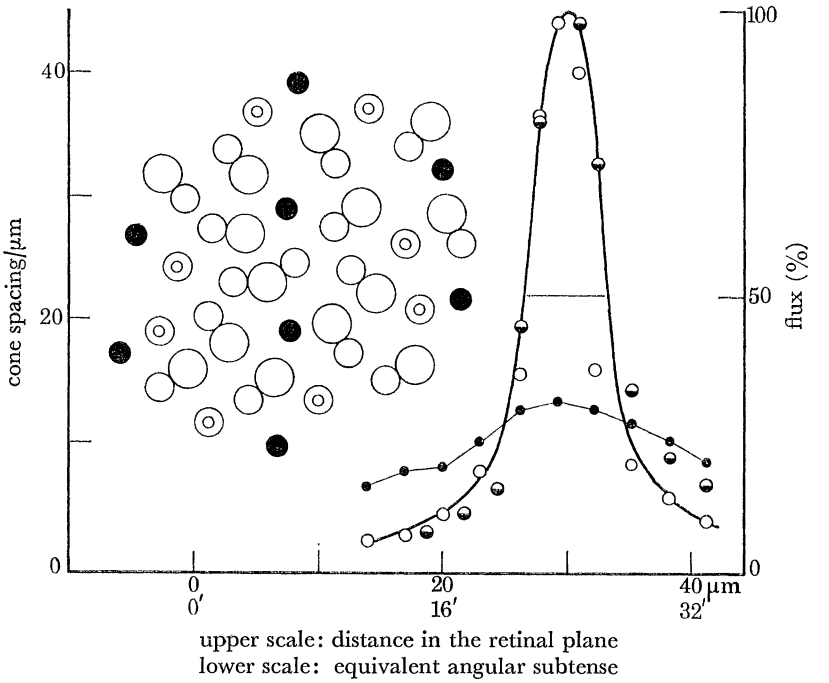

FIGURE 22. A comparison of the optical performance of the fish eye (at single wavelength) with cone spacing. At the right, (open and half-filled circles) the point spread function in the plane of the retina, compiled in 527 and 430 nm light for an eye with 2.0 mm lens diameter. The sketch to the left shows the spacing of the different cone species (notation as in figure 9) in the ventral region of the retina from an eye of the same size. The abscissa shows distance in micrometres in the retinal plane, and equivalent angular subtense into the outside world. The filled circles in the graph represent the blur circle for blue light which accompanies acute focus for green.

A point spread function, compiled in this way for one eye, is shown to the right of figure 22, where the points approximated by the smooth curve are normalized readings at two different wavelengths. The abscissal scale is given in terms both of displacement in the retinal image plane, and of angular subtense into the visual world. The lens diameter was 2.0 mm, so, according to Matthieson's ratio, focal length, which could not be measured directly with any accuracy, was about 2.5 mm.

The width at half height of the point spread function here is about 7.5 μm, or 9′ (minutes of arc). This value is contaminated by slight mechanical drift of the eye during the (randomly scheduled) measurements, and visual inspection of the image plane suggested that resolution was somewhat better than it implies (see also Charman & Tucker 1972). The sketch at the left of figure 22 shows the locations of the different types of cones in a sample area of ventro-temporal retina. Here, the packing density of the cones is highest and their dimensions least, and the average centre separation of principal cones from one another is about 6.5 μm. In this instance, (12 cm fish), the performance of the lens at these single wavelengths is well

balanced to the acuity of the receptor mosaic, and evidently its substance compensates, with remarkable precision, for spherical aberration. This was also true in the eyes of the other cyprinid species measured.

(2) *Chromatic aberration and cone displacement.* At the same time, figure 22 shows that the chromatic performance of the lens is highly imperfect. The open circles are taken from readings of acute focus for light at 527 nm. The small filled circles are measurements of the blur circle that resulted when the green interference filter was substituted by one transmitting at 430 nm, and to regain focus for this light, it was necessary to shift the microscope objective 120 μm closer to the lens, when the set of measurements represented by half-filled circles were taken.

Clark Maxwell (cited by Pumphrey 1961) recognized the possibility that his notional aspheric fish lens might also be achromatic if the optical dispersion of its medium were to vary independently of refractive index. While it is difficult to imagine a way in which this might be realized in a finite, radially symetrical lens, Pumphrey (1961) examined the lenses of various fish, including minnows for chromatic aberration, and, in an arrangement where he expected to be able to detect axial dispersion of red and blue light over distances as small as 2 μm, stated firmly that he found none.

Quite apart from the clear discrepancy of the measurements in figure 22 and Pumphrey's (1961) categorical statement of the achromacy of the fish lens, the issue is potentially useful as an argument for the chromatic identities of the different cone species. In most cone-rich fish retinae, and in many other lower vertebrate eyes, the different cones are separated from one another in depth in the same way as those of the rudd. It is possible that the arrangement might compensate for such chromatic aberration as the lenses show. In turn it would imply a particular ordering of the colour pigments between the different cones.

This has been suggested by Eberle (1967), who showed that the vertical separation of the cone populations in the guppy (*Lebistes*) eye was of the same order as the calculated axial dispersion of red and blue light. Because she gave no details of the assumptions about this complex lens structure upon which her figures for dispersive power were based, the extent of chromatic dispersion was measured in the eyes of rudd and some other cyprinid species, by using the same arrangement as that which provided the data of figure 22, but simply by reading the axial displacement of the microscope objective necessary to bring the point source into visually judged best focus at different wavelengths. Figure 23 shows typical data for the eye of a 15 cm rudd with lens diameter of 3.5 mm and focal length, from Mathieson's ratio, of 4.37 mm.

The ratio of dispersive power in the wavelength interval 465–650 nm, to mean optical power of the lens is approximately 0.035, independent, of course, of eye size. The comparable figure for the chromatic performance of the human eye is 0.02 (Ivanov 1953). The dispersion of 450 and 625 nm light by fish lenses of different diameters was determined, and judged by extrapolation to diminish to 20 μm, the axial separation of the cone types, in eyes with 0.4 mm lenses: rudd fry of around one and a half cm length would have such eye dimensions. So, while over most of its life span the fish is afflicted with far greater chromatic dispersion that could be compensated by the separation of its cones in the depth of the retina, the observations are not altogether inconsistent with Eberle's (1967) conclusion for the *Lebistes* eye, whose adult size is much smaller. Nevertheless, since cone size varies little during eye growth, there is a hyperbolic relation between eye size and receptor mosaic acuity, which means that in an eye sufficiently small that the vertical separation of the cones is the same as the axial chromatic

dispersion, the blur circles of extreme wavelengths will be little or no bigger than the cones themselves.

These measurements were made in the hope that cone displacement and axial dispersion might be related. Were they so, there would be grounds to expect single cones, nearest the lens, to contain blue sensitive pigment, and principal cones, farthest from it, to be sensitive to long wavelength light. But, in the rudd, the results do not strictly permit such teleology, and it remains a curiosity that the lens, while being so limited by its chromatic performance (figure 23), is so perfectly aspheric at single wavelengths (figure 22).

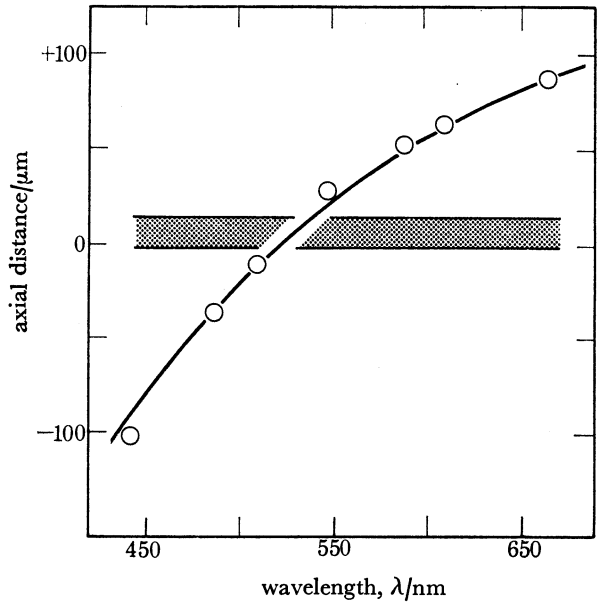

FIGURE 23. Focal length plotted against wavelength for a 3.5 mm fish lens. The stippled horizontal bar represents the extreme vertical separation of the different types of cones in the light adapted retina, and the smooth curve is the first term of the Cauchy formula with constants selected for best fit to the measurements.

2. THE CHROMATIC IDENTITIES OF THE CONES

(*a*) *Introduction*

In spite of its irregular receptor mosaic the rudd retina has the same types of cone cells as many other teleosts, and many of the morphological distinctions between them find their parallel in the cones of other lower vertebrate animals. Liebman (1972), reviewing the microspectrophotometry of cones in a variety of lower vertebrate eyes, shows cone pigment trichromacy to be strikingly ubiquitous: the absorption maxima of cones cluster tightly around 450, 500 or 580 nm, and those of the goldfish cones, the closest relative of the rudd to have been studied are no exception.

The wavelength discrimination performance of both goldfish (Yager 1967) and rudd (Muntz & Northmore 1970) has been analysed behaviourally, and their photopic spectral sensitivity curves are quite similar. They both show three peaks, at red, green and blue wavelengths, whose spectral locations broadly agree with the absorption maxima of the goldfish cones (Marks 1965) measured by microspectrophotometry. While the spectral properties of goldfish cone pigments are known directly, and there is good behavioural evidence that those of the

rudd are similar to them, the question of which anatomical cone species contains which photopigment has been less clearly elucidated. Marks (1965) remarked that the separate elements of the majority of goldfish double cones contained red or green pigment, but was unable to discriminate principal and accessory cones. In the disrupted retinae he used for his measurements, the majority of double cones split apart, and presumably on this account the majority of unpaired cones he measured had red or green spectra. The few (unpaired) cones with blue spectra had a distinctive inner segment morphology, which suggested that they were the true single cones.

In both fish (Liebman 1972) and frog retinae (Liebman & Entine 1968) it has been shown that the principal elements of the double cones contain red-absorbing pigment, while that of the accessory cones is always green. Its pigment is rhodopsin-like, with a λ_{max} similar to that of the rods, and in the frog's metamorphic transition between retinal- and dehydroretinol-based rhodopsins, the spectra of the accessory cones and rods shift in concert (Liebman & Entine 1968). In the frog the single cones as well as the principal elements of the double cones contain red pigment (Liebman & Entine 1968), so that the only receptor substrate for the blue mechanism these creatures are known to possess (Muntz 1962) is the population of Schwalbe rods.

Svaetichin, Negishi & Fatehchand (1965) have measured the photopigments of identified cones in a variety of South American fishes and in the goldfish by microspectrophotometry, and they also found that double cones contain red or green pigments. However, the constituent principal and accessory elements of the double cones were not distinguished from one another in this study, and sometimes both elements of a double cone were found to contain the same photopigment. The two sorts of unpaired cones generally characteristic of fish retinae were recognized; central single cones (morphologically equivalent to the rudd's *single* cones) were held to contain a green photopigment with a similar λ_{max} to the green pigment found in double cones and to the rhodopsin of the rods, while additional single cones (equivalent to the *oblique* cones in the rudd) possessed a blue pigment. However, very few details were given of the exact criteria which enabled these morphological identifications.

Description of plate 2

Figures 10–13. Light micrographs taken from serial horizontal sections through the receptor layer, to show the clarity with which the different cones can be recognized. Osmium fixation and phase contrast. The sequence, from left to right, starts among the rods and the outer segments of the double cones, and ends near to the basement membrane, where (figure 13) the apposed myoids of principal (p) and accessory (a) cones are visible in between more darkly staining outer segment profiles of single (s) and oblique (o) elements. Principal and accessory cones are most easily distinguishable by the depth at which their ellipsoids are situated (cf. figure 12). There is a free principal cone (f) in this area of retina: compare its depth with that of the double cones (e.g. p and a). (Magn. × 1000; cone sizes and packing densities vary by a factor approximately 1.5 between dorsal and ventral retina.)

Figures 14 and 15. The identifiability of the different cones in unfixed retinae stripped of their rods. Figure 14 is a micrograph which isolates the outer segments of accessory cones (a) in optical section and shows also the ellipsoids of the principal (p) elements. Figure 15, with the focal plane deeper in the receptor layer, shows the outer segments of single (s) and oblique cones (o), interspersed among the inner segments of double cones (e.g. a and p). (Magn. × 1000.)

Figures 16–21. Colour separation photographs of the tips of cone outer segments in an unfixed isolated retina stripped of rods. (Magn. × 2000.) The top row are taken by narrow band illumination with, from left to right, red, green and blue light. Immediately afterwards, the retina was exposed to bright white light to bleach the receptor photopigments. Then (lower row, left to right) it was rephotographed in the same sequence of coloured lights. The largest changes in transmission occur in green light. (Compare arrowed cones in figures 17 and 20.)

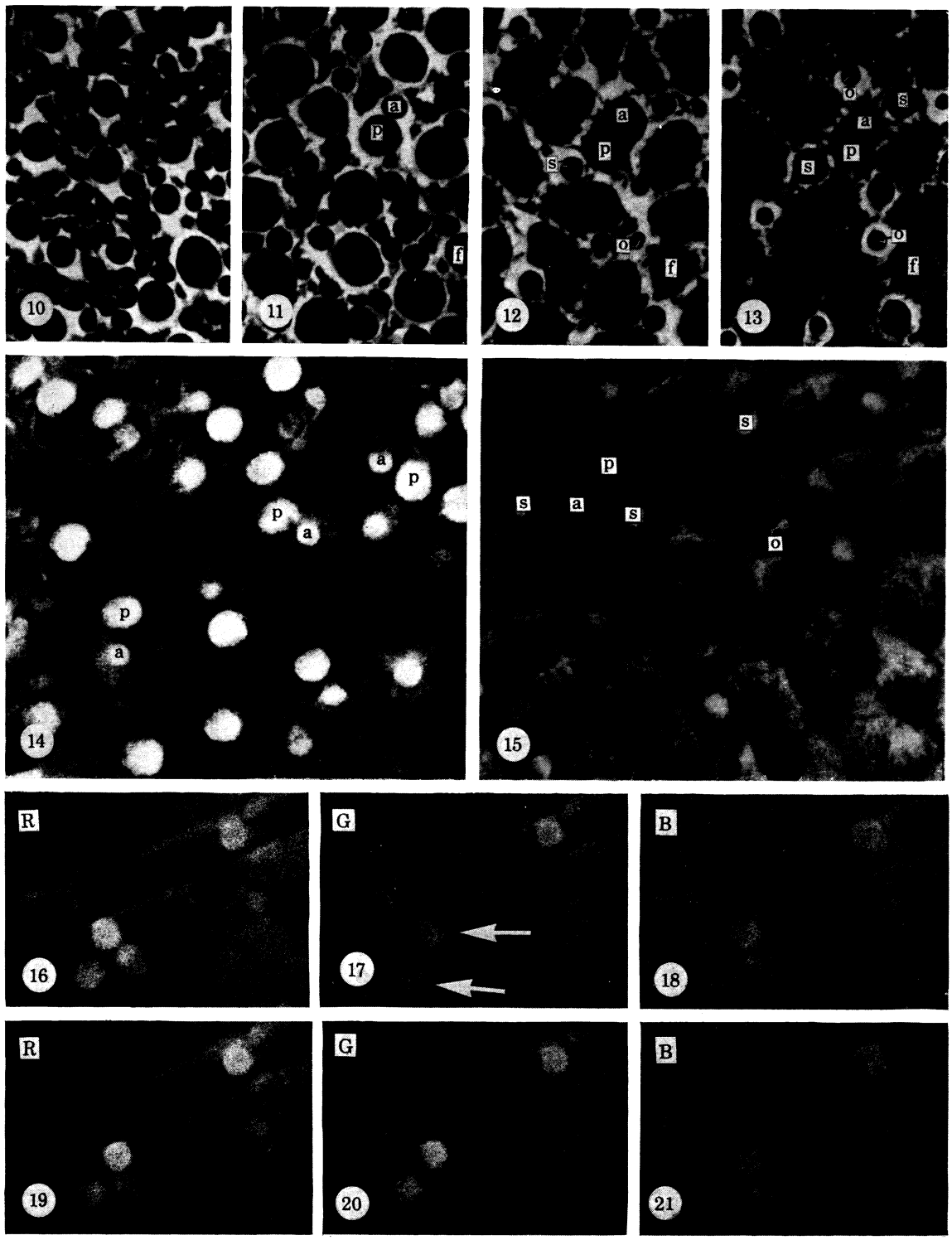

FIGURES 10–21. For description see opposite.

(*Facing p.* 76)

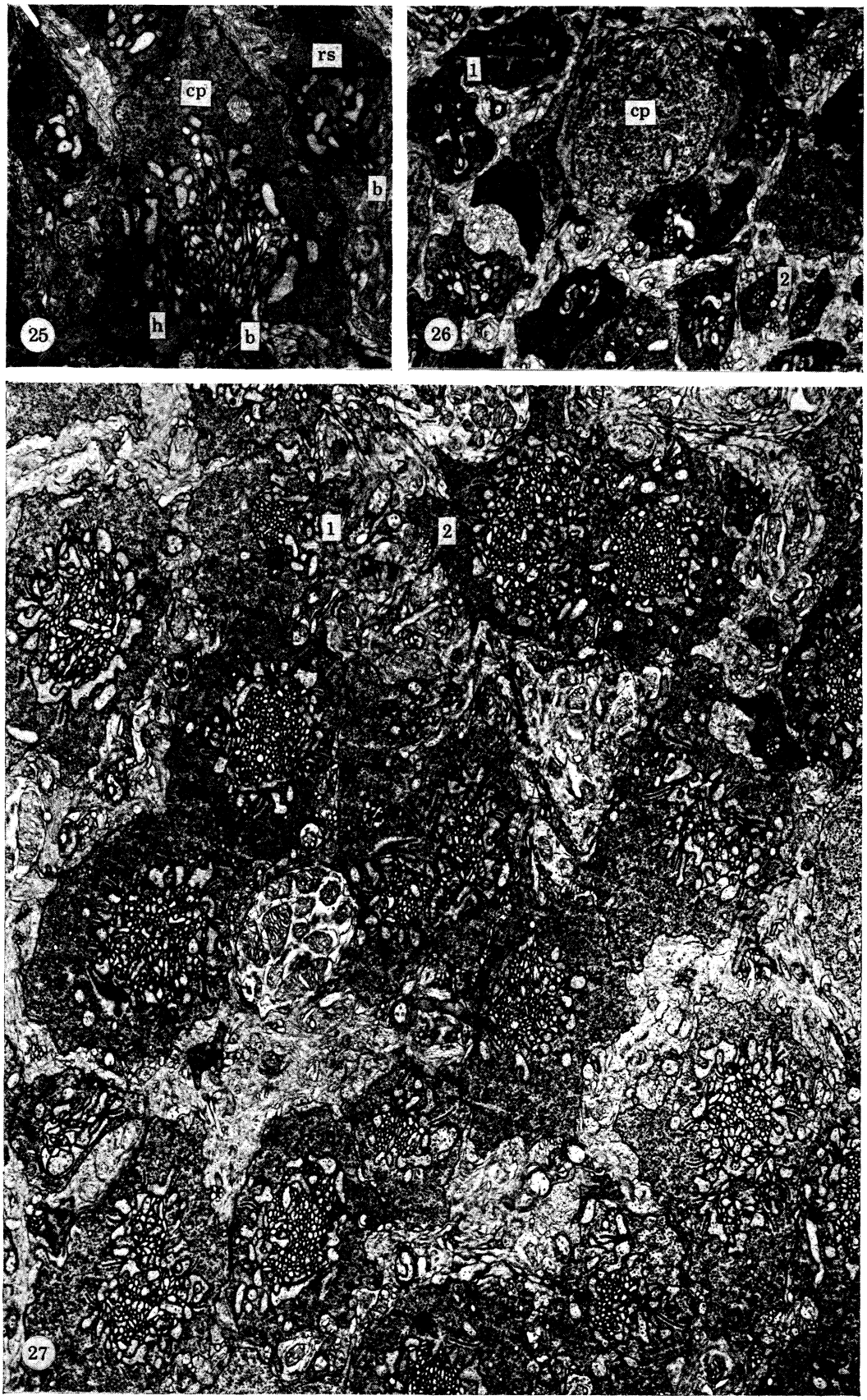

FIGURES 25–27. For description see opposite.

(*b*) *Observations*

The weight of this microspectrophotometric evidence from fish and other lower vertebrate retinae, if it can so be extrapolated between different animals, suggests that principal and accessory cones in the rudd should respectively contain red- and green-absorbing photopigments. The rudd has a photopic blue mechanism that is certainly quite as powerful in determining spectral sensitivity as its red and green cone populations (Muntz & Northmore 1970). This being so, it is most unlikely that the underlying blue sensitive photopigment resides only in the sparse population of small oblique cones that its retina possesses (page 72), as the account of Svaetichin *et al.* (1965) might suggest. Rather, it is more likely that the single cones (equivalent to the central single cones elsewhere) fulfill this role. But it is no more than an assumption, of course, that homologous cones in different species contain similar photopigments, and the red single cones of the frog retina (Liebman & Entine 1968) indicate its uncertain ground.

This being so, an attempt was made to establish the chromatic identities of the rudd cones directly, by photomicrographic densitometry. Some years ago, Denton & Wyllie (1955) photographed the mosaic of rods in the intact frog retina under different wavelengths of illumination, before and after bleaching, and were able to compile accurate absorption spectra for both the rhodopsin and Schwalbe rods. This satisfying technique has never successfully been applied to cones, and there are two reasons, at least, why this may be so. First of all, in duplex retinae, the cones are hidden from axial view by the felt of rods which surrounds their outer segments. Secondly, in the case of cones, it proves, contrary to first intuitions, misguided strategy to work at as low magnification as possible, as Denton & Wyllie did in order most efficiently to utilize quanta transmitted by the receptor outer segments. This is because the refractile optics and outline structure of the cones are such that rays emerging from the tips of their outer segments are highly divergent and unless they are captured with the narrow depth of focus that attends high magnification, mingle with light scattered around the receptors.

A variety of techniques were tried to detach the rods from the rudd retina, and, while none was particularly satisfactory, the following method exposed the cones more frequently than most.

Retinae were stripped from the pigment epithelium of deeply dark adapted eyes, under very dim white light. They were placed in adrenalin-Ringer solution for 5–10 min to contract the

---

Description of plate 3

Electron microscopy of receptor synaptic terminals.

Figure 25. This is a vertical section through the layer of receptor terminals, showing a pedicle (cp) belonging to an accessory or a principal cone, whose neck is surrounded by rod spherules (rs). Bipolar (b) and horizontal (h) cell processes enter the pedicle synaptic cavity basally from the outer plexiform layer (op). (Magn. *ca.* × 12000.)

Figure 26. Horizontal section showing the neck of a cone pedicle (cp) surrounded by rod spherules. Some of them are transected at a level which shows the complexity of the horizontal cell process–synaptic ribbon associations (1). Others, cut basally (2), show that several bipolar processes enter the synaptic cavity of each rod terminal. (Magn. × 5900.)

Figure 27. Cone pedicle profiles in an horizontal section just distal to the outer plexiform layer. Because of their disorderly distribution, there are no cues for identifying their cones of origin, though sometimes double cone terminals (top, right of centre) can provisionally be recognized by their pairing. Though the details of their ultrastructure are the same, there are large scale differences in the *numerical* complexity of the cone pedicles (compare (1) and (2), for example). (Magn. × 5900.)

cone myoids, and then vigorously hand shaken in test-tubes of Ringer to detach the rods. The extent to which this was effective was indicated by the disappearance of the deep rhodopsin colour from the retina, and it was necessary to judge a delicate compromise between just removing it, and disaggregating the tissue. The technique is crude, but more effective than others, such as sonication, which seemed in principle more controllable.

The retinal fragments were mounted receptor side up in a well on a microscope slide, flooded with Ringer, and sealed under a cover slip with vaseline. They were examined with a $\times 100$ oil immersion objective in an optical arrangement that included the stage, condenser and light source of the Leitz Ultropak system. To use light passing through the retina economically, the microscope head was replaced by a prism which could either direct light to a single eyepiece for inspection, or to a 35 mm camera for recording. The condenser imaged the almost closed substage iris onto the plane of the retina, so that, at any time, an area smaller than the field of view of the objective was illuminated. Below the condenser there was a mechanical shutter, opened manually for inspection of the retina, or used to time photographic exposures. Interference filters, whose transmission was adjusted to equality with respect of the spectral distribution of energy from the light source and the sensitivity of the recording film (Kodak 2745, nominal A.S.A. 1600), could be placed in the substage light path.

The retinae were scanned to find areas in which the rods were completely removed, and in which the cones were upright in the light path of the microscope. Such areas, once found, were exposed to light for as short a time as it took to focus the optics on the tips of the cone outer segments, and then the substage shutter was closed while the interference filters and camera were prepared for photography. The microscope light source was preset to such an intensity that half second exposures were sufficient for the recording film. The preparations were photographed by 430, 530 and 625 nm lights (chosen to coincide roughly with the peaks of the rudd's photopic spectral sensitivity curve) in rapid succession, then bleached with intense white light and finally photographed again in the same sequence of monochromatic lights.

Figures 14 and 15, plate 2 are photographs taken at different depths in the retina to illustrate the certainty with which the different cone species can be identified in these partly intact preparations. Figures 16–21, plate 2 show the tips of a small group of cones from a sequence of colour separation photographs, and illustrate the magnitude of density changes upon bleaching which could (sometimes) be captured by this technique. The arrows indicate the two accessory elements of a triple cone, which show a photolabile density maximal at the green wavelength (figures 17 and 20). There is a detached rod lying in the focal plane of these pictures.

Few preparations were achieved in which the cones were both identifiable and showed photolabile densities, though when they were, many cones could be analysed on single frames of the film. Progressive bleaching during preparation and inspection, which could have been avoided by use of infra-red viewing devices, is most likely the reason for this. White light was used for inspection to avoid selective bleaching, and in the initial preparation procedure it was of such an intensity as negligibly to bleach the rhodopsin of the rods. Inspection of the cones under high magnification was of more serious consequence for their pigment: with enough illumination to make them just visible, the quantum flux available to bleach a rhodopsin-like pigment in the outer segment of a single cone was of the order of 10^6 photons s^{-1}, so that only extremely cursory viewing was permissible. Photography was less of a problem, since the flux available to individual cones during the sequence of exposures was less than 5×10^6 photons.

The recording film (Kodak 2745) was about four times faster than that used by Denton & Wyllie (1955), which in part compensates for the increased magnification used in the present measurements.

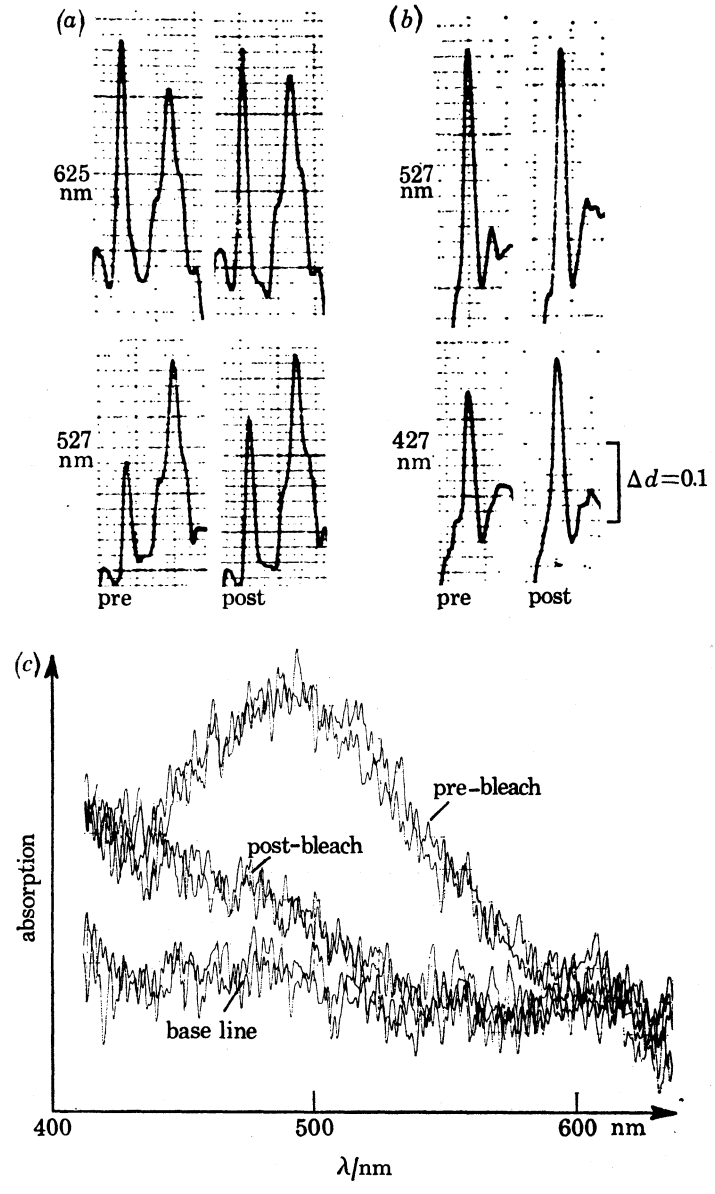

FIGURE 24. (*a*) Upper two traces; microdensitometer scans through the impressions of a double cone in negatives taken by red (625 nm) light, before and after bleaching. No significant transmission change either for the accessory element (left-hand peak) or the principal cone (right-hand peak). Lower two traces; the same scanning path through the impressions of the same double cone photographed in green light (527 nm) before (left) and after (right) bleaching. Transmission by the accessory cone outer segment is increased by the bleaching exposure.

(*b*) Similar scans of colour separation negatives containing the impressions of a single cone outer segment. No significant density change for the photographs taken in green light, but increased transmission for blue (427 nm) as a consequence of bleaching. The absorbance change scale to the right applies to both (*a*) and (*b*).

(*c*) The absorption spectrum of a rudd accessory cone outer segment measured microspectrophotometrically. The peak of the difference spectrum is at rather shorter wavelength than 500 nm. This spectrum was measured by P. A. Liebman and H. J. A. Dartnall, with whose permission it is reproduced here.

The magnitude of the cone density changes was estimated by microdensitometry of the negatives, with a reference provided by frames which had been exposed to a step wedge, using the same mean light intensities and development times as those employed in the retinal photography. The measurements were made with a Joyce–Loebl recording microdensitometer, whose scanning spot size was chosen to be rather smaller than the impressions of the cone outer segments on the negatives. Precautions were taken to ensure that the scanning trajectory through the images of particular cones was the same throughout the series of frames in which they appeared.

Figure 24 shows representative densitometer traces of scans through a double cone (*a*), photographed with the outer segment of the accessory element in the focal plane, and through a single cone (*b*). The slightly out of focus impression of the principal element showed no significant density change at either red or green wavelength after the bleaching exposure but that of the accessory cone showed increased transmission for green light. The single cone scanned in figure 24*b* showed significant increase in transmission for blue light and little or no change for green. These results are typical (table 2) for the majority of cases where photolabile densities were registered. The observed changes upon bleaching (figure 24*a*, *b*, table 2) rarely exceeded a magnitude equivalent to removal of a 0.05 absorbance (*a.* 10 % absorption). This is less than half the longitudinal absorption predicted by microspectrophotometry (pigment density, 0.015 μm^{-1}; Liebman 1972) for cones of the size of the accessory elements, and its low value is most likely due to progressive bleaching during preparation for photography.

TABLE 2. MEAN ABSORBANCE CHANGES AT DIFFERENT WAVELENGTHS UPON BLEACHING THE DIFFERENT CONES, AND THE STANDARD DEVIATIONS OF THE MEANS: MEASUREMENTS FROM COLOUR SEPARATION PHOTOGRAPHS OF 34 CONE OUTER SEGMENTS IN THREE DIFFERENT RETINAL PREPARATIONS

	photolabile density (10^{-2} × absorbance)		
	427 nm	530 nm	625 nm
principal	—	0 ± 1.0	1.0 ± 1.0
accessory	—	3.7 ± 0.5	-0.1 ± 1.2
single	2.7 ± 0.7	0.2 ± 0.7	—

Oblique cones, which were only rarely discernible in the preparations (figure 15, plate 2) never showed a photolabile density, and the same, surprisingly, was true for a larger sample of principal cones.

It is only because of the importance of establishing the chromatic identities of the cones for the study of their neural connexions that these fragmentary data are presented, and an effort has been made to summon arguments from other sources to support the tentative identifications they permit. Clearly, more rigorous identification by microspectrophotometry is needed, and in fact some preliminary measurements have been made on the rod and cone outer segments of the rudd retina.

P. A. Liebman and H. J. Dartnall have compiled spectra from rods and double cones and they have kindly allowed me to quote some of their unpublished findings here. The rods and the accessory cones both contained green absorbing labile pigments with λ_{max} at a rather shorter wavelength in the cones than in rods. One of the accessory cone spectra is shown in figure 24*c*, to confirm the identification, based on photographic densitometry, given above.

Principal cones, in the retinae examined, were universally 'empty', though in one or two cases there was a labile density, just detectable above noise, at around 600 nm. Apparently it is common (P. A. Liebman, personal communication) for red cone pigment to be susceptible to the particular conditions of tissue maintenance (e.g. anoxia, temperature) involved in microspectrophotometry, and it might well be that similar deterioration was responsible for the failure to record the pigment of the principal cones photographically, where the accessories were relatively tractable with this technique. Single and oblique cone spectra were not measured.

To conclude, there is good evidence (table 2, figure 24*a*, *c*) that the green photopic pigment is located in the accessory cones of the rudd retina. There was an indication that the principal cones contain the red pigment, and it will be seen that this is confirmed when the neural connectivity of these receptors is compared (page 111) with the spectral properties of identified bipolar cells recorded electrophysiologically in carp retina (Toyoda 1973). There is evidence that the single cones, like those in goldfish (Marks 1965) contain blue absorbing pigment; nothing, however, is known of the oblique cone pigment.

It is important to note that the relative proportions of red, green and blue receptors are given by the frequencies of the different cone types in the retinal mosaic (table 1 and text). In goldfish, which has a similar retina to that in rudd, Marks (1965) encountered red, green and blue cones by microspectrophotometry in the proportions 11:15:2, and these figures have sometimes inappropriately been used as if they represented the real distribution of the cones (Kaneko 1973), which is not necessarily the case.

3. The rod and cone synaptic terminals

(*a*) *Introduction*

Two aspects of the organization of the receptor synaptic terminals must be considered before the connexions of the bipolars are described. First, it is important to know something of the detailed nature of their synaptic contact with bipolar cells. In mammalian retinae (Missotten 1965; Dowling & Boycott 1966; Boycott & Kolb 1973) and in the turtle (Lasansky 1971) two separate kinds of bipolar cells make two quite distinct sorts of junctions with the cones. Flat contacts are simple appositions of bipolar dendritic processes to the basal surfaces of the pedicles, with a degree of joint membrane specialization, but with no conspicuous aggregations of synaptic vesicles on either side of the junction. Invaginating connexions are quite distinct, and structurally, at least, more specialized, involving the association of the bipolar dendritic processes in the characteristic dendrite 'triads' at the synaptic ribbons of the pedicles. The physiological distinction between these two sorts of synaptic arrangement is not known, though it is clearly one of principle; is there the same dual innervation of the fish cone terminals?

Secondly, it is necessary to have some means of identifying the pedicles of the cones according to their chromatic type: do they show as conspicuous variation in structure as there is between the distal parts of these receptors? It is at least well known that there are large scale differences in the complexity (Cohen 1972) and ultrastructure (see, for example, Evans 1966) of rod and cone terminals.

This part of the paper, then, uses conventional thin section sampling electron microscopy to derive a 'composite illustration' (Sjöstrand 1969) of the organization of rod and cone terminals in the rudd. It is shown that the cone pedicles differ from those in the mammalian retina (Missotten 1966; Dowling & Boycott 1966; Boycott & Kolb 1973) in having a common

synaptic cavity (cf. Pedler 1965) shared by a number of synaptic ribbons, and that the number of separate neuronal processes innervating them is very large.

Generally, in duplex retinae throughout the vertebrate groups, the rod synaptic terminals (spherules) are smaller and simpler than those of the cones (pedicles), and they are usually located in a layer somewhat distal to them (Cajal 1892; Polyak 1941; Missotten 1966; Pedler 1965). Both rod spherules and cone pedicles are innervated by invaginating dendritic processes of bipolar cells, which associate with the intracellular presynaptic ribbons of the terminals deployed around their synaptic cavities (Missotten 1966; Sjöstrand 1969; Stell 1967; Kolb1970). Sections which transect the synaptic ribbons usually show a triad of second order processes clustered around them: it is known (Stell 1967; Kolb 1970) that the lateral processes of triads come from horizontal cells, while the smaller central one is of bipolar origin.

Rod spherules differ from cone pedicles in that, as far as is known, they receive no system of basal flat contacts from the bipolar cells. Also, as far as the invaginating bipolar contacts are concerned, cone terminals are much more complex than those of rods: rather than having just one (or two) synaptic ribbons, they possess many (up to 30). In mammals (Missotten 1966; Dowling 1965; Kolb 1970; Boycott & Kolb 1973), there is a separate, single, synaptic invagination for each (short) synaptic ribbon, which contains just one trio of horizontal and bipolar cell dendritic processes. In the lower vertebrate retina the position is less clearly described, but in general it seems that several ribbons share a common pedicle synaptic cavity, occupied by numerous bipolar and horizontal cell processes (Pedler 1965; Stell 1967; Lasansky 1971).

(*b*) *Observations*

(i) *The structure of rod spherules*

In rudd, like goldfish (Stell 1967), the rod terminals are arranged around the necks of the more complex cone pedicles. In the aldehyde pre-fixed material shown in plate 3 their cytoplasm is conspicuously darker than that of the cone terminals (figures 25 and 26), and the fine structure of their vesicles also differs (cf. Evans 1966; Lasansky 1973). There is just one ribbon in each rod terminal, whose apical specialization (Lasansky 1971) is associated in the usual way with a central bipolar process and flanked by larger processes of horizontal cell origin. In figure 26, plate 3, the section plane passes along one of the rod synaptic ribbons, and shows something of the three dimensional complexity of these horizontal cell processes.

That rod spherules have only one synaptic ribbon is no reason to regard them as single channel terminals in the sense that Pedler (1965) used the term. Horizontal sections through their bases (figure 26, plate 3) show that as many as nine bipolar cell processes invaginate the synaptic cavity, as well as those of horizontal cells, which often enter separately at a slightly higher level (figure 28). The observations on Golgi-impregnated material will suggest that each bipolar process that enters a rod terminal comes from a separate nerve cell; probably this is also the case in mammals (Missotten, Apelmanns & Michiels 1963; Kolb 1970; Boycott & Kolb 1973), but there, the invaginating processes to each spherule are much less numerous.

These features of rod terminal organization are summarized in figure 28*a*. The diagram does not show the entire postsynaptic complement of the spherules, or do justice to the three dimensional complexity of the processes that invaginate them.

(ii) *The structure of cone pedicles*

The pedicles, particularly of double cones, are much larger than rod spherules and bell-shaped (figure 25, plate 3). Horizontal thin sections through their bases show that invaginating

bipolar processes enter the pedicles through a common proximal aperture (figure 27, plate 3).

More distal section planes show a single central synaptic cavity in the pedicle, usually of complex outline (figures 25, 27). The transverse profiles of up to twelve synaptic ribbons, approximately radially oriented, are arranged around it, with their 'apical specializations' projecting from the cavity lining. The apical specializations take the form of ridges projecting into the synaptic cavity, which contain the arciform density (Ladman 1958) and run vertically, rather like vaulting, to end near the neck of the pedicle. They are flanked in the usual way by elaborate horizontal cell processes which line the synaptic cavity (figure 30, plate 4). The cavity outline

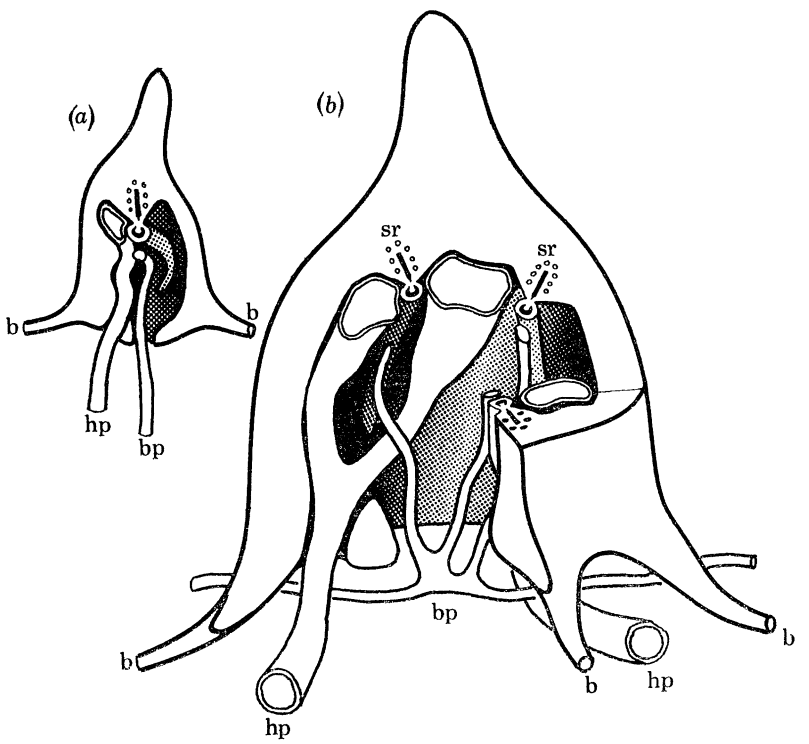

FIGURE 28. Schematic interpretation of the three dimensional structure of rod spherules (*a*) and cone pedicles (*b*).

The internal surface of the synaptic cavities are shown stippled, and of much simplified outline. In the case of cone pedicles, the cavity is lined by elaborations of the horizontal cell processes (hp) which usually enter the terminals basally along with the bipolar processes (bp). In the pedicles, there are several synaptic ribbons (sr), which run vertically up the lining of the synaptic cavity, with their apical specializations (as) projecting into the lumen. In this diagram, a single bipolar dendrite in the outer plexiform layer is represented as sending a branch to each of the ribbons in the pedicle it innervates: evidence that this is the case comes from interpretation of Golgi material, considered in the discussion.

Although rod spheres (*a*) only have one synaptic ribbon, several bipolar processes invaginate each of them. Both rod spheres and cone pedicles have laterally ramifying basal processes (*b*), and both contain many more second order synaptic processes than are shown in the diagram (cf. plate 4).

is complicated by outgrowths of the pedicle cytoplasm, and filled by large numbers (figure 30, plate 4) of vertically oriented (figure 25, plate 3) invaginating bipolar processes. In horizontal sections, 'triad' profiles opposite the ribbons are not usually particularly well defined. Thin process profiles of presumed bipolar origin may be closely and centrally associated with the ridge, but as often are offset or some distance away from it (figure 30, plate 4).

Evidently the bipolar dendritic processes terminate at different levels inside the synaptic cavity, since fewer of their profiles are seen in more distal sections. This, among other things,

suggests that they do so by occupying, in turn, the triad central profile station along successive short lengths of the presynaptic ribbon apical ridge. Ideally, this should be tested by serial reconstruction, which was not seriously attempted: nevertheless interpretation of the Golgi impregnations will provide evidence that it is so (page 109).

Basal (flat) contacts between bipolar processes and cone pedicles were not noticed in the rudd either by conventional or Golgi-electron microscopy. This is not to say that they do not exist, but that if they do, they constitute a much less conspicuous system than that in mammalian and reptilian eyes. In fish, it is possible that such apposition contact could be made *within* the synaptic cavity of the pedicle (rather than basally) and still be functionally remote from the ribbon apparatus; if they were, they might be less easily recognized than those formed on the basal surface of the terminals in other vertebrate retinae.

Figure 28*b*, which is considered more fully in the discussion (page 108), presents this interpretation of pedicle organization. The extent to which it is schematic can best be judged from the vertical and horizontal profile electron micrographs in plate 3, which show, for example, that the synaptic cavity is much more complex in outline than the simplification in the diagram suggests. It will be seen that the vertical extent to which bipolar processes penetrate the pedicle synapse is a feature of this retina which makes analysis of bipolar connexions by Golgi-e.m. particularly convenient.

(iii) *The identities of the cone pedicles, and the structural differences between them*

There is a conspicuous variation in the size and complexity of neighbouring cone pedicles (figure 27, plate 3) but because of their haphazard locations in the plane of the outer plexiform layer (reflecting the disorder of the receptor mosaic), there is little indication in such single sections alone whether this variability is extraneous or reflects the chromatic identities of the cones.

To answer this question, and to make it possible to attack the more central problem of colour selectivity among the synaptic connexions of the bipolar cells, it is obviously necessary to identify particular pedicles with their cones of origin above the outer limiting membrane. Conveniently enough, despite the disorder of the rudd's retinal mosaic and the thickness of the outer nuclear layer, the axons of the three larger cone types do project into the outer plexiform layer in an organized fashion, preserving their neighbour relations. This means that pedicle profiles in horizontal electron microscope sections can reliably and easily be identified by comparing the array of which they are a part with the array of clearly recognizable cone profiles in light micrographs of sections taken in the receptor layer immediately above.

The outline drawings of figure 29, which were traced from light micrographs of a group of cones and electron micrographs of their pedicles, illustrate the typical accuracy of the projection. Double and triple cone pedicles usually pair appropriately to their distal associations, but this is not always so, and their relative orientations commonly change. Single cone axons often wander slightly from their receptor mosaic stations, but not sufficiently to confuse the mapping. The projection of the oblique cones, to which they owe their name, is more complex and will be described separately below (page 85).

The pedicles of the different cones, identified in this way, do in fact differ consistently from one another, though not quite to an extent that would alone enable their firm recognition in Golgi-e.m. material. They differ in size, and this in turn reflects their particular numerical synaptic relations with the nerve cells of the retina, knowledge of which will have bearing on the interpretation of the Golgi impregnations.

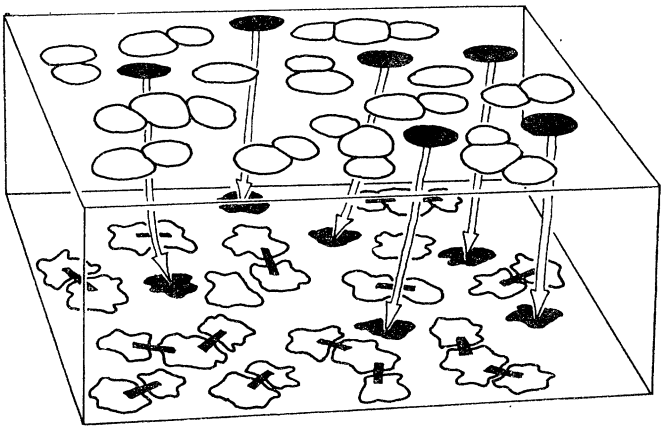

FIGURE 29. This drawing, constructed from light and electron micrographs of the cones and their terminals, shows the typical accuracy with which neighbour relations between the different kinds of cone distal to the external limiting membrane are preserved in the layout of their pedicles at the level of the outer plexiform layer.

Principal cone pedicles are the largest receptor terminals, with around twelve synaptic ribbons, and up to 350 dendritic processes of which the overwhelming majority are of bipolar origin, invaginating their synaptic cavities (figure 30, plate 4). Accessory cone pedicles are somewhat smaller, with about nine ribbons, and up to 250 second order processes (figure 31, plate 4). Predictably, single cone pedicles are smaller than those of the doubles, with about six ribbons and between 80 and 100 bipolar cell processes (figure 32, plate 4), and oblique cones complete the series with just one (sometimes two) ribbon and about twenty invaginating processes (figure 33, plate 4). Their synaptic apparatus, then, is scarcely more elaborate than that of the rod spherules, which are invaginated by about a dozen bipolar dendritic processes.

Numerical details of the synaptic complement of the different receptors are given in table 3. Slight differences were also noticed in the ultrastructure of the pedicle cytoplasm of the various cones, but these were not clear enough to merit consideration here.

TABLE 3. COUNTS OF BIPOLAR PROCESSES AND OF SYNAPTIC RIBBONS ENCOUNTERED IN RANDOM HORIZONTAL SECTIONS THROUGH THE RECEPTOR SYNAPTIC TERMINAL CAVITIES

(Figures at the left of each column are means, and those at the right are maximum counts from a population of fifteen of each cone terminal type in the same area of retina. It is unlikely that individual sections intercepted the same bipolar processes more than once, since they have an uncomplicated, approximately vertical course in the synaptic cavity (figure 25, plate 3).

	principal	accessory	single	oblique	rods
bipolar dendritic processes	285; 367	208: 230	86; 116	16; 19	9; 12
ribbons	9; 12	6; 9	3; 6	1.5; 2	1; 1
processes per ribbon	35	25	19	8	12

(iv) *The projection of the oblique cone axons*

Oblique cones (equivalent to additional cones; see §1), and their pedicles, were omitted from the drawings of figure 29 because their axons do not project through to the outer plexiform layer in register with those of the other cones. The form of their projection is curious enough in its own right to merit a short diversion. Oblique cones easily recognizable in Golgi impregnations by the position of their nucleus below the external limiting membrane (cf.

figure 4, plate 1). The *camera lucida* drawing in figure 34*a* shows a vertical retinal slice containing a number of impregnated receptors, among which the axons of five of these cones are arranged in the same way as those of the Cajal's 'oblique' elements in reptilian and avian retinae, and of Schwalbe rods in the frog. Cajal clearly described these distinctive structures in 1892; since then, to my knowledge, they have not received any attention, and only in the case of the

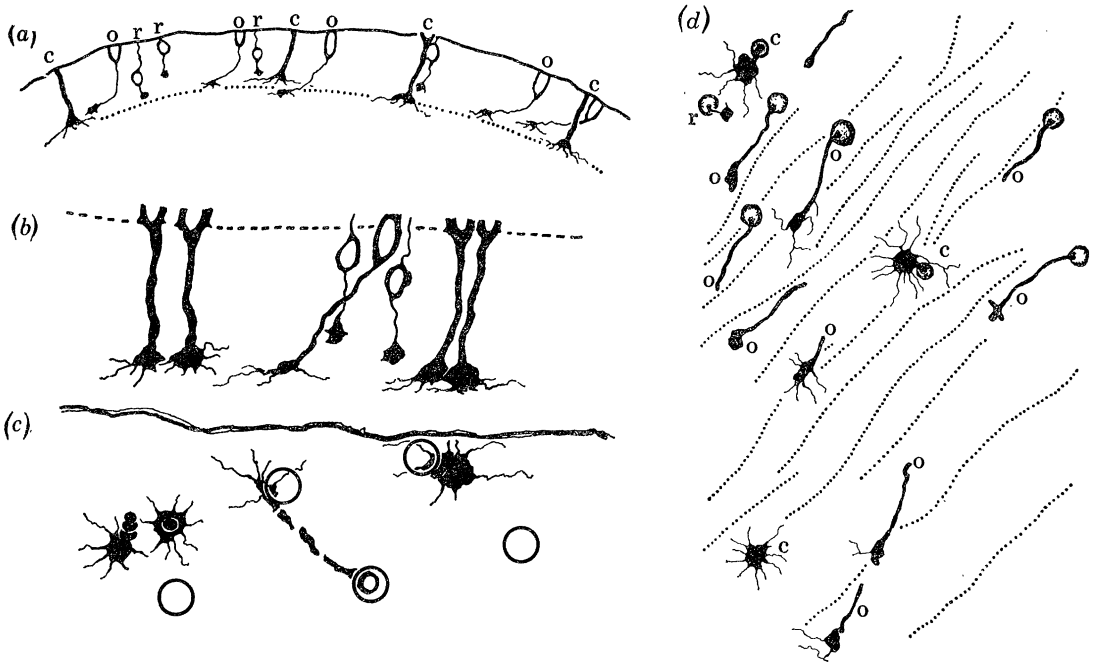

FIGURE 34. The projection of oblique cone axons. (*a*) *Camera lucida* sketch of a group of receptor axons in a vertical slice of the retina. The external limiting membrane is indicated by the upper continuous line, and the dotted lower line represents the boundary of the outer plexiform layer. Several rods (r) and cones (c) are impregnated, and their axons run vertically through the outer nuclear layer. The axons of the oblique cones (o), recognizable by the position of their nuclei, all run sideways in the same direction. (*b*) A small group of impregnated receptor axons, including that of an oblique cone, sketched in vertical profile. (*c*) The horizontal aspect of their axons reconstructed from serial sections, and related to the positions of other oblique cones (circles) in the receptor mosaic. (*d*) Oblique cone fibres (o) always run toward the retinal periphery, irrespective of their location in the eye. This *camera lucida* sketch superimposes a representation (dotted lines) of the orientation of the ganglion cell fibres which could be seen by phase contrast deeper in this impregnated piece of retina.

DESCRIPTION OF PLATE 4

Representative horizontal plane micrographs of pedicles belonging to the four different types of cone cells. Aldehyde prefix and lead section staining.

FIGURE 30. Principal cone pedicle

FIGURE 31. Accessory cone pedicle

FIGURE 32. Single cone pedicle

FIGURE 33. Oblique cone pedicle.

These pedicles, all cut at approximately equivalent levels, in the same retinal area, differ in size, in the number of horizontal cell (h) and bipolar (b) processes they contain, and in the number of synaptic ribbons (sr) they have. Otherwise, the general nature of their ultrastructure is the same. Notice that usually the bipolar and horizontal cell process profiles can be distinguished by their size and cytoplasmic contents, and that both 'dyad' (Lasansky 1971) and triad arrangements can be seen at some of the synaptic ribbons. (Magn. × 18000.)

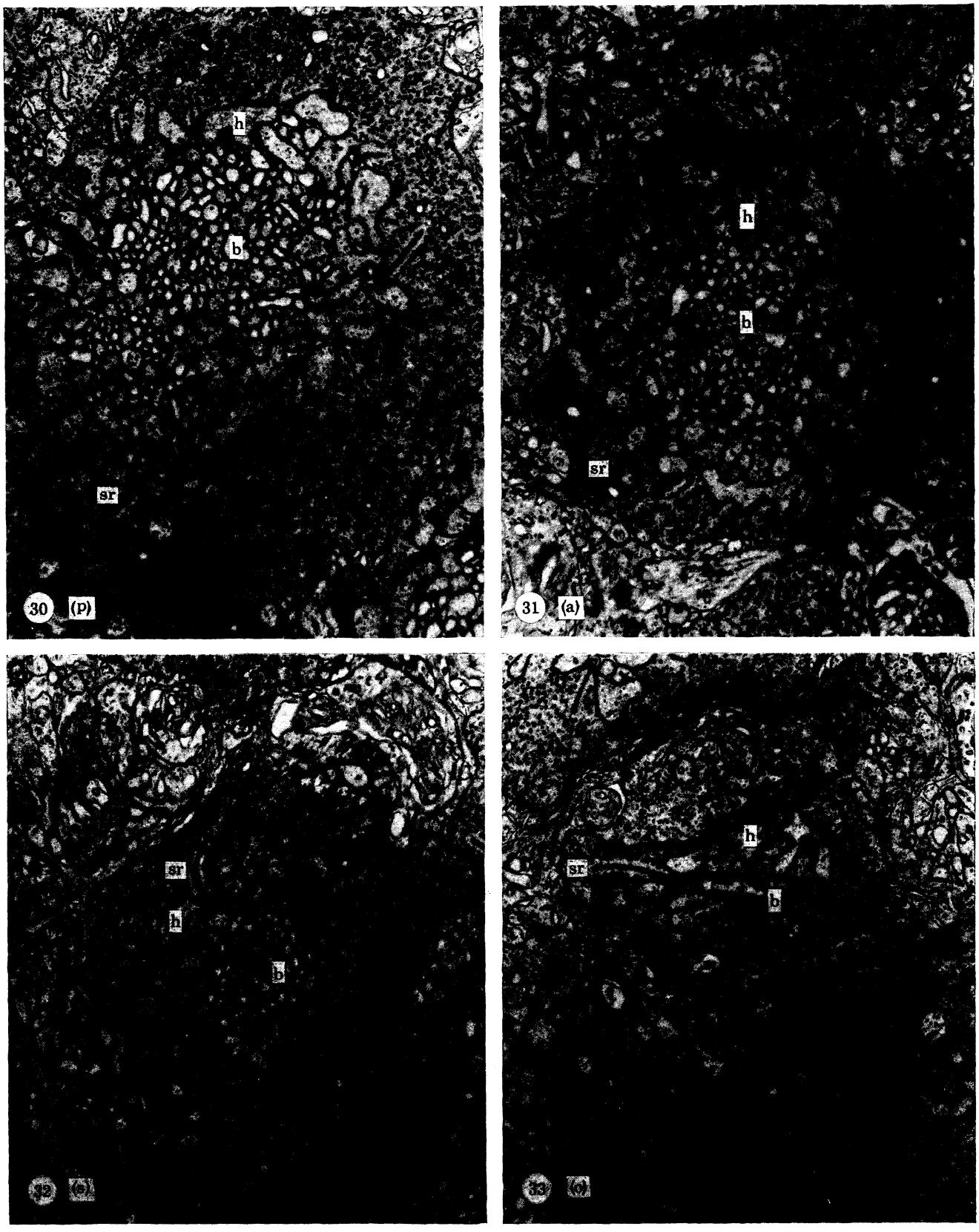

FIGURES 30–33. For description see opposite.

(*Facing p.* 86)

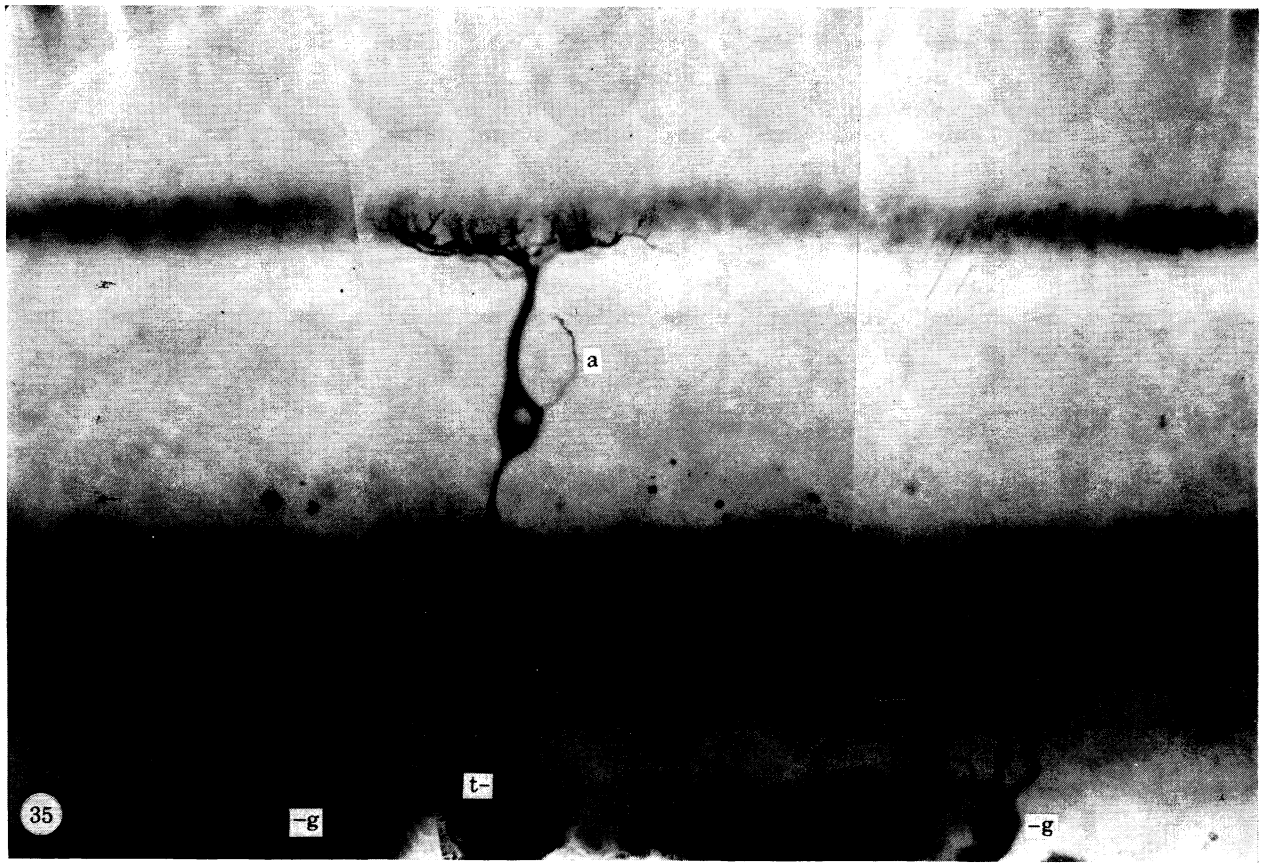

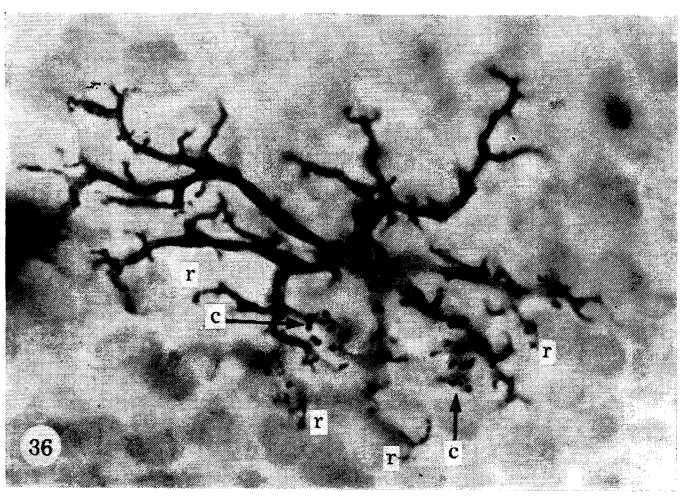

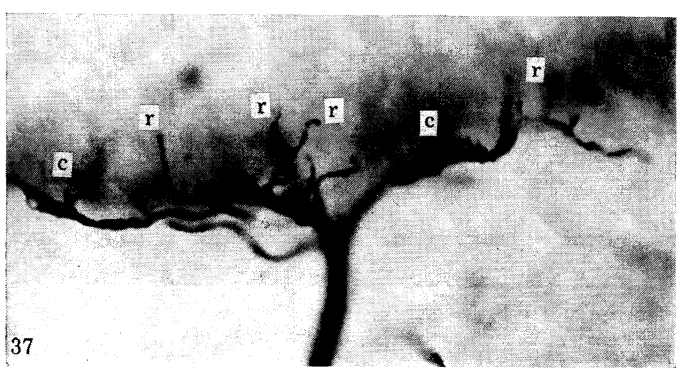

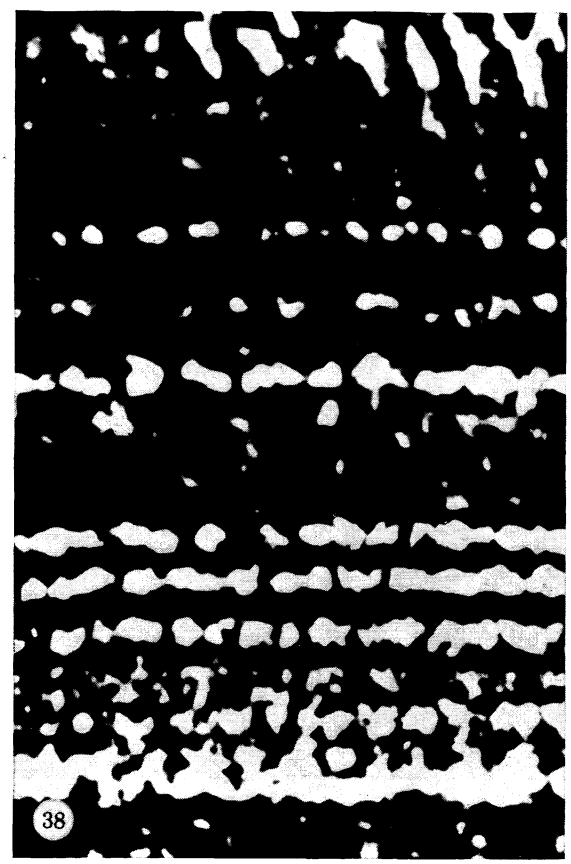

el
on
op
in
1
↑
ip
↓
6
g

el
on
op
in
1
2
3
4
5
6
g

FIGURES 35–38. For description see opposite.

Schwalbe rods are they identified with a named receptor species. Their axons run some distance sideways before terminating in the outer plexiform layer, and, in the rudd this displacement is roughly the same as the separation of adjacent oblique cones in their relatively regular retinal lattice (figure 9*c*).

An attempt was made to discover whether in fact they terminate beneath the mosaic station of a neighbouring cone of the same type, by serial sectioning in the horizontal plane to recover the course of the axons relative to the receptor lattice. Such reconstruction was practicable only in one case, shown in figure 34*b*, *c* where the axon concerned projected in the right direction and over the correct distance to terminate beneath a neighbouring oblique cone. The impregnated receptors were sketched in vertical profile by *camera lucida* (figure 34*b*) before serial sectioning. The sections were photographed and the profiles of the cones and their axons were traced from the micrographs, and superimposed (figure 34*c*) by reference to the edge of the block and the vertical projection of one of the other impregnated cones.

Further reconstructions of this sort were not achieved, but it was possible to show that oblique cone axons side-step in a particular retinal direction. Irrespective of their position in the eye, they always point away from the central area and toward the retinal margin. Figure 34*d* is typical of their arrangement in a number of preparations where they were alined with the ganglion cell fibres which could be seen in the retina by phase contrast microscopy. Perhaps it is no coincidence that this retinal direction is that of the growth axis of the cone mosaic (see figure 9 and text).

No good explanation for this curious projection of the oblique cones has come to mind. In searching for one, it is worth bearing in mind that, while Cajal's (1892) observations indicate the occurrence of these elements to be widespread among the lower vertebrate groups; in fish, at least, they are the smallest, most sparsely distributed (table 1 and text) and least richly innervated (table 3) of all the cone types, and tend to disappear from the retina with increasing age (Fürst 1904; Lyall 1957*a*). This stricture particularly applies to any speculation that they might be the substrate for the apparent 680 nm receptor process found in some cyprinid retinae (Naka & Rushton, 1966*c*; Daw & Beauchamp 1972). Perhaps they might participate in some lateral interaction concerned, say, with the analysis of motion or contour, though this seems unlikely, since the direction, relative to the *visual* world, in which they 'dress' varies all over the retinal surface. Another possibility is that the course of their axons is determined by some

---

Description of plate 5

Bipolar morphological characteristics in the light microscope. Aldehyde prefix, light osmication and multiple Golgi-impregnation.

Figure 35. The relation of a *rod bipolar* cell (see also plate 7) to the major layers of the retina. Numbers on the vertical scale (right) indicate the location of the proximal and distal strata of the inner plexiform layer (ip) (compare with figure 38). g, ganglion cells; t, bipolar terminal; a, bipolar accessory process (see page 90); el, external limiting membrane; on, outer nuclear layer; op, outer plexiform layer; in, inner nuclear layer. (Magn. × 750.)

Figures 36 and 37. Higher magnification views of the horizontal and vertical profiles, respectively, of the *rod bipolar* dendritic field. Single contacts with rod spherules (r) and multiple contacts with cone pedicles (c) can be distinguished. In figure 36, the faint outlines of cone pedicles appear as grey circles. (Magn. × 1500, × 1700 respectively.)

Figure 38. This is a phase contrast micrograph of a thick vertical slice of Golgi-impregnated retina (in which no cells were stained) to demonstrate the stratification of the inner plexiform layer. The vertical scale is identical to that in figure 35, and labelled in the same way. (Magn. × 750.)

developmental mis-specification of the identity of these cones. Perhaps, as their axons differentiate, the oblique cones 'think' that they belong not to the unit of the cone mosaic in which they are located, but to the one next generated by cell division in the peripheral growth zone from which they have themselves just originated. But without knowledge of the detailed cell lineages of the cones, it is not possible to express this idea less colloquially.

4. Patterns of synaptic connexion between receptors and bipolar cells

A. Bipolar morphology

(*a*) *Introduction*

The main concern here is to describe the selectivity with which bipolar cells connect to the rods and the different kinds of cones, and in the extent to which any such order may reflect what is known of the peripheral processing of colour information in the retina. However, as patterns of synaptic connexion in the outer plexiform layer were mapped, it became clear that the specific inputs the bipolar cells receive are firmly correlated with other more general features of their morphology at the level of the light microscope. Analysing the non-specific ratios of amacrine and bipolar cell synaptic input, West & Dowling (1973) have shown in different terms, the same to be true for most (but not all) morphological classes of ganglion cells in the mammalian retina. Most of these distinctions between the fish bipolar cells are descriptive, and therefore less likely to fall into any framework of functional interpretation than the patterns of synaptic connexion with the receptors which they apparently reflect. Nevertheless, to recognize them is useful in more than one way.

At an important practical level, of course, such anatomical features of the bipolars enable them, once their connectivity with the receptors has been determined, to be recognized again by light microscopy of silver-impregnated or Procion-injected material alone. It will be seen that some of the rudd bipolar cells analysed here can confidently be identified with neurons recorded and dye-marked in the goldfish and carp retina (Kaneko 1970; Toyoda 1973). Secondly, the morphological variety of the bipolar population affirms that there is a definite *organization* to retinal connectivity at this level, and that to map bipolar cell connexions in the outer plexiform layer is not merely to undertake an open-ended survey of a population of neurons that, between them might make all possible, or no particular, patterns of synapsis with the different receptors.

(*b*) *Observations*

(i) *Appearance and terminal destination*

Accordingly, before the dendritic tree of each bipolar cell was sectioned for electron microscopy, two general aspects of its morphology, illustrated in plate 5, were examined and recorded. Firstly, in vertical profile (figure 35, plate 5), the cells differ in their process and soma diameters, and in the shape and size of their terminals in the inner plexiform layer. Also, differences in the horizontal profile (e.g. figure 36, plate 5) appearance of the bipolar dendritic trees more directly reflect the various ways in which their synaptic processes sample the array of receptor terminals. The particular *form* of the dendritic fields shown in figures 36 and 37, plate 5, is clearly related to the connexions this cell type makes with rods, and its additional intermittent sampling from cone pedicles.

Secondly, the bipolars can be classified according to the levels of the inner plexiform layer in which their synaptic terminals are located. Usually five, and sometimes more, strata have been recognized in the inner synaptic layer of non-mammalian vertebrate retinae (Cajal 1892; Boycott & Dowling 1969; Wagner 1973*a*, *b*) and of certain placentals (see, for example, West & Dowling 1973), each of which contains the dendritic ramifications of at least one ganglion and amacrine cell type. Individual ganglion cells, of which there are many types, may ramify either in one stratum or in combinations of up to three (Cajal 1892; West & Dowling 1973), and the extents of their fields vary widely between types. Amacrine cells are most frequently uni- rather than multistratified (Cajal 1892; Polyak 1941; Wagner 1973*a*), and the pattern and extent of their dendritic branching varies widely between strata, and also within them. In one of the strata of the fish inner plexiform layer, for instance, Cajal (1892) recognized three quite distinct kinds of amacrine cell ramification. In addition there are many 'diffuse' forms of both amacrine and ganglion cells whose dendritic ramifications are not obviously restricted to particular inner plexiform strata (Cajal 1892; Boycott & Dowling 1969). It is worth remarking that although Cajal's drawings of the fish retina do not show quite as spectacular stratification of neuronal processes in the inner plexiform layer as those, for example, of lizard material, there is abundant evidence in the literature for highly ordered layering, not only of ganglion and amacrine cell dendrites (see, for example, Wagner 1973*a*; Hibbard 1971), but also of bipolar terminal swellings (Vrabec 1966; Goodland 1966) in a variety of fishes.

It is a widely accepted generalization that the feature detecting operations achieved by different ganglion cells result in part from the configuration of their dendrites in different strata of the inner synaptic layer (cf. Lettvin, Maturana, Pitts & McCulloch 1961; West & Dowling 1973), although the rigorous evidence that this is so (Pomeranz & Chung 1970) does not permit function to be related in any detail to morphology. To this extent at least, the strata which the synaptic terminals of the various bipolars address must be as important a characteristic of their participation in retinal function as the detailed patterns of input which they receive from the receptor layer.

In the rudd, the synaptic terminals of impregnated bipolar cells usually appeared as discrete swellings with consistent locations in the depth of the inner plexiform. For example, the cell shown in figure 35, plate 5, ends deep in the layer, close to the ganglion cell bodies; others had multiple terminals at more than one level. Stratification of the inner plexiform layer is not obvious in thin sections of the retina, but could be discerned rather clearly by phase contrast microscopy of thick vertical slices of some of the Golgi-impregnated material. There are six strata in all (figure 38), of which the distal three and the proximal one are the most prominent. They owe their visibility to alinement of the bipolar terminals; for example, the outlines of the terminals of the class of large bipolars can quite clearly be seen in stratum 6 (figure 38).

It was possible to allocate the terminals of named bipolars to numbered inner plexiform strata (figures 35 and 38, plate 5), either directly in this way, or more usually, since the thickness of the synaptic layer varies surprisingly little over wide retinal areas by measurement from its proximal and distal boundaries. Also, in material where numbers of neighbouring bipolars were impregnated, stratification could be distinguished from the alinement of their terminal swellings (figure 39). Bipolars which ended in the three proximal strata were those most frequently impregnated, and the bistratified variety (b) shown in figure 39 was common enough often to provide a reference for the stratification where it was otherwise ambiguous.

The Golgi impregnation, therefore, seems to be selective for cell types *within* neurone classes, a point that should be borne in mind in numerical interpretation (see, for example, Wagner 1973*b*) of the retinal cell populations.

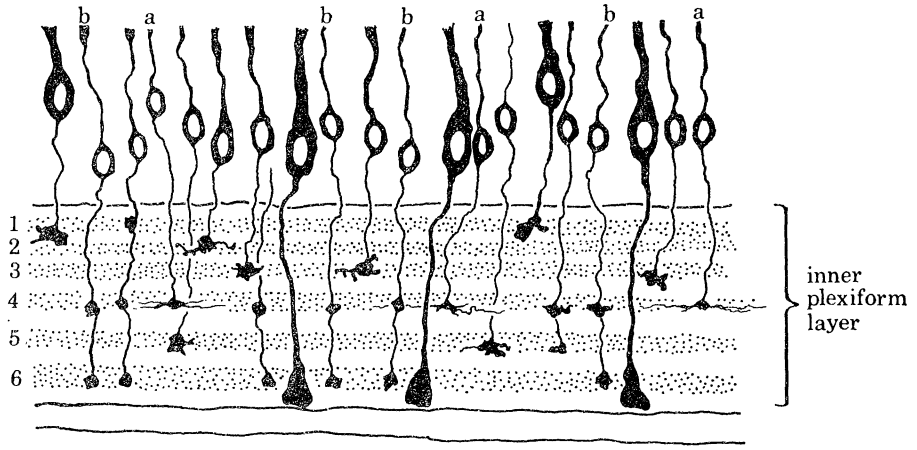

FIGURE 39. These bipolar cell profiles, drawn by *camera lucida* from the same impregnated retina, are superimposed to show the way in which the axon terminal swellings of the different morphological types registered in depth with one another and with the numbered strata of the inner plexiform layer. In most cases (e.g., b), the synaptic terminals appear as simple swellings, of different sizes, according to cell type. Some bipolar terminals (*a*), however, had small dendritic ramifications in the plane of the inner plexiform strata: the instances shown were of diameter approximately 30 μm.

(ii) *Bipolar accessory processes*

The bipolar shown in figure 35, plate 5, has a collateral process which ascends from the soma to the outer plexiform layer and then runs in a single direction out of the focal plane, beyond the limits of the conventional dendritic field. These *accessory processes* were encountered quite often, usually only impregnated over a small part of their maximum length. Not all bipolar types were seen to possess them, which may just reflect capricious impregnation, and among those that did, there was never more than one arising from each. It was not possible to establish their destination in the outer plexiform layer, and if they possess specialized endings, these were not revealed. Their lateral extent was (maximally) greater than the lateral displacement of the axons of the miniature cones. In their departure from the more conventional *concentric* arrangement of retinal dendritic processes, the accessory processes share this characteristic of radial asymmetry with certain of the basal processes of the cone pedicles (see figure 70, and text) and with horizontal cell axons (Cajal 1892), and are mentioned here because they appear not to have been reported elsewhere in the literature.

B. Connexions of the different bipolar classes

(*a*) *Introduction*

In teleosts, Cajal (1892) distinguished two main types of bipolar cells: neurones with massive somata and processes contrast with others (figure 40) whose processes are altogether more delicate. He called these cells simply large and small bipolars, but in discussing their properties he felt confident to describe the former as specific for the rods in the highly duplex retinae he studied, and the latter as connecting only to cones. This was possible because of the more sclerad location of the rod terminals; dendritic processes of the large bipolars leave the plane

of the outer plexiform and ascend to their level, while those of the small bipolars do not penetrate beyond the sheet of cone pedicles that forms its upper boundary (figure 40).

It was only in fish and mammalian material that the rod and cone terminals were clearly separated in depth in this way, so only in these animals could he refer to the large bipolars, found in both, as specific for rods, and, in the case of mammals, name them as such. Stell (1967), in his Golgi-e.m. study of the goldfish retina, recognized the same two kinds of bipolar that

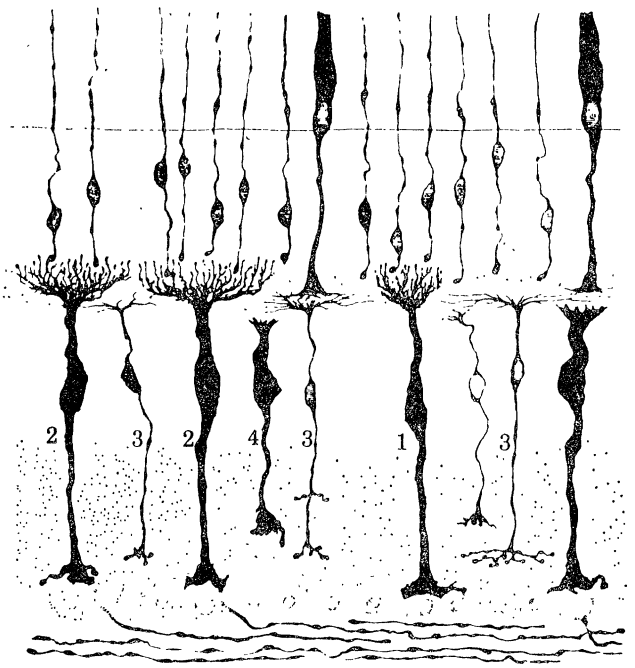

FIGURE 40. Cajal's (1892) drawing of the bipolar cells in the perch retina (relabelled). 1 and 2 are the 'large bipolars destined for rods': notice their different dendritic field sizes, and compare them with the cells in plates 6 and 7. The cells labelled 3 are the 'small bipolars destined for cones', which resemble those shown in plates 8 and 9 in their filamentous structure. The bipolar labelled 4 is referred to on page 97.

Cajal distinguished in a number of widely separated representatives of teleost phylogeny. He confirmed that the small bipolars only synapse with cones, but showed that the large cells as well as connecting to the numerous rods within their dendritic fields, also receive input from cones, in which respect they differ from the morphologically similar rod bipolars of the mammalian retina (Kolb 1970; Boycott & Kolb 1973).

Both these cell types were impregnated in the rudd retina, and their connexions with identified receptor terminals were studied in the electron microscope. For each, more than one sub-class was recognized either on grounds of specific receptor input or general morphology. In addition, there were morphologically intermediate cells with a mixed receptor input distinct from either of them.

(*b*) *Observations*

(i) *Criteria for synaptic connexion*

The dendritic trees of impregnated bipolar cells were sectioned in the horizontal plane for electron microscopy, so that the profiles of the cone pedicles could be identified by comparing their relative locations with the layout of the receptor mosaic above the external limiting membrane (cf. figure 29 and text). Synaptic connexion between particular receptor terminals

and the bipolars was judged to exist when silvered processes were seen clearly within the outline of their synaptic cavities. In assigning the connexions, no account was taken of the finer synaptic structures of the terminals, though the silvered processes were often noticed occupying the central station of the 'triads'.

To use this single criterion for functional connexion, of course, evades any ultrastructural issue of what detailed relations between the cells really constitute physiological synapses. It is necessary, though, to state some justification for this unsophisticated index. First of all, no silver impregnated bipolar cells were found which lacked invaginating connexions with the receptor terminals. This suggests that the fish lacks a separate class of bipolar cells which make exclusively basal apposition contacts with the pedicles, like those in turtle (Lasansky 1969) or in the mammalian retina (see, for example, Missotten 1966). Furthermore, it was noted earlier (page 84) that no basal junctions were seen by conventional electron microscopy on the external surfaces of the fish pedicles, which makes it unlikely that the bipolars have mixed apposition and invaginating connexions with the receptors. Secondly, that different bipolars *do* have quite characteristic patterns of invaginating contact with the receptors in itself confirms the functional status of those connexions. Finally, it will be shown that the physiologically measured scotopic and photopic spectral sensitivities of one bipolar type exactly agree with those inferred from the pattern of its invaginating connexions with the receptors (page 111).

Although the detailed mode of termination of the invaginating processes was not usually recorded during scrutiny of the e.m. sections, it will be possible to give statistical evidence that most, if not all, of them associated with the synaptic ribbons (pages 108–109).

(ii) *Bipolar nomenclature*

Although most of the bipolar cells to be described can be identified in the literature, considerations both of their dendritic field dimensions and their connectivity with the receptors make it desirable to rename the two existing classes of fish bipolars, and necessary to erect a new one.

Therefore, Cajal's prominent 'large' fish bipolar cells (figure 40) are referred to as *rod bipolars* (cf. Parthe 1972). This takes cognizance of their numerically predominant scotopic input, and serves to emphasize their morphological similarity (possible homology) with the exclusively rod connected rod bipolars (Cajal 1892; Boycott & Dowling 1969; Kolb 1970) in mammals. However, in the fish, the following caveat must straightaway assume equal emphasis; unlike mammalian rod bipolars they do not receive synaptic input *only* from rods, but also from some of the cones (cf. Stell 1967). Nor are they the only bipolars to be connected to the rods.

Likewise, it is desirable not to follow Cajal (1892) in naming the 'small' bipolars (figure 40) according to their size, for despite their delicate structure, their dendritic fields can be very extensive (Parthe 1972). Because these cells were found to be connected exclusively to cones, and in the event, each to particular types of cones, they are called *selective cone bipolars.*

The third (new) class of bipolars receives input both from cones and rods, but differs from the first one (rod bipolars) in that the photopic input is provided by more than one (*though not all*) species of cones. Acknowledging this, and the relative numerical subordinacy of their rod input, they are called *mixed cone bipolars.* There are also some cells which receive input from all three main cone types. The examples which were seen had dendritic fields of intermediate size, but because they were not properly identified by light microscopy, they are not considered further here.

Naturally, one hesitates to complicate the extant terminology, and is aware that these class names do not comprehensively describe the cell characteristics they invoke. They are chosen more to draw attention to those features of bipolar organization which are likely to be important for retinal function. In describing observations, the cones are referred to by their anatomical names: in discussing implications of their connexions they are often called red or green cones, etc., in accordance with the identities argued in §2.

(iii) *Rod bipolars*

Perhaps intentionally, Cajal's drawings of his large bipolars (figure 40) indicate that their dendritic fields may vary in size, and Parthe (1972) has also recently subdivided them on this basis. In the rudd retina also, there are large and small field rod bipolars, which have an overlapping spatial distribution in the retina, and their synaptic input from rods and cones has been characterized in detail. It will be important to stress features of their morphology which indicate them to be functionally distinct, rather than extreme examples from a spectrum of dendritic field size, because it turns out that they both receive the same pattern of input from the different receptors and both have the same synaptic address within the inner plexiform layer.

(1) *Narrow field rod bipolars.* Plate 6 shows the light and electron microscopic analysis of this bipolar category. Figures 43 and 45 are *camera lucida* sketches of its vertical and horizontal profiles, viewed under oil immersion before thin sectioning in the plane of the outer plexiform layer. It is characteristic that the ascending synaptic processes from the outer plexiform dendrites are dense and can clearly be seen to penetrate up to the level of the rod spherules where they terminate as small looped figures. Also, the soma, vitreal process and axon are stout, and as Cajal noted, the axon terminal is large, compact and located in the deepest stratum (no. 6, figures 35 and 38, plate 6) of the inner plexiform layer. Cajal (1892) stated that they contacted the somas of the ganglion cells; in fact there is a thin intervening sheet of particularly fine neuropil processes in between.

As well as innervating most, if not all, of the rod terminals within their dendritic fields, the narrow field rod bipolars, as Stell (1967) showed, are also connected to cones. Figure 44 shows the outlines, in the horizontal plane, of the cone pedicles within the dendritic field of this cell. It is traced from electron micrographs at this level, and reduced to the same scale as the *camera lucida* sketches in figures 43 and 45. Silvered invaginating processes, indicated in this drawing, as in the similar reconstructions in plates 7–10, by filled squares, were found only in the synaptic cavities of principal cone pedicles. This selectivity for principal cone and rod terminals is illustrated at higher magnification by the slightly oblique electron micrograph of figure 41. Several silvered processes are seen in the central principal cone pedicle, and none in closely adjacent accessory and single cone pedicles. Only one dendritic process invaginates each rod spherule, though frequently two profiles are seen in single sections (figure 41) because of the characteristic looped form of the endings inside the synaptic cavity (figure 42).

Seven examples of this bipolar type (which was that most frequently impregnated in the retinal material available) were analysed in this way, and all of them were found to receive their input exclusively from rods and principal cones. Cone terminals were recognized according to type by comparing their locations with those of the receptors distal to the external limiting membrane (§3(*b*)). The rather narrow dendritic fields of these cells embraced four or five principal cones only, and where (in two instances) there were 'free' principal elements

(§1(*b*)(ii)) within their margins, they also were innervated. This is one further reason for regarding free and paired principal cones as chromatically equivalent to one another (see page 69).

This bipolar type, then, which is richly connected to rods, also receives (photopic) input from the most numerous and largest of the cones, which have been argued (§2) to constitute the red mechanism.

(2) *Wide field rod bipolars.* Plate 7 shows the morphology and synaptic connexions of this rather similar cell type, an example of which also appears in figures 35–37, plate 5. It is characteristic that the axon terminal swellings of these cells, located in the deepest stratum (no. 6) of the inner plexiform layer, are less precisely restricted in depth than those of the narrow field rod bipolars, as it is that their dendritic fields in the outer plexiform layer are much wider (cf. figures 45 and 50 in plates 6 and 7). They do not innervate all of the rod terminals within the outlines of their outer plexiform fields, since their dendrites are more widely spaced than those of the small field cells. Sometimes, they had accessory processes (figure 35, plate 5).

The cone connectivity patterns of three examples were examined electron microscopically, and that of one of them is shown in figure 51, plate 7. Like the narrow field rod bipolars, it connects exclusively to principal cones; again, while several synaptic processes invaginate the pedicles of these cones, just one enters each rod spherule (figures 47 and 48, plate 7). The other two cells contacted between 15 and 20 principal cones, and also innervated the pedicles of two or three accessory cones. Though it is impossible to prove this in retrospect, it is most unlikely that these minority connexions belonged to some other, unnoticed, neuronal processes

---

Description of plate 6

Narrow field rod bipolars.

Plates 6–10 give information about the different bipolar classes in a more or less standard fashion. There are *camera lucida* sketches of examples of each cell type in horizontal and vertical profile, and the stratum of termination in the inner plexiform is indicated (e.g. S6 in figure 43). Tracings from electron micrograph montages show, at the same scale, the location of the cone pedicles within their dendritic fields and indicate with filled squares which of them are innervated, and which are not. Small areas of the original electron microscope montages are shown at higher magnification mainly to record the quality of the material upon which assertions about synaptic connectivity are based.)

Figure 41. Oblique section plane through the layer of receptor terminals. The silvered invaginating processes of a narrow field rod bipolar (some of them are indicated with white rings) show in the synaptic cavities of principal cone (p) pedicles and in rod spherules (r), but not in closely neighbouring accessory (a) and single (s) cone pedicles. (Magn. × 8500.)

Figure 42. This electron micrograph shows the looped configuration adopted by the impregnated processes of these bipolars where they invaginate rod spherules (r) (cf. also figure 46). A basal process (b) from this spherule contacts (arrow) another nearby rod terminal. (Magn. × 18000.)

Figure 43. *Camera lucida* sketch of the vertical profile of a narrow field rod bipolar. The dashed horizontal line indicates the distal boundary of the inner plexiform layer (ipl). (Magn. × 1100.)

Figure 44. The outlines (horizontal plane) of the cone pedicles within the denditic field of the cell of figure 44. Double cone pairing is indicated by the short bars, and smaller profiles represent single and oblique cone terminals. The pedicles which were innervated by the bipolar dendrites are identified with filled squares; they all belonged to principal cones. (Magn. × 1100.)

Figure 45. The horizontal profile of the dendritic tree of this bipolar, drawn by *camera lucida*. (Magn. × 1100.)

Figure 46. This light micrograph shows the synaptic processes of a narrow field rod bipolar in the layer of rod spherules, isolated in a thin horizontal section. Compare their characteristic appearance with that of the synaptic processes of the large field rod bipolar (figure 52, plate 7). (Magn. × 2500.)

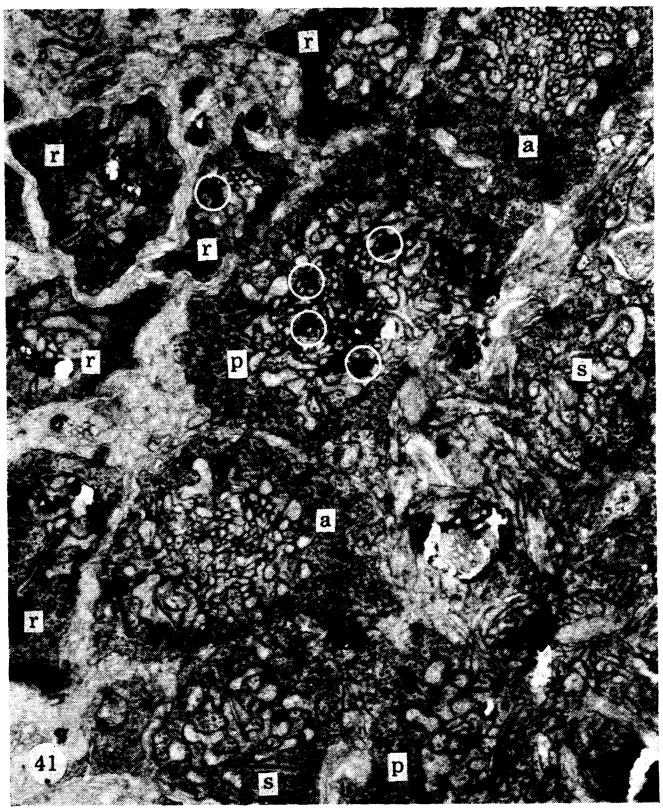

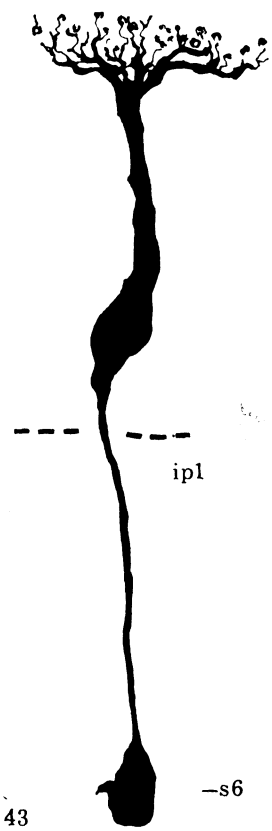

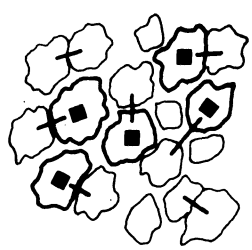

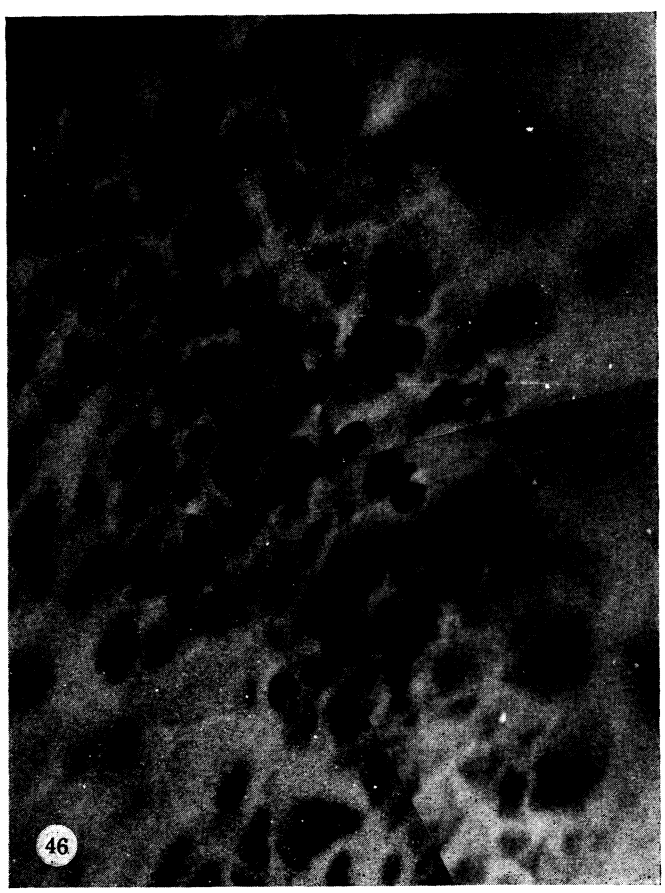

FIGURES 41–46. For description see opposite.

(*Facing p.* 94)

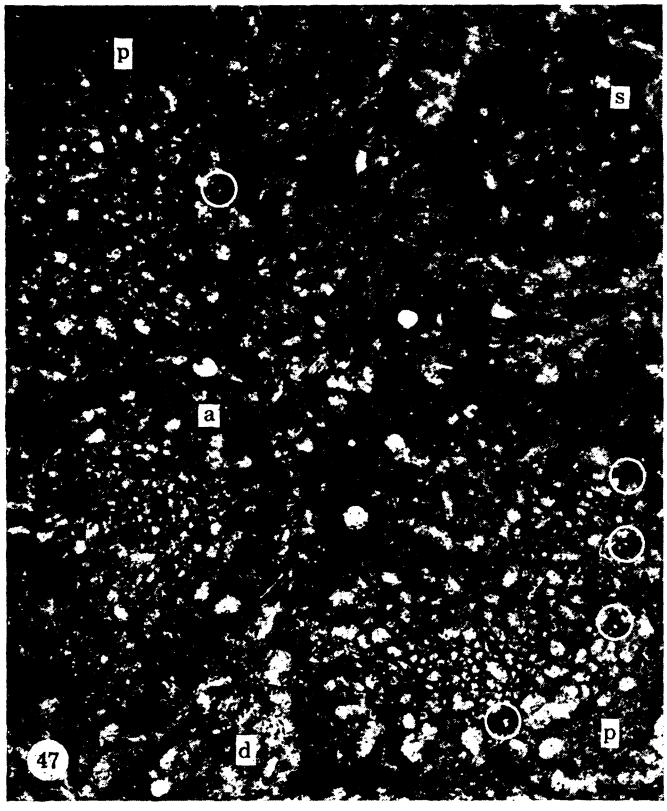

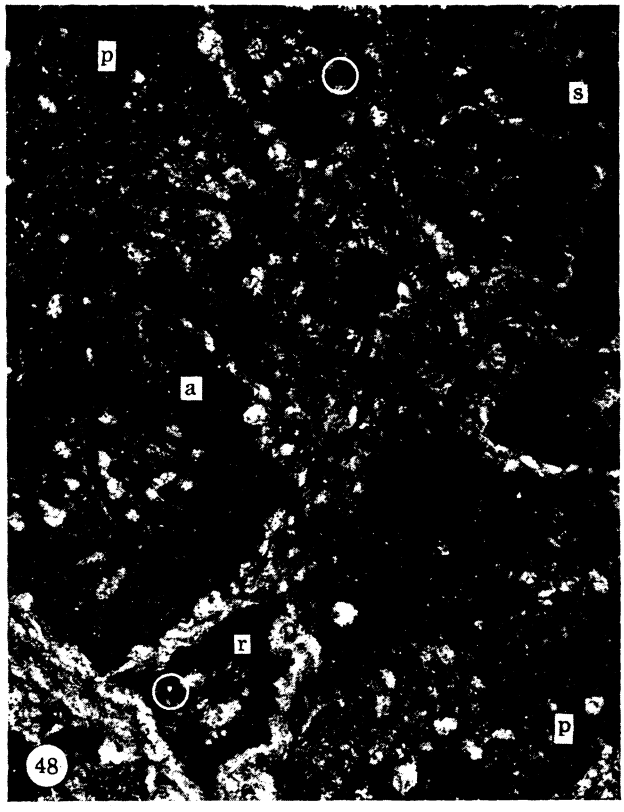

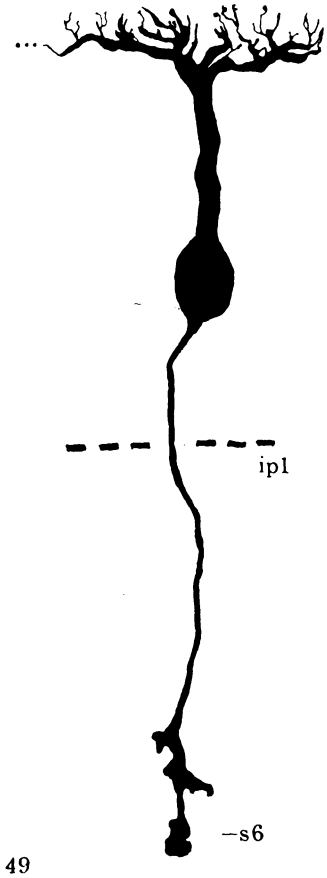

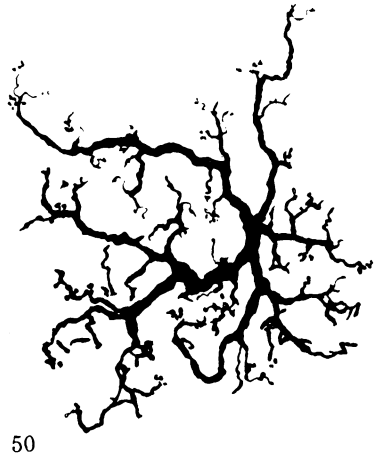

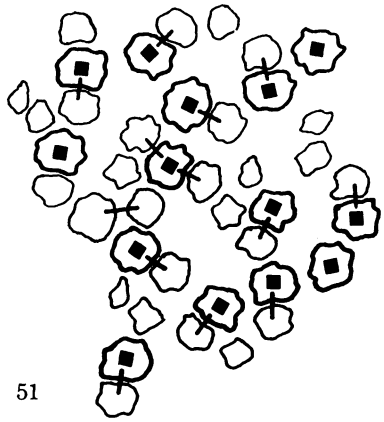

FIGURES 47–52. For description see opposite.

within these bipolar dendritic fields. It seems likely that they represent a degree of lability in the morphogenetic specification of patterns of synaptic connexion in the retina (see also page 106).

This apart, it can be said of both categories of rod bipolar that their synaptic destination is the same, and that they both receive input from rods and from principal cones and no other receptors. Examples of both cell types were impregnated in closely neighbouring retinal areas, so that the difference between their field sizes is unrelated to retinal position (cf. Parthe 1972). The two cell types differ from one another most strikingly in the form of the synaptic processes they send to invaginate the terminals of the rods (figures 46 and 52, plates 6 and 7). Those of the small field bipolars are thick, and terminate in the spherules as incomplete loops (figures 42 and 43, plate 6), while the processes of the large field cells are finer and relatively straight (figure 49, plate 7). It is likely that the looped appearance of the small field bipolar processes is a consequence of their occupying a substantial length of the curved presynaptic ribbon in the spherule, since in conventional e.m. sections (e.g. figure 25, plate 3), the triad central process profile is most usually of the large diameter characteristic of these cells.

This consistent difference in the synaptic arrangements of the two kinds of rod bipolar seems rigorous ground for what otherwise might be a contentious distinction between them. But beyond observing that the more extensive synaptic invaginations of the small field cells make it likely that individual rods exert a more powerful influence on them than upon the large field bipolars, there is no scope for speculation upon its functional implications.

(iv) *Selective cone bipolars*

The strikingly different appearance of this class of cells (small bipolars, cf. figure 40) is sufficient to suggest a distinct role for them in retinal function, and Cajal's (1892) observation that they connect only to cones has been confirmed by Golgi-electron microscopy (Stell 1967). Two variants were examined in the rudd retina, and their synaptic arrangements indicate that they comprise, or are a part of, a bipolar population whose members carry signals from the individual colour channels to particular strata of the inner plexiform layer. Neither type has the exact morphology (with respect, for example, to the levels of the inner plexiform layer they

---

Description of plate 7

Wide field rod bipolars.

Figure 47. Silvered synaptic processes (some of them marked by white circles) invaginate the pedicles of two principal (p) cones, coming into close proximity with the apical specializations of the synaptic ribbons (cf. figure 30, plate 4). Accessory (a) and single (s) pedicles in the vicinity are spared. (Magn. × 11000.)

Figure 48. The same retinal area earlier in the sequence of serial sections to show that other dendritic processes (e.g. that labelled d in figure 47) end higher up in the rod spherules (r). Other labels as in figure 47. (Magn. × 11000.)

Figure 49. Vertical profile of a wide field rod bipolar. Part of its dendritic tree (left) was obscured from this angle of view. (Magn. × 1100.)

Figure 50. The horizontal dendritic profile of the same cell. (Magn. × 1100.)

Figure 51. Cone pedicle outlines within the dendritic field of this bipolar traced from electron micrographs. Same scale as figures 49 and 50, and same notation as figure 44 in plate 6: only principal cone pedicles (filled squares) are innervated. The pedicle outlines are smaller since this is a different area of the retina.

Figure 52. Dendritic processes of a wide field rod bipolar ending in the rod spherules, isolated in a thin horizontal light microscope section. They are characteristically finer and simpler in their configuration than those of the small field cell shown in figure 46, plate 6.

address) of those illustrated by Cajal; nevertheless, the filamentous structure of their processes, and the width and radially symmetrical branching of their outer plexiform dendritic fields are sufficient ground to identify them with his 'small' bipolars.

(1) *Accessory cone bipolars.* The first type, whose analysis is shown in plate 8, made exclusive (or majority; see page 106) connexions with accessory (green, figure 24) cones. These cells (two examples were examined in detail) had synaptic terminals in strata 4 and 5 of the inner plexiform layer, and their characteristic morphology can easily be seen by comparing figures 54 and 55 in plate 8 with the drawings of the rod bipolar profiles in plates 6 and 7. Figure 57, plate 8, shows a small area of the layer of cone pedicles where the dendritic fields of an accessory cone bipolar overlapped with that of a narrow field rod bipolar, making it clear that this distinction of process size extends also to the dendritic branches that penetrate the pedicle synaptic cavities.

It is of interest to note that the morphology (e.g. branching pattern) of the dendritic field and the spacing of the visible sites of synaptic contact (figure 54, plate 8) directly and conspicuously reflects the punctate sampling of the array of pedicles which characterizes these accessory cone bipolars. This congruence of the light and electron microscope pictures of the synaptic field (figures 60 and 61 in plate 9 provide a better example) is reason to be confident in the completeness of the Golgi-impregnation and retrieval of synaptic processes in the e.m. Nevertheless, the bipolar illustrated in plate 8, as well as sending processes to most of the 30 accessory cone pedicles within the outline of its dendritic tree, also apparently innervated one single cone terminal (open square, figure 53, plate 8). As with the wide field rod bipolars which were apparently connected to one or two accessory cones in addition to their majority connexions with principal cones, it is not possible to rule out the intrusion of other neuronal processes into the area analysed, but that is certainly most unlikely (page 106).

(2) *Single cone bipolars.* Another bipolar type, similar in appearance to the accessory cone bipolar had synaptic terminals located in strata 1, 4 and 6 of the inner plexiform layer, and was connected exclusively to single cones (blue receptors, §2). The analysis of one of these cells is shown in plate 9; the *camera lucida* sketch of its dendritic tree horizontal profile in figure 61, illustrates particularly well how easily the *selectivity* of these cell's synapsis with the receptors can be recognized by light microscopy alone. Only one other example was examined in the electron microscope, and that incompletely; its connectivity also was exclusive to single cones. It would be pleasing to complete the picture by presenting a third cell type for the principal (red) cones, but in the material examined, there was no evidence that such exists. This might

---

Description of plate 8

Selective (accessory) cone bipolars.

Figures 53–55. The cone connectivity pattern and the horizontal and vertical profiles of a bipolar specific for accessory cone pedicles. The scale and notation are the same as those of the comparable drawings of rod bipolars in plates 6 and 7. Notice how some of the synaptic sites recognized by light microscopy (e.g. 1–5 in figure 54) were retrieved in the same relative locations in the reconstruction from electron microscopy (1–5 in figure 53). Apparently, though, neither the drawing of the dendrites nor the reconstruction of their connexions is entirely exhaustive. In addition to innervating 25 accessory cone pedicles, this cell synapsed with one single cone terminal (open square, figure 53). (Magn. × 11 00.)

Figure 56. Part of the montage on which figure 53 is based. Impregnated bipolar synaptic processes ringed, lettering as in figure 41, plate 6. (Magn. × 11 000.)

Figure 57. Shows a retinal area where the field of a narrow field rod bipolar (rb) innervating principal cones (p) or rods (r) overlaps with that of an accessory cone bipolar. The synaptic processes, visible in the accessory cone pedicle (a), of the latter are distinctly finer. (Magn. × 15 000.)

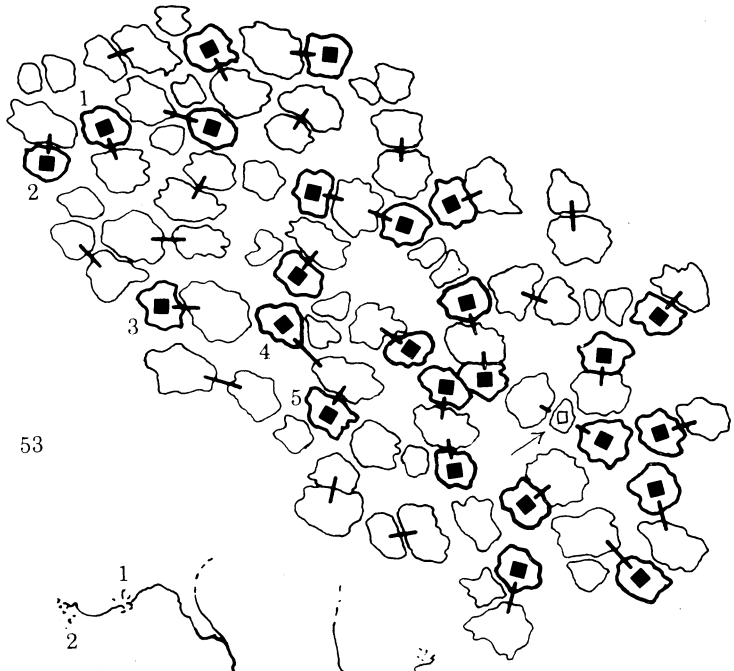

53

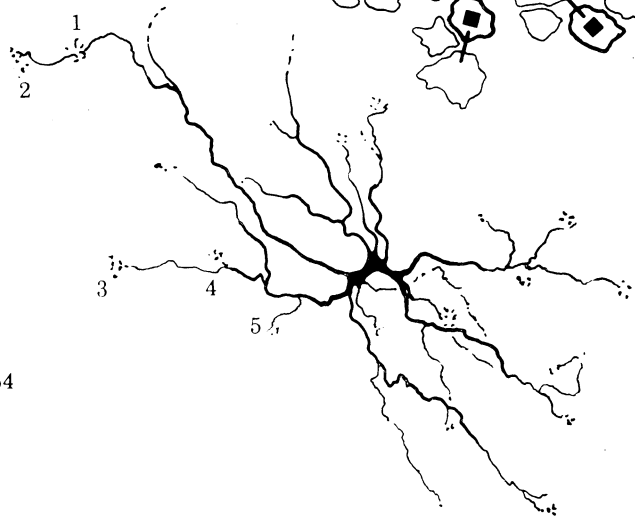

54

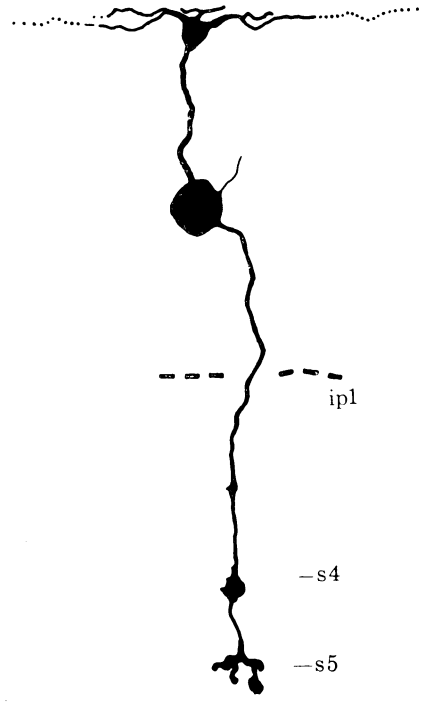

55

56

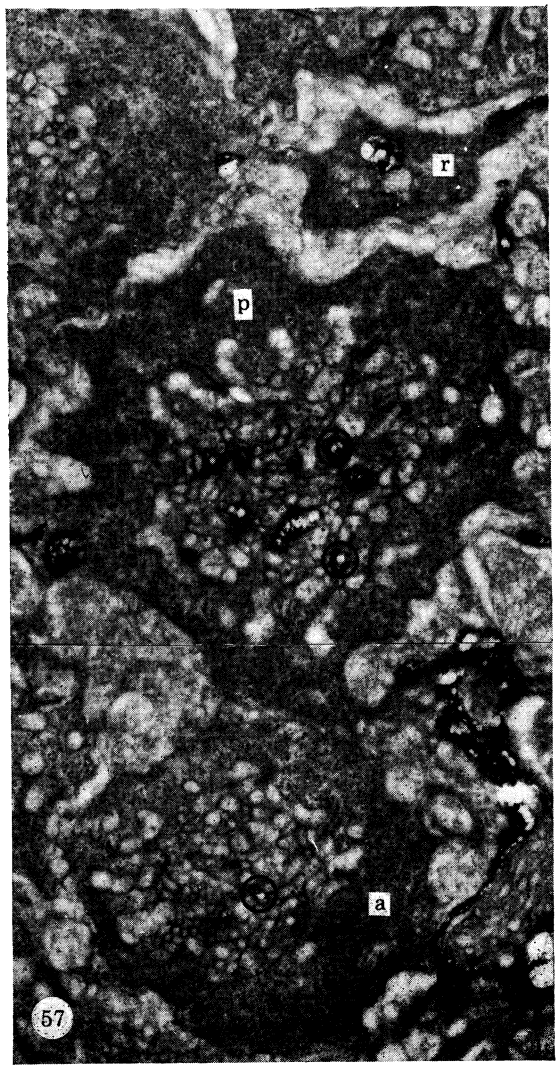

57

FIGURES 53–57. For description see opposite. (*Facing p.* 96)

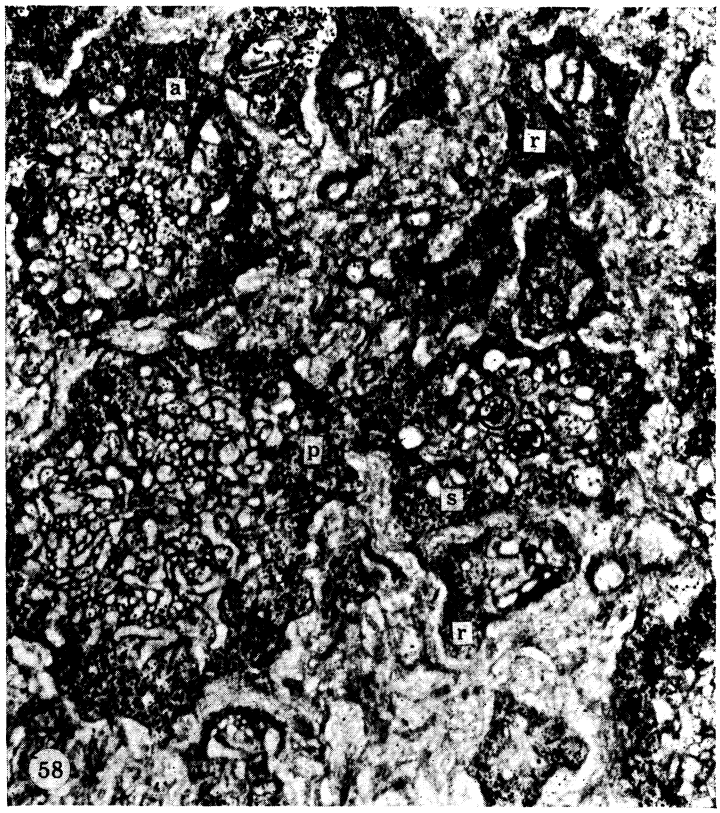

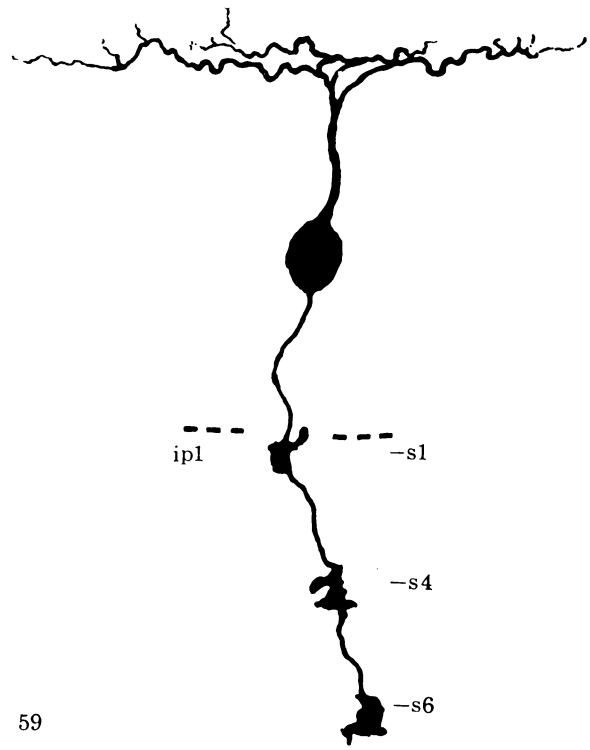

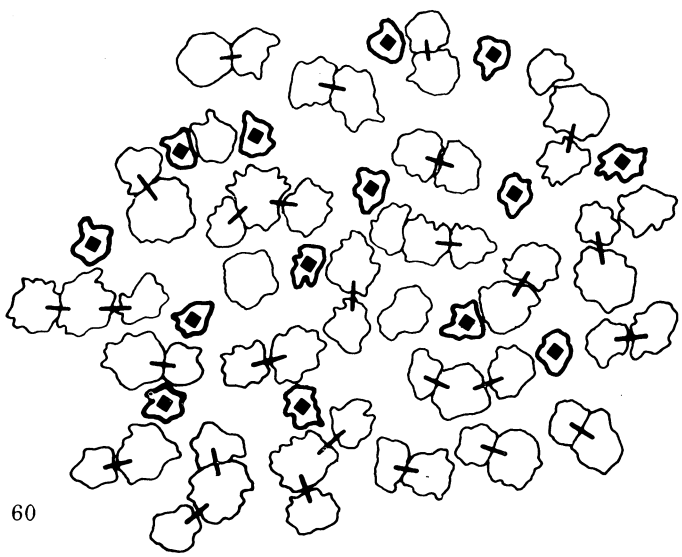

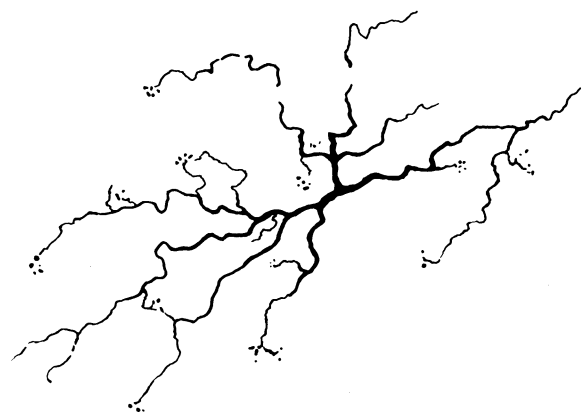

Selective (single) cone bipolars.

FIGURES 58–61. Analysis of the morphology and connexions of a bipolar specific for single cones; the scale and notation is the same as that used in comparable figures in plates 6–10. Figure 58 shows part of the array of pedicles drawn in figure 60, where a single cone (s) pedicle receives silvered processes from the bipolar (circles), but a principal (p) and an accessory (a) do not.

well be a sampling error, and there are certainly other sorts of these delicate bipolar cells (cf. figures 39 and 40) whose outer plexiform connexions were not examined.

The likelihood is that the selective cone bipolars are the only vehicle for transmission of information from individual cone species through the depth of the retina. They have the widest dendritic fields of all the cells encountered (see also Parthe, 1972), while those whose narrower fields should relay more acute spatial information receive synaptic input from combinations of cones rather than from single types.

(v) *Mixed cone bipolars*

Cajal (1892) remarked of his large bipolars in the fish retina (rod bipolars, here) that, while the majority of them had their terminal feet in the deepest level of the inner plexiform, he sometimes encountered examples which terminated in the more distal strata of the synaptic layer. His drawing (figure 40) shows one, but he unfortunately did not sketch in the appearance of its dendritic field.

In the rudd, a number of cells were observed which fall into a morphological category intermediate between Cajal's large and small bipolars (rod and the selective cone bipolars). They have thick vitreal processes, and fairly large somas located at the distal border of the inner nuclear layer. These features are not as marked as they are in the small field rod bipolars, and the dendritic processes are not at all as thick and prolific as they are in those cells. The two types observed had terminal swellings of intermediate size, either in stratum 1 or stratum 2 of the inner plexiform layer. Probably these cells are the same as Cajal's exceptional large distally addressed bipolars (figure 40(4)); it is interesting that the axon of the single example he shows has the narrow diameter characteristic of the cells seen in the rudd. This is one of the main features in which they differ from the rod bipolars (plates 6 and 7), and if the identification be correct, it speaks a lot for the impartiality of Cajal's draughtsmanship.

Plate 10 shows details of the morphology and receptor connexions of two examples of the mixed cone bipolar cell type. Their dendritic fields are slightly smaller than those of the narrow field rod bipolars, and it is characteristic that their synaptic processes are more sparse. The subtle features of appearance in which they differ (shape of perikarya, outline of terminals, etc.) should also be noted. The receptor connectivity of three examples were analysed, and in each case (two examples of the variety terminating in stratum 2 and one of that for stratum 1), they were connected to rods and to both principal and accessory cones (figures 65–67, plate 10). They did not innervate all of the rods within their dendritic fields (hence the sparseness of their ascending synaptic processes (cf. figures 62 and 64), which embraced 3–4 double cone pedicles.

Cells of this type were rarely encountered, but there are reasons for thinking that this is a caprice of impregnation and that they are in fact relatively numerous. First of all, their dendritic fields are the smallest of all the bipolars, which means, unless they sample the receptor array intermittently, that their packing density must be relatively high. Secondly, it is likely that they provide the dominant input for the two distal strata of the inner plexiform layer. With the exception of the single cone bipolars, no other cells were seen to be directed to these strata, and it is tempting to conclude that the prominence of these layers in phase contrast microscopy (figure 38, plate 5) is due to the large size of the mixed cone bipolar terminals located in them, just as that of stratum 6 is attributable to the rod bipolar terminals.

There are two other cell types which properly belong under the heading of mixed cone input,

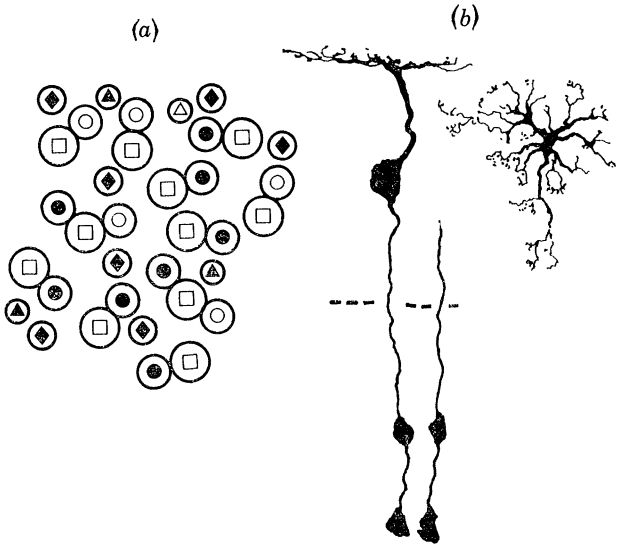

FIGURE 68. (*a*) The outer plexiform connexions of a bipolar cell type whose general light microscope morphology was not recorded. It connects (filled symbols) with accessory (○), single (◇) and oblique cones (△), and with a few rod spherules, but not with principal cone terminals (□). (*b*) The light microscopic appearance of a class of bipolars specific for principal and accessory cones, which also connects to a few of the rod terminals within its dendritic field. The morphology of these cells is intermediate between that of the mixed (plate 10) and the selective (plates 8 and 9) cone bipolars, and their axon terminals register with strata 4 and 6 of the inner plexiform layer (cf. *b* in figure 39). (Magn. × 700.)

neither of which was completely analysed. The first comprises a population of cells which terminated at two levels, strata 4 and 6, of the inner plexiform layer. These cells were one of the types most commonly impregnated, and their light microscope appearance (figure 68*b*) was more like that of the selective cone bipolars than the two types described above. However, their dendritic fields were significantly smaller, and their receptor input mixed. Partial reconstructions were made of the dendritic fields of three of these cells, all of them far from complete, but sufficient to show that these cells also connect to both principal and accessory cones, and to a small percentage of the rods within their fields.

In the preliminary report of this work (Scholes & Morris 1973), these cells (figure 68*b*) were placed in a separate class from the mixed cone bipolars which terminate in strata 1 and 2 of the inner synaptic layer (plate 10). The latter, on account of their small dendritic trees, were

---

DESCRIPTION OF PLATE 10

Mixed cone bipolars.

This plate shows two morphologically distinct bipolars from the same retinal area, which connect to principal and accessory cones, and to rods.

FIGURES 62–63. Morphology and cone connexions of a cell which terminates in stratum 2 of the inner plexiform layer. Notation and scale as in the comparable diagrams in plates 6–9.

FIGURE 64. Electron microscope section early in the series through the dendritic field of this bipolar, showing (e.g., circles) its innervation of rod spherules. (Magn. × 11000.)

FIGURE 65. Later section in the same retinal area, now at a level which shows the innervations (e.g., circles) of principal and accessory cone pedicles (a and p). Two single cones (s) however are spared. (Magn. × 11000.)

FIGURE 66. This bipolar terminates in stratum 1 of the inner plexiform (cf. figures 62–63).

FIGURE 67. Like the cell of figures 62–65, it innervates rods (r, insert), principal (p) and accessory (a) cone pedicles, but not single cones (s). (Magn. × 11000.)

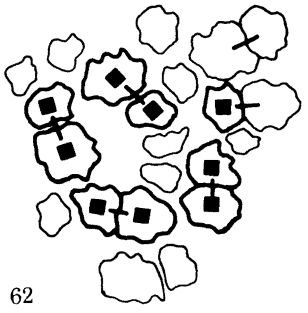

62

63

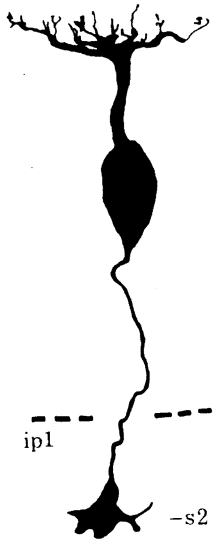

63

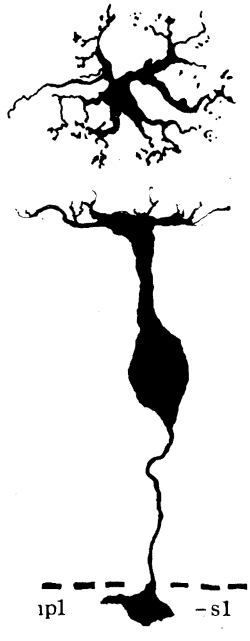

66

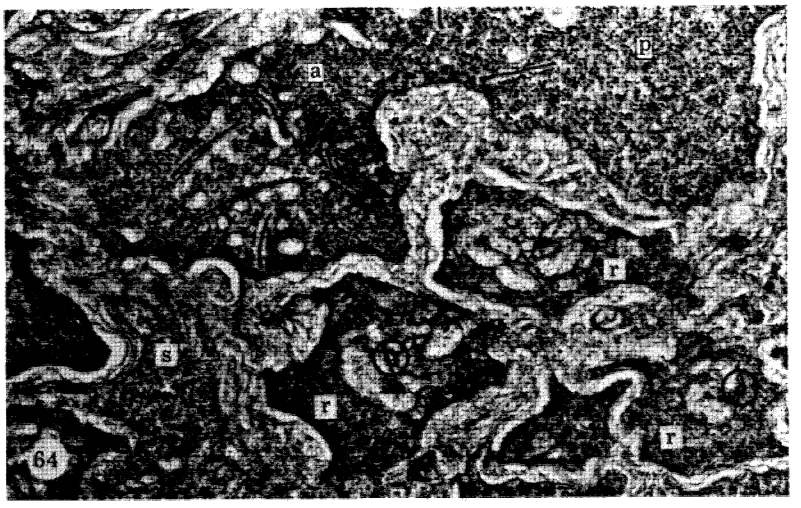

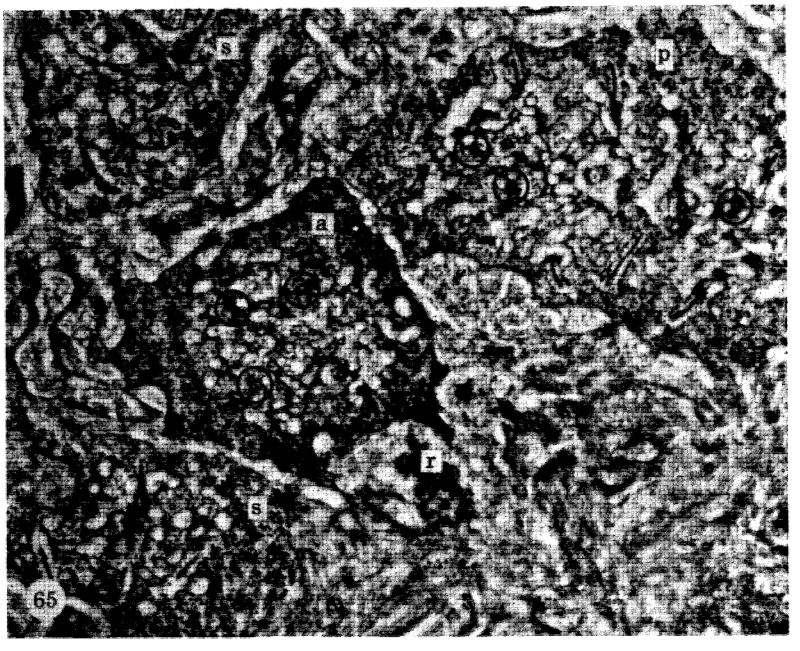

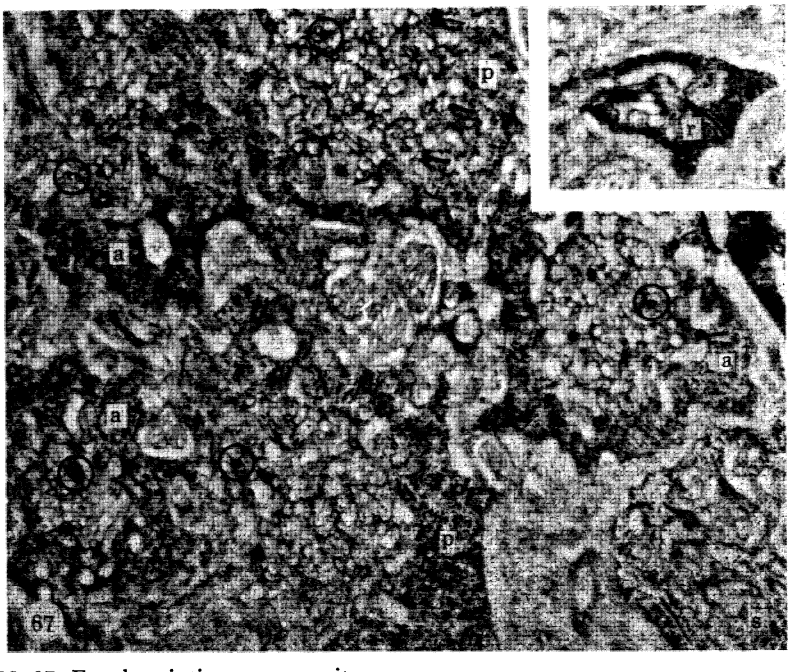

FIGURES 62–67. For description see opposite.

(*Facing p.* 98)

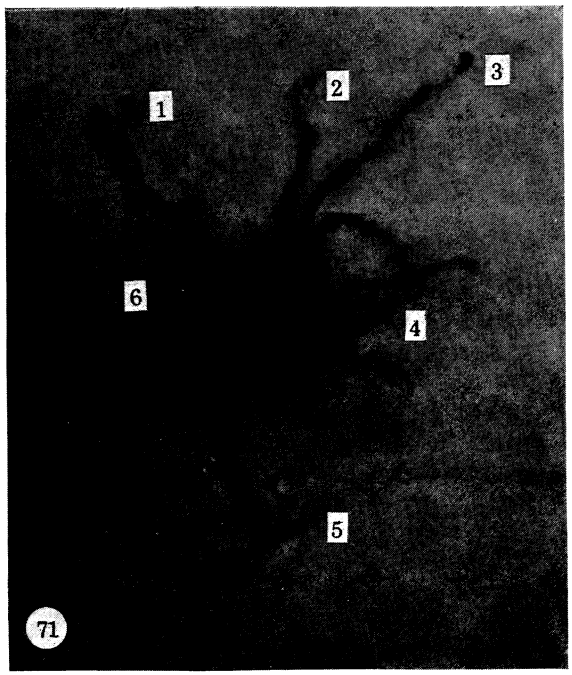

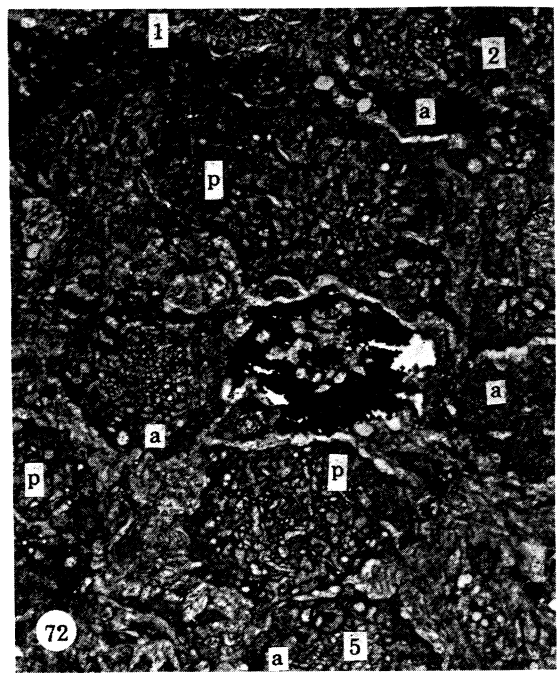

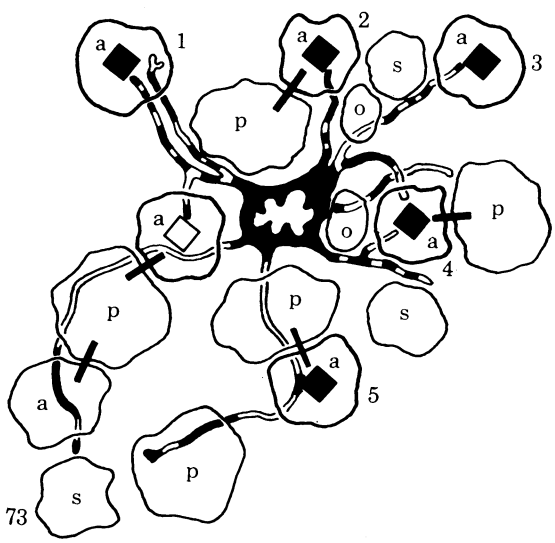

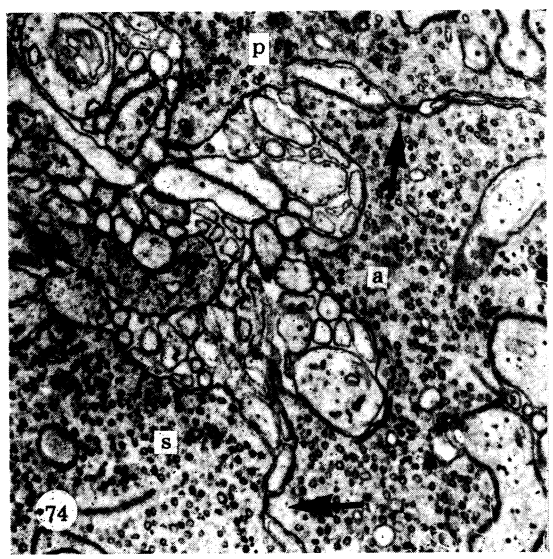

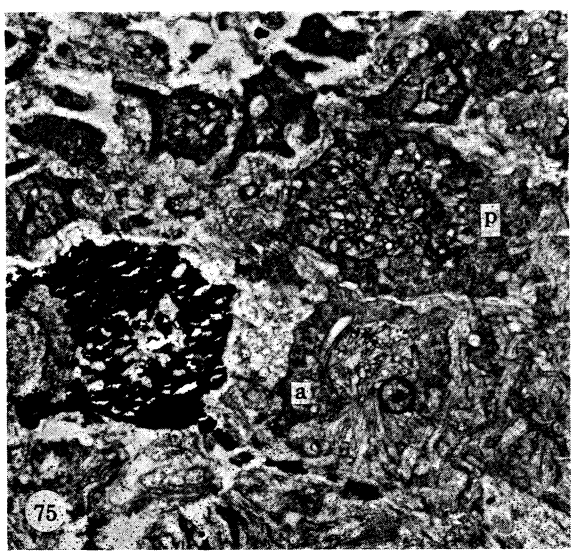

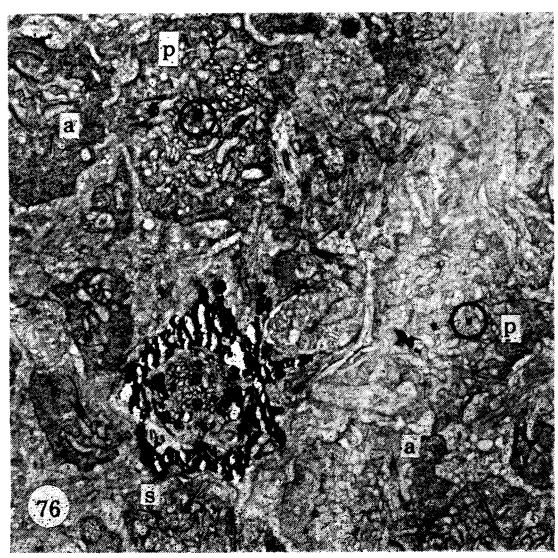

FIGURES 71–76. For description see opposite.

identified with a cell type which Parthe (1972) termed small cone bipolars. This identification was wrong, for the vertical profile appearance of Parthe's cells is quite different (see his figure 24, 1972); they more resemble the rudd's bistratified bipolar (figure 68*b*).

Yet another bipolar species which received input from more than one cone type and from a few rods is shown in figure 68*a*. It connects mainly to single and accessory cone pedicles, but in addition, a few processes clearly invaginated oblique cones and rods. The dendritic field is approximately the same size as that of the bistratified cell (figure 68*b*) and the cone input is 'complementary' to that of the other mixed input (red and green) bipolars. The light microscopic profile appearance was not recorded, and the cell is only mentioned here to show (*a*) that not only the red and the green channels, but also the blue and green cones, converge along with rods onto common bipolars in the outer plexiform layer, and (*b*) that oblique cones can have the same status as the other receptors in their connexions with bipolar cells.

(vi) *The chromatic organization of the bipolar population*

Figure 69 summarizes the selective receptor connexions of the bipolars which have successfully been analyzed. The outlines of the rods and cones are drawn to suggest their stratification in depth, and their chromatic identities are allocated in accordance with the arguments presented in §2. Above each bipolar, the outlines of one of each of the receptor types it innervates is filled in, and since the receptors are drawn to roughly the same scale as the bipolars, the numbers that converge onto each can roughly be estimated from the size of the dendritic fields which are indicated below (see plates 6–10 for more exact details). The alinement of the terminals of the different bipolar cells with the numbered strata of the inner plexiform layer is also shown.

The diagram shows seven neuronal types, which differ in their receptor connectivity patterns or morphology (or both), but this figure by no means represents the total bipolar complement of the retina. Quite different receptor connectivity patterns were seen in a few cells whose light

---

Description of plate 11

Innervation patterns of invaginating basal processes.

Figure 71. Horizontal plane light micrograph of a Golgi-impregnated single cone pedicle. Those of its basal processes which end by turning back out of the outer plexiform into the layer of cone pedicles are indicated with numbers; not all of them do this.

Figure 72. Thin section through the same cone terminal, in the electron microscope. The profiles of neighbouring unimpregnated cone pedicles (a, p) can now be seen, along with the silvered invaginated terminals of three of the basal processes (circles). The numbers correspond with those in figure 71.

Figure 73. Reconstruction of the destinations of the basal processes of this single cone pedicle. Invaginating contacts are made exclusively with neighbouring accessory cone pedicles (black squares, 1–5, cf. figures 71 and 72). One basal process judged in the light microscope to make invaginating contact (6), was not retrieved in the electron microscopic examination (open square). p, principal; a, accessory; s, single; o, oblique cone pedicles. The configuration of the basal processes is slightly distorted by section compression.

Figure 74. Gap junctions (arrows) between an accessory cone (a) and adjacent principal (p) and single (s) cone pedicles.

Figure 75. An impregnated principal cone pedicle and one of its invaginating basal processes (circle) in a nearby accessory cone terminal. See also figure 77; lettering as in figure 74.

Figure 76. An impregnated accessory cone pedicle, and its basal processes invaginating the synaptic cavities of two nearly principal cone pedicles. See also figure 77; lettering as in figure 74.

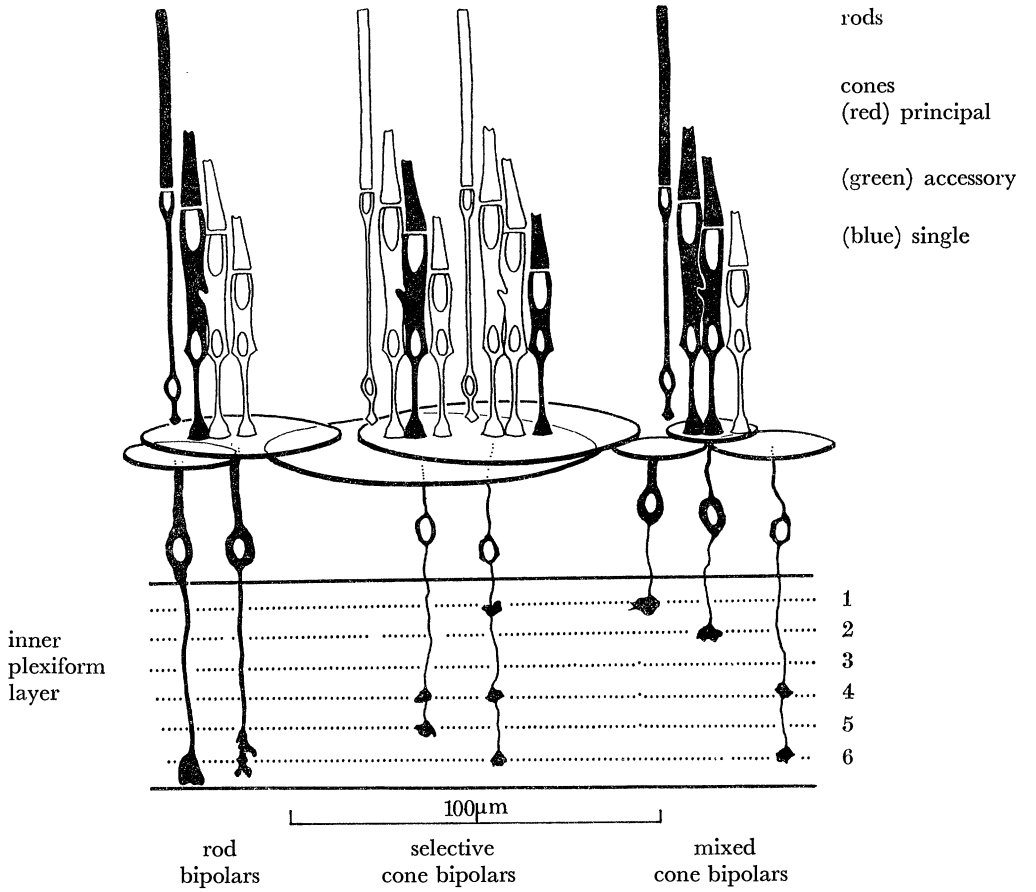

FIGURE 69. Summary of the receptor connexions and the inner plexiform destinations of the bipolar cell types analysed. The outlines of receptors and bipolars are drawn roughly to scale, and the identities of the cones are indicated to the right. The particular receptors to which the different bipolars connect are filled black, and the approximate dimensions of the bipolar dendritic fields are indicated by the (overlapping ellipses). The relative numbers of these different neurones in the retina are not known, but the excess of all bipolars over all cones is about 5:1.

microscopic morphology was not established (e.g. figure 68*b*) and other types were distinguished by their patterns of termination in the inner plexiform layer, but not analysed by electron microscopy. Figure 39 shows examples of these cells, whose single axon terminals were addressed to strata 3, 4 or 5 of the inner synaptic layer.

It appears, then, that there are at least ten species of retinal bipolar cells, which differ not only in their superficial morphology but also in the detailed patterns of synapsis they make with the different kinds of colour cones and rods in the outer plexiform layer. There are not many plausible comments that can be made on the functional significance of this considerable intricacy of neuronal architecture in the periphery of the visual system, but it is worthy of emphasis that the kind of morphological variety among neurones in the lower vertebrate that Cajal (1892) most strikingly portrayed has its basis in functional differentiation of patterns of synaptic input and output. These numerous bipolar cells convey information about different spatial (dendritic field areas) and chromatic (combinations of rod and cone input) aspects of the retinal image.

Initially, it was envisaged that bipolars *specific* for different cone types might synapse in

different layers of the inner plexiform layer. Accordingly, ganglion cells, whose responses are driven by more than one colour channel, might collect excitation or inhibition from separate 'colour coded' layers with their multi-stratified dendrites. However, it is clear in figure 69 that the anatomical findings lend no support at all to this view. Those inner plexiform strata for which there seems to be an approach to complete information are addressed by bipolars carrying quite complex combinations of colour information from the receptor layer. Thus rod and red and green cone signals from one bipolar population, and blue cone signals channelled through another, are all available to stratum 1. Ignoring those strata whose bipolar input is obviously incompletely known (3 and 5, see figures 39 and 69), there is no layer which receives input from just one receptor channel. Of course, in considering bipolar convergence into the inner plexiform strata, it should be borne in mind that within some of these layers at least there are separate populations of amacrine and ganglion cell dendrites which are likely to be specific for the different bipolar terminals (Cajal, 1892).

An unexpected observation was that different colour channels may converge onto the same (mixed cone) bipolars. Although in the Golgi impregnations, cells of which this was true were relatively infrequently encountered, it was argued that this is likely to be an artefact of the stain, and that the condition is relatively common. This convergence of the red and green (plate 10), or blue and green (figure 68*a*), channels might at first suggest additive interaction between them, but there are a number of considerations which argue against this simplest interpretation of the anatomical connexions. It seems unsound teleology that wavelength-specific information, once segregated by the differing action spectra of the cones should immediately be recombined by neural convergence. And if it were combined by these bipolars in order to participate in some luminosity signalling system independent of retinal channels concerned with the analysis of hue (e.g. plates 8 and 9), why should only two of the cone channels contribute? Again, as far as both behavioural and physiological measures of retinal sensitivity in fish go, there is very little evidence for additive combination of excitation from the various colour mechanisms. At threshold, the colour mechanisms are independent in determining discrimination performance, so that the photopic sensitivity curve is of the envelope type (Muntz & Northmore 1970), and in other behavioural circumstances, the only interaction detectable between the red and green channels is an antagonistic one (Northmore 1973).

The same is true of physiological measures of retinal activity. None of the recordings from fish retinal neurons have demonstrated spectral sensitivity curves which can easily be interpreted as unweighted sums of the excitation in red and green cones. Most commonly, as in the case of the ganglion cell responses (Wagner, MacNichol & Wolbarsht 1960; Daw 1968; Spekreijse, Wagner & Wolbarsht 1972), there is a powerful opponent interaction between these two channels, and it has been known for a long time that a chromatic opponency process is located as far peripherally as the outer plexiform layer in the chromatic *S*-potential compartments (Svaetichin *et al.* 1965; Naka & Rushton 1966*a*, *b*). These considerations suggest that the interaction mediated by convergence of the red and green cones onto common bipolar cells may be antagonistic. In a simple interpretation, this would imply that the red and green terminals possess different transmitter substances, or, less likely, that the synaptic processes of the bipolar dendrites respond differentially to the same transmitter substance liberated by different cones. But before further considering bipolar organization in this respect, another set of peripheral anatomical connectivity patterns should be described. These are the direct connexions between the synaptic terminals of the cones, effected by their basal processes.

5. Connexions between receptor terminals

(*a*) *Introduction*

Basal processes seem to be a universal feature of the cone pedicles in all the vertebrate groups (Cajal 1892), though they are certainly inconspicuous in the primate fovea (Missotten *et al.* 1963; Polyak 1941). Possibly because they do not appear in Golgi-impregnations of mammalian rod spherules (Cajal 1892; Polyak 1941), it is often overlooked that rod terminals in most of the lower vertebrate groups certainly possess them (Cajal 1892).

They are fine processes which radiate in the horizontal plane from the vitread margins of the receptor terminals, extending laterally around one to three receptor diameters and sometimes more. The size of their fields, and the density of processes within them varies according to species, retinal locus, and, among lower vertebrates at least, to cone type (Cajal 1892).

Although the basal processes in some vertebrates are known to contact neural processes of unknown origin in the outer plexiform layer (Lasansky 1971), the junctions they make with adjacent receptor terminals have received the greater emphasis in the literature. There seem to be no conventional synaptic junctions between the receptor terminals or their basal processes; however membrane appositions (gap junctions; Lasansky 1972), of varying degrees of specialization, have been found in most of the vertebrate groups (Sjöstrand 1969; Nilsson 1964*b*; Cohen 1965; Missotten 1966; Lasansky 1972). As well as involving basal processes, the junctions also directly link the bodies of closely adjacent spherules and pedicles.

The status of these inter-receptor contacts is particularly important in relation to physiology, for just as their structure suggests they may be involved in electrical interactions between the receptors, so it is now known, in the turtle retina at least (Baylor & Hodgkin 1973), that cones (of like spectral sensitivity) are in local electrical continuity with one another. However, where this question has been examined, it is generally true to say that gap junctions are made between receptors more or less indiscriminately of chromatic identity or functional type.

In man, the cone pedicle basal processes are directed to the bodies or processes of other neighbour cone terminals, where they end in quite extensive areas of membrane apposition (Missotten, Apelmanns & Michiels 1963). In addition they make rather less prominent *en-passant* contact with some of the rod spherules, though there is no evidence that these terminals themselves are linked together in the same way as the cones. In the guinea-pig retina rod and cone terminals all contact each other without discrimination (Sjöstrand 1969). Only in the frog is it held that apposition contacts between the receptor terminals are selective according to morphological type. Nilsson (1964*b*) found that principal and single cones, and rods, all contact one another according to rules related to their relative numerical density in the retina, while, by contrast, accessory cones and Schwalbe rods connect neither to each other nor to any other receptor type. However, Schwalbe rods indisputably possess basal processes (Cajal 1892), and it is most likely that frog accessory cones do as well, so Nilsson's result is not without its puzzling features.

In all of these cases, the (gap) junctions link unlike, as well as like, receptors, and the difficulties this raises for physiological interpretation are exacerbated by Raviola & Gilula's recent (1973) freeze fracture study of their ultrastructure. In the mammalian retina, the contact between cones, and between cones and rods, are qualitatively identical at the finest level of detail. These authors, as well as earlier workers (Missotten 1966; Cohen 1965; Dowling & Boycott

1966), have been careful to acknowledge the possibility that the inter-receptor contacts may fulfil a function other than physiological interaction.

Recently, Lasansky (1972) made the important observation that there is another, distinct, pathway for communication between cones beside these systems of membrane contacts between receptors. He showed that certain of the basal processes of cones in the turtle retina may invaginate the synaptic cavities of neighbouring pedicles. It is not yet known whether a similar pathway exists between the somewhat differently organized terminals of mammalian cones. The evidence is that there are not, since the rule seems to be that just one bipolar cell process and two horizontal cell processes are found in each 'triad' invagination into the pedicles (Kolb 1970), but it is true to say that primate material has not explicitly been examined with this point in mind. Fish, however, certainly possess invaginating basal processes.

In principle, the invaginating basal processes might be either pre- or postsynaptic, and they might have that relation either with the cones whose pedicles they enter, or with one or other of the neuronal processes that do so in common with them. Lasansky (1971) was able to recognize the invaginating basal processes in conventional electron microscope material, and showed that they do not have the same relation with the pedicle synaptic ribbons as the post-synaptic processes of bipolars (triad central processes). They terminate at 'distal' junctions with the lateral elements of horizontal cell 'dyad' complexes. They lack, however, any aggregation of synaptic vesicles at their endings that might firmly indicate them to be *presynaptic* to any of the cellular components of the receptor terminals they enter.

(*b*) *Observations*

(i) *Light microscopy*

The variation in the size and complexity of the terminals of the rods and the different cones recognized by electron microscopy (table 4) can also easily be seen in Golgi impregnations (figure 70). Both rod and cone terminals have basal processes; the fields of the rod processes are smaller than those belonging to cones, but between cone types basal process field size is roughly the same. However, the larger pedicles, which belong to the most numerous kinds of cones

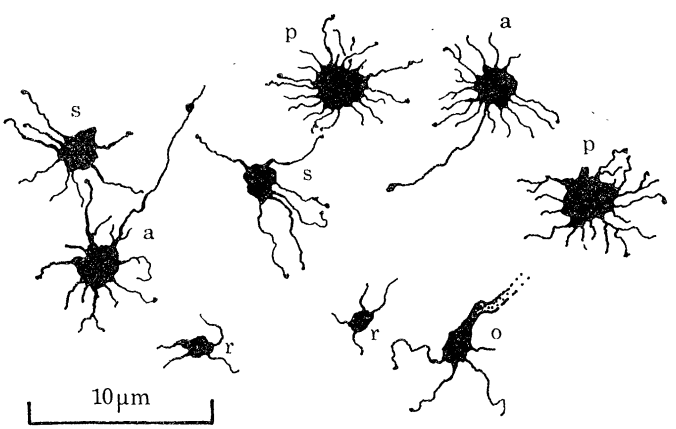

FIGURE 70. Horizontal view of a group of impregnated receptor synaptic terminals (*camera lucida*) r, rod spherules; p, principal; a, accessory; s, single and o, oblique cone pedicles. Generally, the cones which are the most numerous in the retina (principals, table 1) have the most densely branched basal processes. However the basal process fields of the different cone types are approximately the same size. Notice the locus of joint termination of processes from a principal and single cone; and the single long processes characteristic of the accessory cone pedicles.

(e.g. principals) have *more* basal processes than the smaller ones (e.g. obliques), and more frequent branching. Accessory cone pedicles usually possess a long additional process which runs horizontally well outside the conventional basal process field, apparently in no particular retinal direction (figure 70).

Cone basal processes do not ramify in the plane of the pedicles themselves, but below them in the outer plexiform layer; this is evident in figure 71, plate 11, where the processes are shown sharply, but the outline of the pedicle body is somewhat out of focus. The shorter range basal processes of the rod spherules (figure 70), however, ramify at their own level, and never penetrate the outer plexiform layer.

A proportion of the basal processes of each type of cone pedicle terminates by leaving the outer plexiform layer and penetrating the pedicle layer again. Those which do so can be clearly distinguished in the light microscope, since they end in slight swellings (figure 70; figure 71, plate 11). The remainder end 'blind' in the plane of the outer plexiform layer, without any specialized terminal structure (figure 70; figure 71, plate 11), and it is true to say that such blind basal processes are more numerous in the larger (more numerous, table 1) cone types than in the smaller ones (figure 70). Perhaps this hints there is a system of connexions between the basal processes of like cones (see also below).

(ii) *Intereceptor contacts*

The receptor terminals are isolated from one another over most of their surface area by a matrix of Müller glial membranes. At intervals, however, it attenuates, allowing neighbouring spherules and pedicles to make what are interpreted as 'gap' junction contacts with one another (figure 74, plate 11). The pedicles of like and dissimilar cones contact one another in this way, and rod spherules contact each other and cones as well, with no evident regard for type. The junctions are similar to the intereceptor contacts described in other retinae (Sjöstrand 1969; Nilsson 1964*b*; Cohen 1965; Missotten 1966), though the rudd material was not examined at a resolution which would reveal the detailed ultrastructure they have recently been shown to possess (Lasansky 1972; Raviola & Gilula 1973). Although they are numerous in the fish retina, their lack of selectivity for receptor type (figure 74, plate 11) again firmly raises the issue whether such contacts do represent sites for physiological communication between the receptors.

In addition, the basal processes of the cones make similar, often more extensive, contacts with one another in the outer plexiform layer, as do those of the rods at their own more distal level. The clear morphological differentiation of the basal processes leads one to the thought that *their* contacts might represent a distinct, and functional, pathway between the receptors. They might possess the selectivity for receptor type which the physiological demonstrations of electrical continuity between cones demand (Fuortes 1972; Baylor & Hodgkin 1973), but which the more commonly studied appositions between the receptor synaptic bodies conspicuously lack.

Nilsson's (1964*b*) observation that Schwalbe rods in the frog make no 'intereceptor' contacts, when they certainly possess basal processes (Cajal 1892), hints at such a distinction, and it does seem that the junctions between the basal processes of primate cones are more specialized than the contacts they make *en passant* with the rod spherules (Missotten *et al.* 1963).

However, the Golgi-impregnated material from the rudd retina was of inadequate quality confidently to identify sites of basal process apposition in the outer plexiform layer, and the

much more difficult task of analysing their selectivity for cone type by conventional electron microscopy was not attempted.

(iii) *Invaginating basal processes*

The cone pedicle basal processes which terminate by leaving the plane of the outer plexiform layer invaginate the synaptic cavities of neighbouring pedicles, in the same way as those of the turtle retina (Lasansky 1971). Normally, any particular cone pedicle sends just one process into each of the nearby pedicles with which it makes this invaginating connexion, though occasionally two or three may be involved. This condition contrasts with the multiple (5–12, see table 3 and text) processes the bipolar cell dendrites direct into the synaptic cavities of the pedicles they innervate, and presumably reflects the detailed mode of termination of the basal processes, which, as in the turtle, never assume the triad central process station, although they are frequently seen in the proximity of lateral process 'dyads'.

In the fish, cone pedicle basal processes do not invaginate rod terminals, and rods have no invaginating connexions with one another or with cones. The cone basal processes make their invaginating contacts with strict selectivity according to cone type; they link cones of *different* colours.

The single cone pedicle seen in horizontal profile by light microscopy in figure 71, plate 11, was cut in this plane for the electron microscope. Figure 72 is an electron micrograph of one of the sections, showing three of its invaginating contacts located in the pedicles of nearby accessory cones, and the drawing in figure 73 shows the complete reconstruction of the connexions of the invaginating basal processes. The parts of the silvered pedicle which were retrieved in the (semi-serial) sections are filled black, and the neighbour terminals which its processes invaginated are indicated by filled squares. All five of them belonged to accessory cones. A process directed to the vicinity of a sixth accessory cone pedicle (open square) seemed in the light microscope to make invaginating contact, but could not be found in the e.m. sections of the synaptic cavity of this terminal. The remaining four processes, including two rather long and prominent ones, terminated blind in the outer plexiform layer; none of them were obviously directed *toward* other nearby accessory cone pedicles. The two large ones rather clearly converge on another single cone pedicle (which they do not quite reach).

In the same way one other reconstructed single (blue) cone pedicle had invaginating contacts exclusively with accessory cones (green), and extra basal processes which suggested a separate system of connexions in the outer plexiform layer, which could involve apposition junctions.

Several impregnated principal and accessory cone pedicles were also examined, and their invaginating contacts were likewise found to be selective; those of principal (red) cones were exclusive for accessory pedicles (actually, for 19 contacts exclusive to accessories, evidence was found of invagination into just one principal cone terminal). The invaginating basal processes of accessory (green) cones were connected only to principal (red) cones: none were observed to go to single cones. Reconstructions of these patterns of invaginating contact of a principal and an accessory pedicle are shown in figure 77. Here, again, many of the processes end in the outer plexiform layer at points unrelated to the positions of other cone terminals in the vicinity. Figures 75 and 76, plate 11 show representative e.m. sections from which these reconstructions were made.

To summarize, basal processes are involved in the following sorts of (presumably functional)

connexions. Some, but not all, of those belonging to cone pedicles invaginate the synaptic cavities of neighbouring cones. Their structure suggests that they may be postsynaptic to the cones involved, but their status may well be much more complicated than this, for it is known that they have a more intimate relation of proximity to horizontal cell processes in the pedicle than they do to the presynaptic apparatus of the receptors themselves (Lasansky 1971).

Principal cone basal processes innervate the pedicles of nearby accessory cones, and vice versa, so that they constitute a possible vehicle for direct interactions between the red and green receptor channels. Single cone basal processes innervate accessory pedicles, but the reverse is

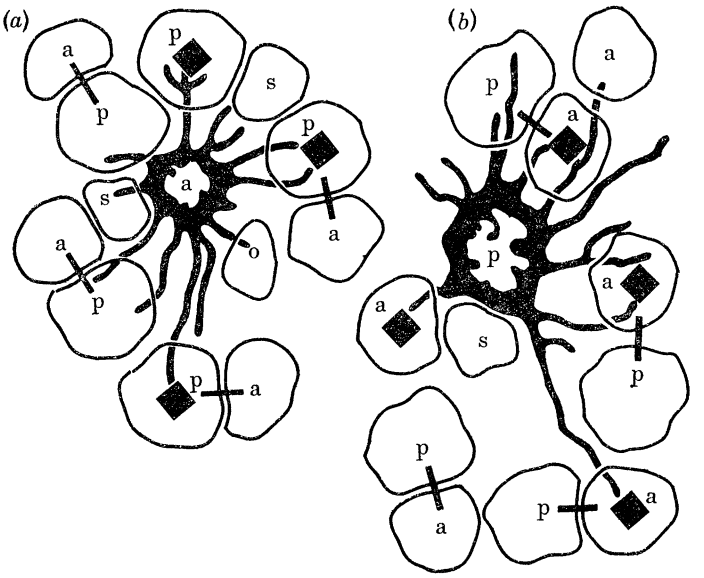

FIGURE 77 .(*a*) Reconstruction, from semi-serial electron microscope sections, of the destinations of the basal processes of an accessory (green) cone. Four of them terminate by invaginating some of the nearby principal (red) cone pedicles, while the remainder end within the outer plexiform layer. (*b*) The same for an impregnated principal cone terminal, four of whose basal processes invaginated neighbouring accessory cone pedicles. Figures 75 and 76 in plate 11 show representative sections from the series upon which these drawings are based.

not the case, so that any interaction they mediate between the blue and the green channels is not the reciprocal one characteristic of red and green.

Rod terminals do not have invaginating contacts, either with one another or with cone pedicles. Their basal processes make apposition contacts (gap junctions) with one another and also with neighbouring cones. Besides the gap junctions on the synaptic terminal bodies of the cones, which link them to one another and to rods, basal processes of nearby pedicles also contact one another in a similar way in the outer plexiform layer.

DISCUSSION

1. THE SPECIFICITY OF SYNAPTIC CONNEXIONS IN THE OUTER PLEXIFORM LAYER

Alongside repeated assertions of the selectivity with which the different types of receptors and bipolar cells make their majority synaptic connexions in the outer plexiform layer, it has been necessary almost as often to acknowledge exceptional minority receptor connexions. To name one instance, large field rod bipolars make their majority photopic connexions with the pedicles of principal cones, but on occasion they were seen to innervate one or two accessory

cones as well (page 94). The reader will require assurance that this does not hint, for example, at some selective failure of silver impregnation that could make nonsense of the goals of mapping connectivity in this way.

These minority connexions, which accounted for some 5 % of all those retrieved, cannot be attributed to the intrusion of processes from other impregnated retinal neurones, since the bipolar cells analyzed were carefully selected by light microscopy for their isolation. Also, in most of the cases where they were encountered, there were grounds for confidence that, in reality, there were no further connexions of the same type which for some reason were not revealed by the impregnation. These were that the morphological *patterns* of bipolar dendritic trees and cone basal process fields very conspicuously reflected the selectivity (or otherwise) of the *majority* synaptic connexions. This can be seen, for instance, by comparing the branching patterns of the accessory and single cone bipolar fields in plates 8 and 9 with the locations of the cones they are connected to, or by examining the basal process patterns of the different kinds of cones in figure 70. Apparently, therefore, specificity in the way these retinal cells connect to one another is not absolute, although it is sufficient that the 'errors' which the bipolars can make in their developmental selection of receptor input are infrequent enough to be of negligible functional consequence.

The gross morphology of the bipolar cells is consistently correlated with the patterns of connexion they make, and this suggests that they possess phenotypic identities which embrace more characteristics than the details of their synapsis with other cells. In the rod bipolars, for instance, these characteristics seem sensibly related to functions their synaptic connexions demand; their thick processes and proximal address in the inner plexiform layer appear well suited to convey the notionally feeble signals of the scotopic receptors. In the other types of bipolar cells the relation is more obscure; why, for example, are the dendritic fields of the selective cone bipolars so large? It would be interesting to know, in this context, whether such morphological differentiation among the bipolar cell population is as conspicuous in that region of the growing peripheral retina where these neurones have fully differentiated their processes and dendrites into the two plexiform layers, but where (unpublished observations) the axons of the rods and cones have not yet grown down to synapse with them.

2. Numerical synaptic relations between bipolars and receptor terminals

The fish retina is afoveate, and has no counterpart of the simian midget bipolar system. Because of their special relation with individual cones (Polyak 1941; Boycott & Dowling 1969; Kolb 1970) the midget bipolars are the only second order nerve cells which can securely be inferred to carry wavelength specific information in the mammalian retina, and it is an important contrast that the fish bipolars which also have direct synaptic input from just one photopic channel have, by contrast, very wide dendritic trees (figure 69 and plates 8 and 9), and connect to many cones.

It is by no means clear what relation there is between the size of the bipolar cell dendritic fields (or, indeed, those of other retinal cells) and the geometry of the eye. It is not known, for example, whether as fishes grow and their retinal mosaic acquires finer grain in relation to the image cast upon it, neuronal fields also extend to embrace a constant angular subtense into the outside world. As far as we have seen, bipolars connect to the greater majority, if not to all

the appropriate receptor terminals that fall within their dendritic fields (plates 6–10). A consequence, therefore, of an increase in the size of the fields and their (commensurate) degree of overlap, would not only be that the thickness of the outer plexiform layer should increase, but also that the receptor terminals should expand in order to accommodate the proportionately larger number of presynaptic invaginating processes that would accrue. No evidence was found that this in fact occurs in the fish.

If, then, the size of the bipolar fields bears little relation to the scale of the image whose 'analysis' they begin, it is no more easy to find a reason why, between functional types, their dimensions should vary. An explanation might be that there is (in some sense) a required numerical receptor input, and that to collect it, the bipolars which connect only to one species of cone must embrace a wider retinal area than those connected to several. This is true in measure only (mixed cone bipolars have smaller fields than selective cone bipolars), and it goes nowhere toward explaining the difference in dendritic spread between the two kinds of rod bipolars (plates 6 and 7) which are connected to exactly the same combinations of receptors, namely principal cones and rods.

The numerical relations between the receptors and the bipolars are defined by two quantitative synaptic properties. The first, which refers to the bipolar cells, is *convergence*; its degree, in particular cells, is simply given by the number of receptors connected to each of them. It is a function, therefore, of the density of those receptors in the retinal mosaic, and of the width of the bipolar dendritic trees. As we have seen, different degrees of convergence characterize different morphological classes of bipolars. The second, a property of the different types of receptors, is *divergence*, the number of bipolars synaptically connected to them. Its degree is determined by the numerical excess of bipolars over receptors (according to type), the width of their dendritic fields, and the extent, therefore, to which they overlap.

The numerous (up to 350, table 3) invaginating processes accommodated by the cone pedicles implies a highly divergent connectivity in the outer plexiform layer between receptors and second order nerve cells. Actually, if each of the 350 bipolar processes in a principal cone pedicle came from a separate nerve cell, the *average* bipolar dendritic field would embrace (assuming a bipolar excess of $\times 5$; Muntz & Northmore 1971*b*) some 70 principal cones, a much higher number than that observed in the Golgi material (plates 6–10). However, the situation is not as extreme as it at first appears, for each bipolar sends more than one process to each of the pedicles it invaginates, and figure 47, plate 7, for example, suggests the possibility that as many processes from a particular cell enter the pedicle cavity as there are synaptic ribbons around its outline, each eventually coming to participate in a 'triad' association with one of them.

The important feature of this suggestion is that it proposes a quite different organization for the synaptic sites to that found in primate retinae. In primate cone pedicles there are many short ribbons (10–30; Missotten 1966; Dowling 1965; Dowling & Boycott 1966; Kolb 1970), and each is associated with just one 'triad' of bipolar and horizontal cell processes: that is to say, there is a ribbon for each invaginating bipolar process. In the fish, many more processes enter the synaptic cavity than there are synaptic ribbons, but the ribbons are longer than those in primates. It is quite clear from table 3 that if only a small fraction of all the processes which enter the synapses are to be accommodated in triad configurations, then more than one must share each ribbon.

To prove, in Golgi impregnated material, that each of the several silvered processes which

enters a pedicle cavity (e.g. figure 47, plate 7) eventually comes to occupy a segment of the length of a (different) synaptic ribbon in a 'triad' arrangement, requires serial section analysis. Unfortunately, when such sections were available, the issue had not come to mind, so strategic micrographs only were made to record the bipolar connectivity patterns discussed in §5, and their levels and resolution are inadequate to answer this question directly.

Nevertheless, they yield quite good statistical evidence, whose power rests in the numerical differences between the innervation of the pedicles of the various cones (table 3, figures 30–33, plate 4). Table 4 presents counts of the numbers of silvered processes encountered in the pedicles sectioned for examination of bipolar connectivity patterns (plates 6–10), classified according to the receptor type they invaginated, and to the bipolar type from which they originated. As with the data in table 3, the average figures are underestimates, and the maxima more probably approach a realistic estimate of the numerical innervation of the synapses.

Both the averages and the maximum counts vary systematically between pedicle types in just the same way as did the counts of presynaptic ribbons, and of total numbers of process profiles, in table 4. It can immediately be discounted that this is a property more of the particular bipolars involved than of the cone pedicles they innervate, since, for example, principal and accessory cone terminals receive different numbers of processes from the cells which jointly innervate them both (column 5, table 4).

TABLE 4. THE NUMBER OF SILVERED DENDRITIC PROCESSES FROM DIFFERENT BIPOLAR CELL TYPES (COLUMNS) FOUND TO INVAGINATE THE SYNAPTIC TERMINALS OF THE DIFFERENT RETINAL RECEPTORS (ROWS)

The figures (maximum counts, with means in brackets) are compiled from horizontal electron micrographs at the edge of the outer plexiform layer; they compare with the distribution of synaptic ribbons in the different receptor terminals (table 3).

	rod bipolars (n = 5)		selective cone bipolars (n = 2)		mixed cone bipolars (n = 4)
receptor field	small field	large field	accessory cone	single cone	
principal cone (n = 55)	14 (9.9)	12 (6.9)	—	—	13 (7.3)
accessory cone (n = 44)	—	—	7 (3.3)	—	8 (4.9)
single cone (n = 13)	—	—	—	5 (2.5)	—
rods (n = 107)	1	1	—	—	1

The numbers of synaptic ribbons in the pedicles of the Golgi-e.m. material were also counted, and strikingly agree with the counts of silvered processes in the different pedicle types (figure 78). The width of the distributions must be due in part to the sampling error inherent in counting from isolated sections, but the register of both means and ranges for each pedicle type surely asserts that the bipolars send as many processes into a pedicle cavity as there are presynaptic ribbons around its margin, and implies a relation between them. To find this numerical equality between the organelles of separate cells suggests an ontogenetic *tropism* of bipolar synaptic processes toward the ribbons; an intuition nourished by cases such as that shown in figure 61, plate 9, where branches from adjacent but quite separate bipolar dendrites each contribute part of the innervation of a pedicle lying in between them.

Divergence in the outer plexiform layer, therefore, can simply be estimated by dividing the process profile counts by the number of ribbons characteristic of each terminal type. This was done in row 3 of table 3, (page 85) which shows that the real innervation of the cones only differs between types by a factor of approximately two. The reader will also notice that a direct relation now appears between the variation in the degree of divergence at the synapses of the different cones, and the variation in the frequency with which those cones occur in the retinal mosaic (compare row 2 in table 1 (page 72) with row 3 in table 3 (page 85)).

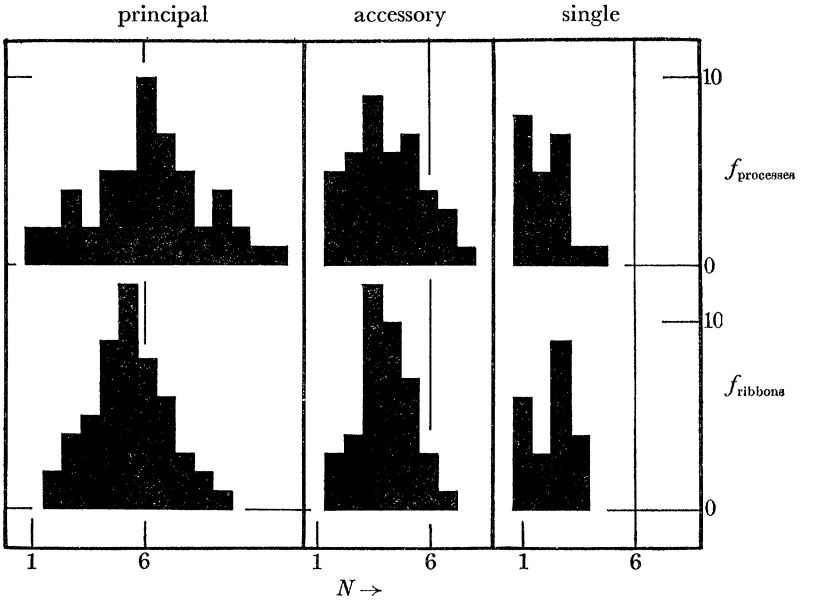

FIGURE 78. The top row of histograms are frequency (f) distributions of counts of the numbers, N, of silvered bipolar processes recognized in e.m. sections of principal, accessory and single cone pedicles. The lower row of histograms show the frequency distributions of counts of synaptic ribbons in the same population of pedicles.

Although it is characteristic of the different kinds of receptors that each displays a different degree of divergence in its synaptic relations with the second order neurons of the retina, this is less a property of the cones than of the neuronal populations with which they synapse. It reflects, I have argued, the degree of overlap in particular bipolar cell dendritic fields, determined, in turn, by their density in the retina and their lateral extent. Because the overall excess of bipolar cells over cones in the retina (× 5, Northmore & Muntz 1971*b*) is considerably less than the divergence at the synaptic terminals of each of the cone classes (row 3, table 3), there must be a substantial degree of overlap in the dendritic fields of the bipolar cells, each of which contact most, if not all, of the appropriate cone pedicles within their reach (see, for example, figure 60, plate 9).

What has been observed of the Golgi-impregnated bipolars certainly does not exclude that the population of cells connected to different kinds of cones (or combinations of them) have approximately the same *range* of dendritic field sizes. If this is so, the curious relation between the retinal density of particular cone types and the degree of synaptic divergence at their terminals would mean no more than that the cells connected, for example, to red cones, comprise the same fraction of the total bipolar population as red receptors represent of the total complement of cones.

It is hardly likely that there are as many functional types of bipolars in the retina as there are bipolars connected to individual cones. Therefore it must overall be true that the fields of bipolars of the *same* functional type overlap substantially with one another, as well as with those of different cell classes. We have already remarked that the Golgi impregnations indicated that bipolars innervate most, if not all, of the appropriate synaptic terminals within the bounds of their dendritic fields, rather than sample intermittently. Our understanding of dendritic field overlap therefore suggests a substantial degree of redundancy in the bipolar populations, within their functional classes.

The various ways in which the four cone species differ from one another seem likely to determine their relative power in generating visual excitation. Thus, their effectiveness in capturing light is related to their (varied) size and frequency of occurrence. Likewise, both the number of synaptic ribbons their pedicles contain, and the number of second order neurons they are connected to, should determine the functional dominance of their postsynaptic effect in the retina. It is interesting that all of these features quantitatively co-vary: in the principal cones, for example, each assumes a *value* consistent with this receptor system functionally dominating the others (tables 1 and 3). At the other end of the scale, the oblique cones are least well equipped in every respect to play an important visual role.

3. Rod bipolars and red cones

Fish, unlike mammals, seem to have no bipolar channel exclusive to the rods. The two neuron types described under the heading of rod bipolars (plates 6 and 7 and text), not, in fact, the only cells connected to these receptors, also synapse with principal cones (both paired and free, see §1). It was argued in §2 that principal cones contain the red absorbing photopic pigment, and recent recordings from bipolar cells in the carp retina provide a pleasing confirmation of this view.

Procion-injected rod bipolars are easily recognizable (cf. Kaneko 1970), and Toyoda (1973) has recently shown physiologically that, during dark adaptation, they are depolarized by a receptor mechanism sensitive at 520 nm, reasonably attributed to rods, while, in light adaptation, their maximal sensitivity shifts to red light at 620 nm. This 'Purkinje shift' is entirely consistent with the anatomical connexions here demonstrated for the rod bipolars, and with the chromatic identity attributed to the principal cones.

More recently still, Kaneko (1973) has distinguished two physiological types of red centre depolarizing (rod) bipolar cells in goldfish retina: both have antagonistic surround mechanisms in their receptive fields, evidently mediated by horizontal cells, which in one case is driven by both red and green cones, and in the other by red cones only. It is not impossible that these types correlate with the distinct large and small field rod bipolar cell types that can be distinguished anatomically in the rudd (plates 6 and 7) and other fish (Parthe 1972).

The rod bipolars are the only cells for which a firm identification can be made between Golgi-impregnated and Procion-injected material. That identification permits the conclusion that the depolarizing action of light upon these 'on-centre' neurons is mediated, in the case of both their rod and cone input, by invaginating postsynaptic processes which form central profiles at the receptor terminal triads (figure 41, plate 6). It would be interesting to know whether the same is true of hyperpolarizing bipolars, bearing in mind the possibility that the difference in their responses reflects the difference between invaginating and basal junction

(Missotten *et al.* 1963; Lasansky 1969) synapsis with the receptors. But it must again be stressed that basal junctions have yet to be found in the fish retina (page 84).

Rod bipolars in the mammalian retina have rather the same general morphological characteristics as those in fish; their processes are thick and their synaptic terminals are located in the most vitread stratum of the inner plexiform layer, next to the ganglion cell perikarya (Cajal 1892). However, they appear not to be connected to cones. Kolb (1970) who sectioned an impregnated rod bipolar for the electron microscope, proved this to be the case in the rhesus monkey retina and Boycott & Kolb have recently (1973) shown the same to be true in the cat. Perhaps lack of cone input to mammalian bipolars has interesting implications for the location of the interactions responsible for scotopic hue effects (Stabell & Stabell 1965; McCann & Benton 1969) in man.

It is not impossible that the 'rot-scheu' behaviour (Bauer 1910) characteristic of many fish, including rudd (Burkamp 1923), is some reflexion of the curious red cone specific connectivity of their rod bipolars. It is difficult to suppose they have an achromatic photopic role, equivalent to their scotopic function, because it is known that some have chromatic receptive field surrounds (Kaneko 1973), and because such would suggest they should connect indiscriminately to all types of cones.

4. Bipolar chromatic opponency

The most complex of the fish retinal ganglion cells are double opponent (Daw 1973). They have a spatial antagonism between their receptive field centres and their annular surrounds, and a separate chromatic (red-green) opponency embedded in each of these receptive field regions. Thus, for example, red centre *on*-responses are antagonized by green centre *off* and red periphery *off*. At light intensities below those at which the red and green fields are functional, the double opponent cells receive input from a co-extensive spatially opponent field of rods, which always exert the same sign of control on the responses as do the red cones in light adaptation, opposite to that of the green channel (Beauchamp & Daw 1972; Raynauld 1972). The present findings have a bearing on the morphological substrate of the chromatic interactions mediated *within* these regions of the receptive fields; those *between* regions are presumably conveyed by neurons with much more extensive lateral ramifications than those of the bipolars, for fish ganglion cell receptive field regions are commonly measured in millimetres.

It is unlikely that the signals of the rods and the red and green cones are conveyed separately through the depth of the retina to converge onto the ganglion cells in the inner plexiform layer, since neither a bipolar channel exclusive to rods nor a class of cells connected only to red cones has been found. Of the cells examined, either the rod bipolars or the mixed cone bipolars could be involved in transmission between the receptors and the opponent colour ganglion cells. The rod bipolars, connected to rods and red cones, could convey their synergist signals (Toyoda 1973) to the ganglion cells, and interact at some level with an antagonistic green channel.

Two possibilities suggest themselves: Kaneko (1971) showed that the rod bipolars have an antagonist receptive field surround, mediated presumably by horizontal cells, and sometimes driven in part (Kaneko 1973) by a green receptor mechanism. He has suggested (Kaneko 1973) that convergence of many such concentric bipolar fields onto the ganglion cells might be the basis of their complex double opponent organization, and this model has the appeal that its hierarchical organization (in a different context) resembles that proposed by Hubel & Wiesel

(1968) to underlie the transition between 'concentric' and 'simple' receptive fields in the mammalian visual pathway. Alternatively, the green signals could be conveyed to the inner plexiform layer by a separate bipolar channel (e.g. selective cone bipolars) to interact with the rod bipolar messages at that level.

Neither of these alternatives is entirely acceptable in view of the almost equal status of the red and the green channels in their interaction to generate the ganglion cell responses (MacNichol, Wolbarsht & Wagner 1961; Spekreijse *et al.* 1972); on an equal area basis, the rod bipolar green surround is much less sensitive than the 30–60 μm (plates 6 and 7) centre dendritic fields (Kaneko 1970). Likewise the distinctive filamentous morphology of the selective cone bipolars suggests that their signals would have a quite different status to those of the rod bipolars in the inner plexiform layer.

Suggestively, the mixed cone bipolars are connected to all of the receptor types known to drive the double opponent ganglion cells, and it is certainly not impossible that the red and green cones have opposite synaptic effects upon them, thereby establishing the chromatic opponency of the ganglion cell responses in the outer, rather than the inner, synaptic layer of the retina. However, some physiological findings argue against the convergence of red and green cones onto these small field bipolars alone mediating ganglion cell colour opponency.

Spekreijse & Van den Berg (1971) showed that the phase and modulation depth of flickering red and green light patches placed in the receptive field can be arranged to achieve a particularly sensitive cancellation of the ganglion cell discharges that each alone evokes. The parameters of cancellation are independent of the positions of the lights, providing neither transgresses the boundaries of the receptive field regions at which they are directed. In the simplest interpretation, this strongly suggests that convergence of the red and green opponent channels occurs at that station whose morphology determines the extent of the receptive field regions, presumably the ganglion and amacrine dendrites in the inner plexiform layer. They could not so interact via outer plexiform structures (mixed cone bipolar dendrites) embracing only a few cone diameters (plate 10).

This result does not, in fact, absolutely preclude that mixed cone bipolars mediate the red-green opponency, but requires that, if they do so, these cells must individually be capable of passing on to the ganglion cells both excitation and inhibition in measure to the balance of antagonistic input which it is suggested they receive from the red and green cones.

5. Direct chromatic interactions between cones

The characteristics of horizontal cell responses have made it clear for a long time (Svaetichin & MacNichol 1958) that opponent colour processes are carried on in the outer plexiform layer. So-called chromatic *S*-potentials, evoked by stimuli of 'opponent' wavelengths, have opposite sign, and a more interesting interaction between the colour channels appears in the responses of the luminosity *S*-potential compartments (Naka & Rushton 1966*c*), whose polarity is the same irrespective of wavelength. Long wave adapting lights depress the dominant red component of their action spectrum, but considerably enhance the sensitivity of the green channel, and vice versa. Because the responses caused by both the colour channels are of the same sign, and because the adapting lights necessary to produce the effect need only make trivial displacements of the *L*-compartments resting potential, it is likely that the (antagonistic) interaction between these colour channels is mediated at some level peripheral to the site at which the

responses are measured. Since the horizontal cells are connected directly to the cones, this might well be between the receptors themselves.

Arguing between turtle and fish retinas (page 102), there seem to be two kinds of pathway between individual cone cells. It is now well established that turtle cones of like spectral sensitivity are in selective electrical continuity with one another (Baylor, Fuortes & O'Bryan 1970; Baylor & Hodgkin 1973), over a range probably insignificant in relation to the optical blur of the retinal image (cf. §1, figure 22). Apposition contacts between the basal processes of the cone pedicles are a likely substrate for this pooling of signals *within* the colour channels.

The invaginating connexions of the basal processes seem to constitute a separate pathway between the cones, for we have seen in the fish that they link opponent colour cone pedicles (plate 11, figure 77 and text). What is known of their anatomy does not in fact firmly show that they *directly* link the cones they concern, for they terminate in more close spatial association with the lateral elements (horizontal cell) of triads than with the ribbon apparatus of the pedicles they invaginate (Lasansky 1971).

However, very infrequently, recordings from cones have demonstrated physiological interactions between neighbouring receptors that are more complex than the selective electrical continuity. Baylor *et al.* (1970) described an instance where polarization of one cone resulted in an opposite voltage deflexion in its neighbour, transmitted directionally between them. It is tempting to speculate that the invaginating basal processes might be the substrate of this interaction, the more so in view of the present finding that, in fish at least, these connexions link just the colour channels that are known at one stage or other to participate in antagonistic interactions.

However, clear though the morphological connexions between different cones may be (figures 71 and 72, plate 11, figure 77), and difficult though it is to imagine they underlie anything but physiological antagonism, there are substantial reasons to question this speculation. First of all, it is odd that complex physiological interactions between cones are so rarely found (Baylor *et al.* 1970) when the invaginating basal processes, their putative basis, form such a prominent system of connexions. Also, action spectra intercepted physiologically or behaviourally at a variety of levels in the visual pathway can closely fit the pigment absorption spectra (Naka & Rushton 1966*c*; Spekreijse *et al.* 1972; Muntz & Northmore 1971*a*). Were the cones themselves to antagonize one another, responses *throughout* the visual pathway ought without exception to reflect the distortion of the action spectra of the three colour channels such interaction should necessarily involve.

6. Synaptic organization in the outer plexiform layer and the univariance principle

The particular way receptor terminals are organized in the outer plexiform layer enabled the synaptic connexions of the bipolars to be recognized with ease and certainty. At that level of scrutiny, it was unnecessary to raise any of the ultrastructural issues as to the exact criteria for functional synaptic connexion, and there was a reassuring correlation between the morphology of bipolars in the light microscope and the consistent patterns of receptor synapsis that they make. It is natural to consider the combinations and segregations of cone input these connexions effect as *operations* upon the basic colour signals generated by the cones.

Nevertheless, while it is *anatomically* correct to speak of rod bipolars, say, as connecting to

red cones, this does not go as far as to describe the wavelength characteristics of the signals they convey. There is now a lot of evidence that the Univariance principle (Naka & Rushton 1966*b*) holds only for the basic transduction process in the cones, and that their electrical activity is also profoundly dependent upon activity in different colour channels. In the turtle, red and green cones over a wide retinal area antagonize, via the horizontal cells, the responses of individual red cones (Fuortes *et al.* 1973), and presumably equally complex interactions govern the activity of the other types of cones. It would be surprising to find that the complex horizontal cell population in fish did not effect similar colour coded feedback onto the cones. Furthermore, the invaginating basal processes of the cone pedicles are most likely to mediate more local and direct interactions between the colour channels.

Evidently, therefore, the responses conveyed even by the selective cone bipolars, which connect directly only to uniformly coloured cone populations within their dendritic trees, are likely to contain information from the other colour channels, collected in these two quite distinct (and indirect) ways. The situation is yet more complex in the case of the mixed cone bipolar cells: convergence of differently coloured cones onto their dendrites provides a third, sequential, station for chromatic interaction at this most peripheral level in the visual pathway.

This research was supported by a grant from the Science Research Council. It owes a great deal to the capability and enthusiasm of my assistant in Sussex, Mrs Jacqueline Morris, whom I thank, as I do also, Dr W. R. A. Muntz and Dr D. P. M. Northmore for many conversations about visual mechanisms. I am greatly indebted to Professor B. B. Boycott, F.R.S., for much helpful work on the manuscript, which was largely written in London with the support of the Medical Research Council.

REFERENCES

Bauer, V. 1910 Uber das farbenunterscheidungsvermögen der Fische. *Archiv. ges. Physiol.* **133**, 7–26.

Baylor, D. A., Fuortes, M. G. F. & O'Bryan, P. M. 1970 Receptive fields of cones in the retina of the turtle. *J. Physiol., Lond.* **214**, 265–294.

Baylor, D. A. & Hodgkin, A. L. 1973 Detection and resolution of visual stimuli by turtle photoreceptors. *J. Physiol., Lond.* **234**, 163–198.

Beauchamp, R. D. & Daw, N. W. 1972 Rod and cone input to single goldfish optic nerve fibres. *Vision Res.* **12**, 1201–1212.

Boycott, B. B. & Dowling, J. E. 1969 Organization of the primate retina: light microscopy. *Phil. Trans. R. Soc. Lond.* B **255**, 109–184.

Boycott, B. B. & Kolb, H. 1973 The connections between bipolar cells and photoreceptors in the retina of the domestic cat. *J. comp. Neurol.* **148**, 91–114.

Brown, P. K. & Wald, G. 1964 Visual pigments in single rods and cones of the human retina. *Science, N.Y.* **144**, 45–52.

Burkamp, W. 1923 Versuche über das Farbenwidererkennen der Fische. *Zeit. Psychol. Physiol. Sinnesorgane. Abt. II.* **55**, 133–170.

Cajal, S. R. 1892 La rétine des vertébrés. *Cellule.* **9**. Trans. by S. A. Thorpe & M. Glickstein in *The structure of the retina.* Springfield, Ill.: Thomas.

Charman, W. N. & Tucker, J. 1972 The optical system of the goldfish eye. *Vision Res.* **13**, 1–8.

Cohen, A. I. 1965 Some electron microscopic observations on interreceptor contacts in the human and macaque retina. *J. Anat., Lond.* **99**, 595–610.

Cohen, A. I. 1972 Rods and cones. In *Handbook of Sensory Physiology* (ed. M. G. F. Fuortes), VII/1.B. Berlin: Springer Verlag.

Daw, N. W. 1967 Colour coded units in the goldfish retina. Ph.D. Thesis, Johns Hopkins University, Baltimore.

Daw, N. W. 1967 Goldfish retina, organisation for simultaneous colour contrast. *Science, N.Y.* **158**, 942–944.

Daw, N. W. 1968 Colour coded ganglion cells in the goldfish retina: extension of their receptive fields by means of new stimuli. *J. Physiol., Lond.* **197**, 567–592.

Daw, N. W. 1973 Neurophysiology of colour vision. *Physiol. Rev.* **53**, 571–611.

Daw, N. W. & Beauchamp, R. D. 1972 Unusual units in the goldfish optic nerve. *Vision Res.* **12**, 1849–1856.
Denton, E. J. & Wyllie, J. A. 1955 Study of the photosensitive pigments in the pink and green rods of the frog. *J. Physiol., Lond.* **127**, 81–89.
Dowling, J. E. 1965 Foveal receptors of the monkey retina: fine structure. *Science, N.Y.* **147**, 57–59.
Dowling, J. E. 1968 Synaptic organization of the frog retina: an electron microscopic analysis comparing the retinas of frogs and primates. *Proc. R. Soc. Lond.* B **170** 205–228.
Dowling, J. E. & Boycott, B. B. 1966 Organization of the primate retina: electron microscopy. *Proc. R. Soc. Lond.* B **166**, 80–111.
Eberle, H. 1967 Cone length and chromatic abberation in Lebistes reticulates. *Z. vergl. Physiol.* **57**, 172–173.
Engström, K. 1960 Cone types and cone arrangements in the retina of some Cyprinids. *Acta. Zoologica* **41**, 277–295.
Evans, E. M. 1966 On the ultrastructure of the synaptic region of visual receptors in certain vertebrates. *Z. Zellforsch.* **71**, 499–516.
Fletcher, A., Murphy, P. & Young, A. 1954 Solutions of two optical problems. *Proc. R. Soc. Lond.* A **223**, 216–225.
Fuortes, M. G. F., Schwartz, E. A. & Simon, E. J. 1973 Colour dependence of cone responses in the turtle retina. *J. Physiol., Lond.* **234**, 199–216.
Fuortes, M. G. F. 1972 Responses of cones and horizontal cells in the retina of the turtle. *Invest. Ophthalmol.* **11**, 275–284.
Furst, C. 1904 Zur Kenntnis der Histogenese und des Wachstums der Retina. *Lunds Univ. Arsskrift* **40**, Avd. 2(1), 1–45.
Goodland, H. 1966 The ultrastructure of the inner plexiform layer of the retina of *Cottus bubalis*. *Exp. Eye Res.* **5**, 198–200.
Greef, R. 1900 Die mikroscopische Anatomie der Sehnerven und der Netzhaut. In *Handbuch der gesamten Augenheilkunde.* (ed. Graefe-Saemisch), 1–212. Leipzig.
Hamburger, V. 1926 Versuche über Komplementär-Farben bei Ellritze (*Phoximus laevis*). *Z. vergl. Physiol.* **4**, 286–304.
Hibbard, E. 1971 Grid patterns in the retinal organisation of the cichlid fish *Astronotus ocellatus*. *Exp. Eye Res.* **12**, 175–180.
Hubel, D. H. & Wiesel, T. N. 1968 Receptive fields and functional architecture in monkey striate cortex. *J. Physiol., Lond.* **195**, 215–243.
Ivanov, A. 1953 *Les aberrations de l'oeil.* Paris: Editions de la Revue d'optique.
Kaneko, A. 1970 Physiological and morphological identification of horizontal, bipolar and amacrine cells in goldfish retina. *J. Physiol., Lond.* **207**, 623–633.
Kaneko, A. 1971 Physiological studies of single retinal cells and their morphological identification. *Vision Res. Suppl.* **3**, 17–26.
Kaneko, A. 1973 Receptive field organisation of bipolar and amacrine cells in the goldfish retina. *J. Physiol., Lond.* **235**, 133–153.
King-Smith, P. E. 1969 Absorption spectra and function of the coloured oil droplets in the pigeon retina. *Vision Res.* **9**, 1391–1399.
Kolb, H. 1970 Organisation of the outer plexiform layer of the primate retina: electron microscopy of Golgi-impregnated cells. *Phil. Trans. R. Soc. Lond.* B **258**, 261–283.
Ladman, A. J. 1958 The fine structure of the rod-bipolar cell synapse in the retina of the albino rat. *J. biophys. biochem. Cytol.* **4**, 459–466.
Lasansky, A. 1969 Basal junctions at synaptic endings of turtle visual cells. *J. Cell. Biol.* **40**, 577–581.
Lasansky, A. 1971 Synaptic organization of cone cells in the turtle retina. *Phil. Trans. R. Soc. Lond.* B **262**, 365–381.
Lasansky, A. 1972 Cell junctions at the outer synaptic layer of the retina. *Invest. Ophthalmol.* **11**, 265–274.
Lasansky, A. 1973 Organization of the outer synaptic layer in the retina of the larval tiger salamander. *Phil. Trans. R. Soc. Lond.* B **265**, 471–489.
Laties, A. M. & Liebman, P. A. 1970 Cones of living amphibian eye: selective staining, *Science, N.Y.* **168**, 1475–1477.
Lettvin, J. Y., Maturana, H., Pitts, W. H. & McCulloch, W. S. 1961 Two remarks on the visual system of the frog. In *Sensory communication* (ed. W. A. Rosenblith). Cambridge and New York: Technology Press and Wiley.
Liebman, P. A. 1972 Microspectrophotometry of photoreceptors. In *Handbook of sensory physiology*, vol. VII/1, 482–528. Berlin: Springer Verlag.
Liebman, P. A. & Entine, G. 1968 Visual pigments of frog and tadpole. *Vision Res.* **8**, 761–775.
Liebman, P. A. & Granda, A. M. 1971 Microspectrophotometric measurements of visual pigments in two species of turtles (*Pseudemys scripta* and *Chelonia mydas*). *Vision Res.* **4**, 105–114.
Lyall, A. H. 1957*a* The growth of the trout retina. *Q. Jl micr. Sci.* **98**, 101–110.
Lyall, A. H. 1957*b* Cone arrangements in teleost retinal. *Q. Jl micr. Sci.* **98**, 189–201.

MacNichol, E. F., Wolbarsht, M. L. & Wagner, H. G. 1961 Electrophysiological evidence for a mechanism of color vision in the goldfish. In *Light and life* (ed. W. D. McElroy & Bentley Glass). Baltimore: The Johns Hopkins Press.

Marks, W. B. 1965 Visual pigments of single goldfish cones. *J. Physiol., Lond.* **178**, 14–32.

Marks, W. B., Dobelle, W. H. & MacNichol, E. F. 1964 Visual pigments of single primate cones. *Science, N.Y.* **143**, 1181–1183.

McCann, J. J. & Benton, J. L. 1969 Interaction of the long wave cones and the rods to produce color sensations. *J. Opt. Soc. Am.* **59**, 103–107.

Missotten, L. 1966 *The ultrastructure of the human retina.* Brussels: Arscia. Uitgaven N.V.

Missotten, L., Apelmanns, M. & Michiels, J. 1963 L'ultrastructure des synapses des cellules visuelles de la rétine humaine. *Bull. Mém. Soc. franc. Ophthal.* **76**, 59–82.

Morris, V. B. & Storey, C. D. 1967 An electron microscope study of types of receptor in the chick retina. *J. comp. Neurol.* **129**, 313–340.

Müller, H. 1952 Bau and Wachstum der Netzhaut des Guppy (*Lebistes reticulatus*). *Zool. Jahrb., Abt. f. Zool. u. Physiol.* **63**, 275–322.

Muntz, W. R. A. 1962 Microelectrode recordings from the diencephalon of the frog and a blue sensitive system. *J. Neurophysiol.* **25**, 712–720.

Muntz, W. R. A. & Northmore, D. P. M. 1970 Vision and visual pigments in a fish, *Scardinius erythrophthalmus*, the Rudd. *Vision Res.* **10**, 281–298.

Muntz, W. R. A. & Northmore, D. P. M. 1971*a* The independence of the photopic receptor systems underlying visual thresholds in a teleost. *Vision Res.* **11**, 861–867.

Muntz, W. R. A. & Northmore, D. P. M. 1971*b* Visual pigments from different parts of the retina in rudd and trout. *Vision Res.* **11**, 551–561.

Naka, K.-I. 1971 The horizontal cells. *Vision Res.* **12**, 573–588.

Naka, K.-I. & Rushton, W. A. H. 1966*a* *S*-potentials from colour units in the retina of fish (*Cyprinidae*). *J. Physiol., Lond.* **185**, 536–555.

Naka, K.-I. & Rushton, W. A. H. 1966*b* An attempt to analyse colour reception by electrophysiology. *J. Physiol., Lond.* **185**, 556–586.

Naka, K.-I. & Rushton, W. A. H. 1966*c* *S*-potentials from luminosity units in the retina of fish. *J. Physiol., Lond.* **185**, 587–599.

Nilsson, S.-E. G. 1964*a* An electron microscope classification of the retinal receptors of the leopard frog. *J. Ultrastruct. Res.* **10**, 340–416.

Nilsson, S.-E. G. 1964*b* Interreceptor contacts in the retina of the frog (*Rana pipiens*). *J. Ulstrastruct. Res.* **11**, 147–165.

Northmore, D. P. M. 1973 Ph.D. Thesis; University of Sussex.

Parthe, V. 1972 Horizontal, bipolar and oligopolar cells in the teleost retina. *Vision Res.* **12**, 395–406.

Pedler, C. 1965 Rods and cones: a fresh approach. In *Ciba Foundation Symposium on colour vision* (ed. A. V. S. deReuck & J. Knight), 52–83. London: J. & A. Churchill.

Polyak, S. L. 1941 *The retina.* Chicago: Chicago University Press.

Pomeranz, B. & Chung, S. H. 1970 Dendritic-tree anatomy codes form-vision physiology in tadpole retina. *Science, N.Y.* **170**, 983–984.

Pumphrey, R. J. 1961 Concerning vision. In *The cell and the organism* (ed. Ramsay, J. A.), 193–208. Cambridge University Press.

Raviola, E. & Gilula, B. N. 1973 Gap junctions between photoreceptor cells in the vertebrate retina. *Proc. natn. Acad. Sci. U.S.A.* **70**, 1677–1681.

Raynauld, J. P. 1972 Goldfish retina: sign of the rod input in opponent colour ganglion cells. *Science, N.Y.* **177**, 84–85.

Scholes, J. H. & Morris, J. 1973 Receptor-bipolar connectivity patterns in the fish retina. *Nature, Lond.*, **241**, 52–54.

Sjöstrand, F. S. 1969 The outer plexiform layer and the neural organization of the retina. In *The retina: morphology, function and clinical characteristics. U.C.L.A. forum in medical sciences* 8, (ed. B. R. Straatsma, M. O. Hall, R. A. Allen & F. Crescitelli), 63–100. Berkeley and Los Angeles: University of California Press.

Spekreijse, H. & Van den Berg, T. J. T. P. 1971 Interaction between colour and spatial coded processes converging to retinal ganglion cells in goldfish. *J. Physiol., Lond.* **215**, 679–692.

Spekreijse, H., Wagner, H. G. & Wolbarsht, M. L. 1972 Spectral and spatial coding of ganglion cell responses in goldfish retina. *J. Neurophysiol.* **35**, 73–86.

Stabell, V. & Stabell, B. 1965 Rods as color receptors. *Scand. J. Psychol.* **6**, 195–200.

Stell, W. K. 1965 Correlation of retinal cytoarchitecture and ultrastructure in Golgi preparations. *Anat. Rec.* **153**, 389–397.

Stell, W. K. 1967 The structure and relationships of horizontal cells and photoreceptor-bipolar synaptic complexes in goldfish retina. *Am. J. Anat.* **121**, 401, 423.

Stell, W. K. 1972 The morphological organization of the vertebrate retina. In *Handbook of sensory physiology* (ed. M. G. F. Fuortes), VII/1.B. Berlin: Springer Verlag.

Stiles, W. S. 1959 Colour vision: the approach through increment threshold sensitivity. *Proc. natn. Acad. Sci. U.S.A.* **45**, 100–114.

Svaetichin, G. & MacNichol, E. F. 1958 Retinal mechanisms for chromatic and achromatic vision. *Ann. N.Y. Acad. Sci.* **74**, 385–404.

Svaetichin, G., Negishi, K. & Fatehchand, R. 1965 Cellular mechanisms of a Young-Hering visual system. In *CIBA Foundation symposium on colour vision* (ed. A. V. S. deReuck & J. Knight), 178–203. London: J. & A. Churchill.

Tomita, T., Kaneko, A., Murakami, M. & Pautler, E. L. 1967 Spectral response curves of single cones in the carp. *Vision Res.* **9**, 453–463.

Toyoda, J-I. 1973 Membrane resistance changes underlying the bipolar cell response in the carp retina. *Vision Res.* **13**, 283–291.

Vrabec, Fr. 1966 A new finding in the retina of a marine teleost, *Callionymus lyra* L. *Folia Morphol.* **14**, 143–147.

Wagner, H. J. 1973*a* Die nervösen Netzhautelemente von *Nannacara anomala* (Cichlidae, Teleostei). I. Darstellung durch Silberimprägnation. *Z. Zellforsch.* **137**, 63–86.

Wagner, H. J. 1973*b* Die nervösen Netzhautelemente von *Nannacara anomala* (Cichlidae, Teleostei). II. Quantitative Verteilung. *Z. Zellforsch.* **137**, 87–95.

Wagner, H. G., MacNichol, E. F. & Wolbarsht, M. L. 1960 The response properties of single ganglion cells in the goldfish retina. *J. gen. Physiol.* **43**, *suppl* **6**, 45–62.

Walls, G. L. 1963 *The vertebrate eye and its adaptive radiation.* New York: Hafner Publishing Company.

Werblin, F. S. & Dowling, J. E. 1969 Organization of the retina of the mudpuppy *Necturus maculosus*. II. *J. Neurophysiol.* **32**, 339–355.

West, R. & Dowling, J. E. 1973 Synapses onto different morphological types of retinal ganglion cells. *Science, N.Y.* **178**, 510–512.

Yager, D. 1967 Behavioural measures and theoretical analysis of spectral sensitivity and spectral saturation in the goldfish (*Carassius auratus*). *Vision Res.* **7**, 707–727.

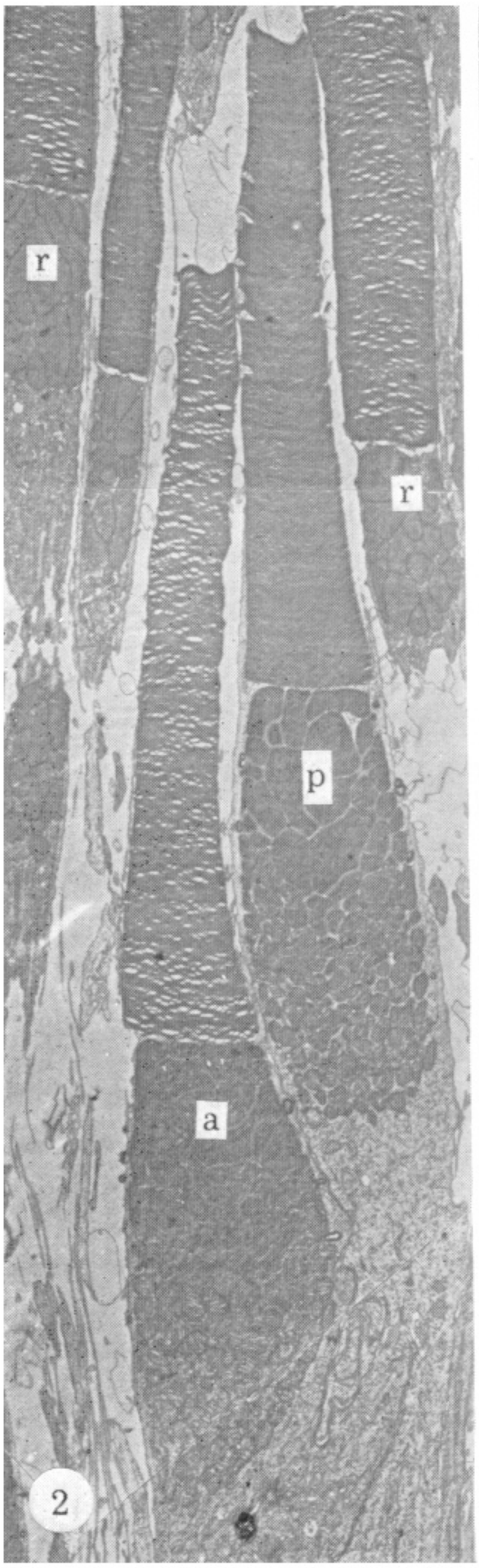

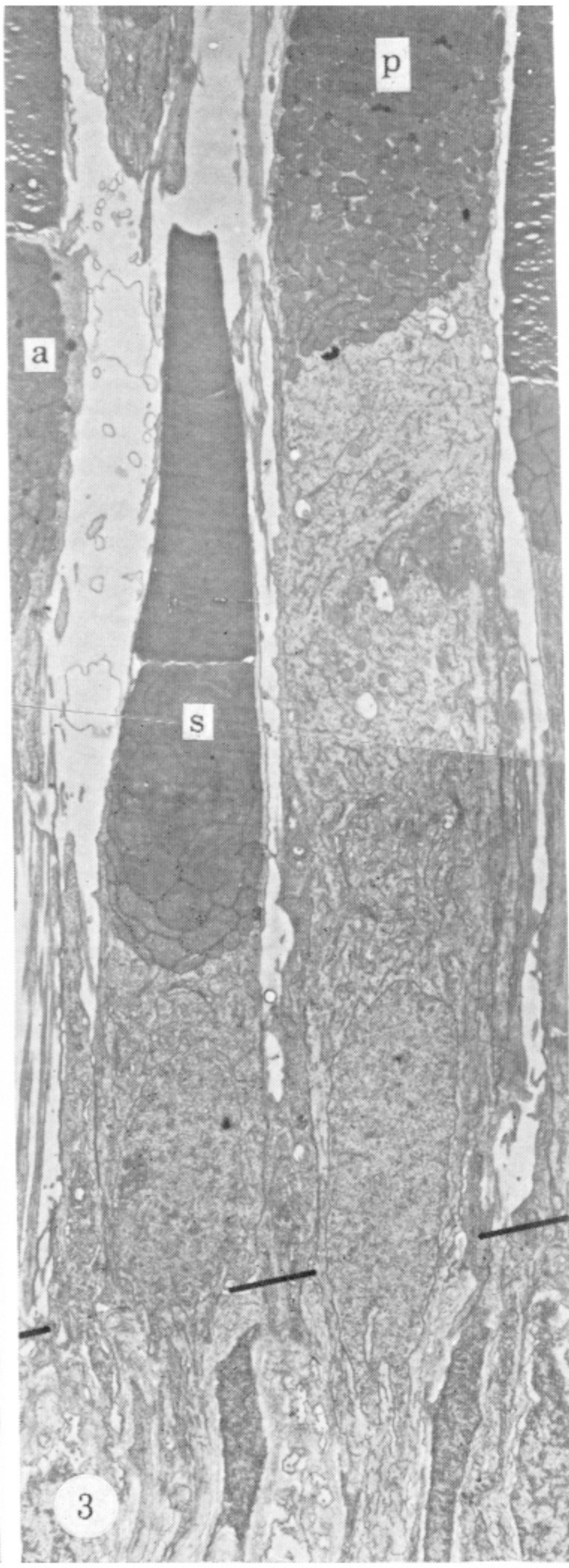

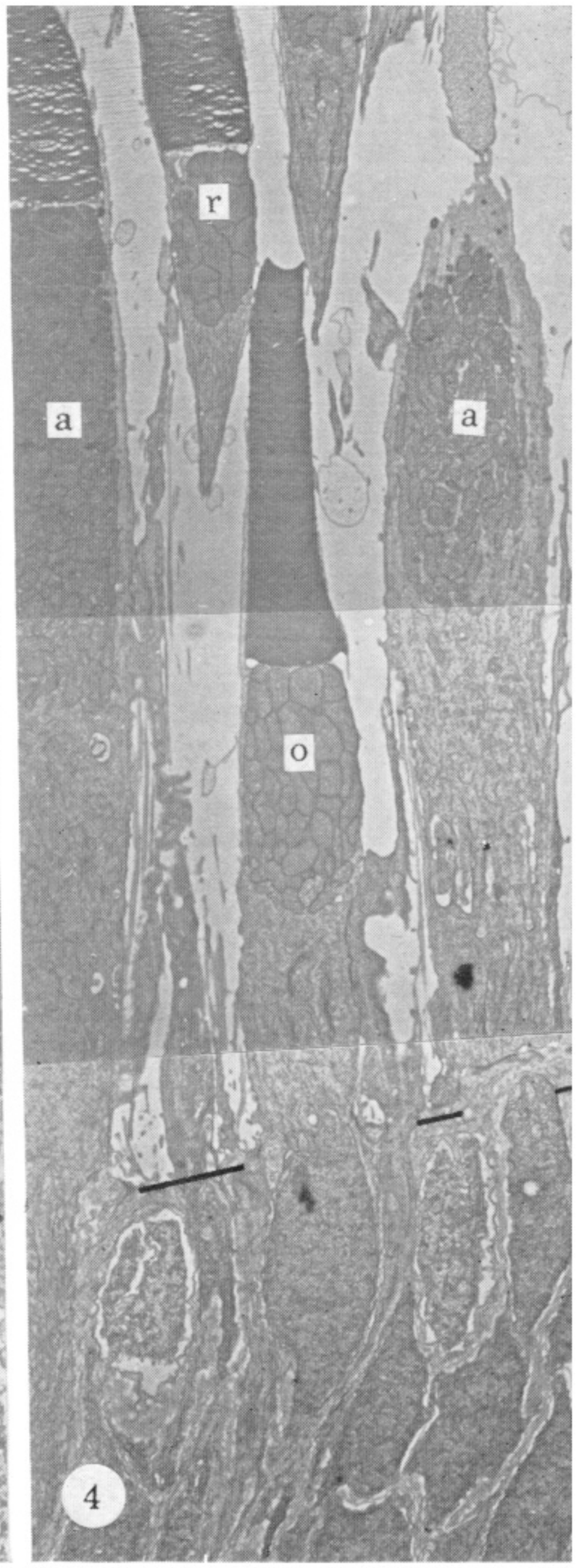

2

3

4

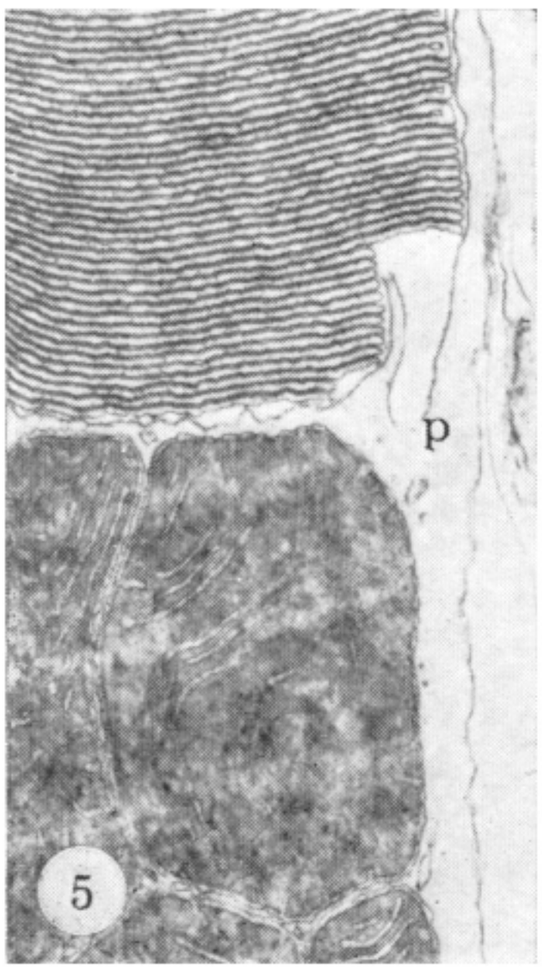

5

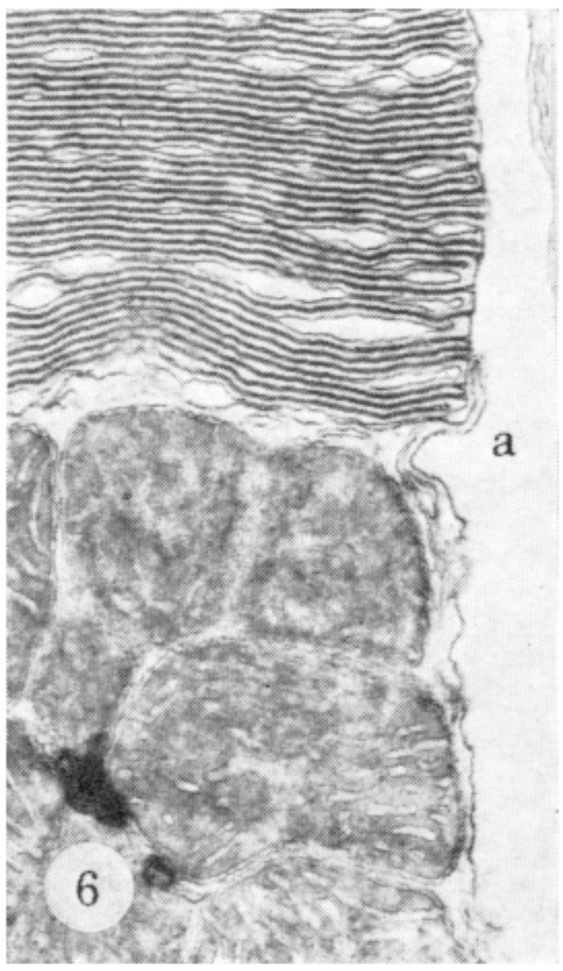

6

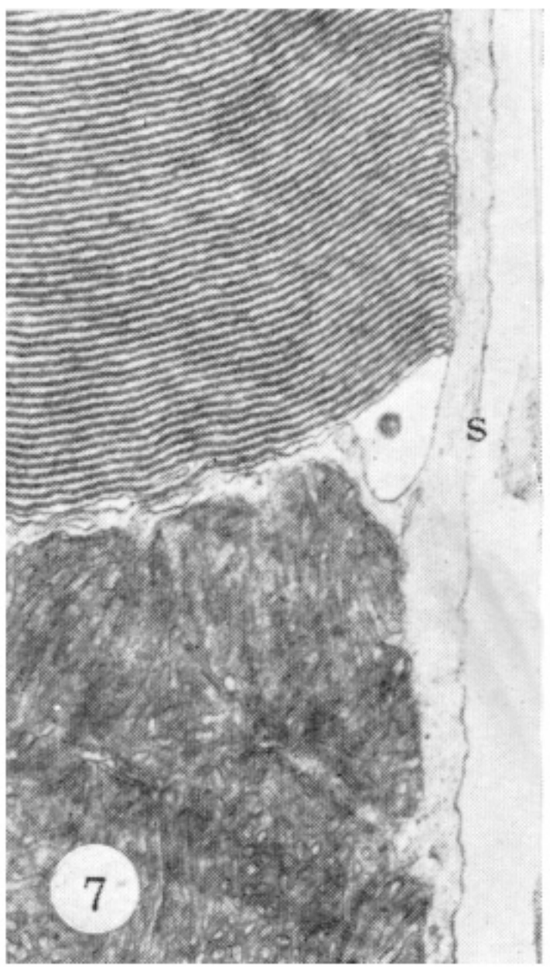

7

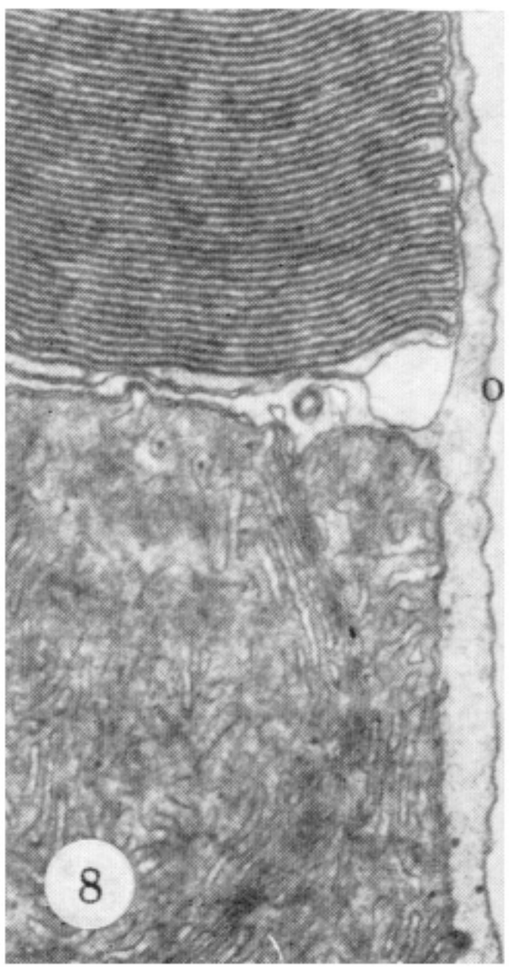

8

FIGURES 2–8. For description see opposite.

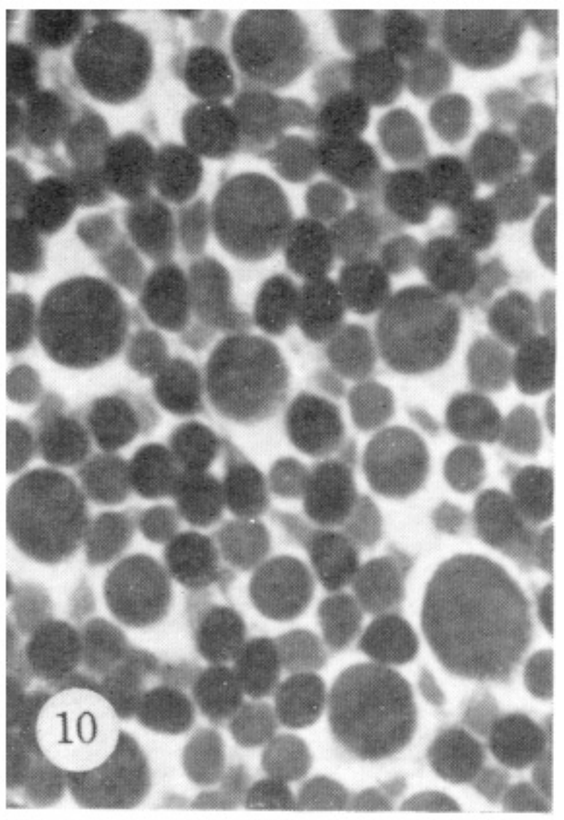

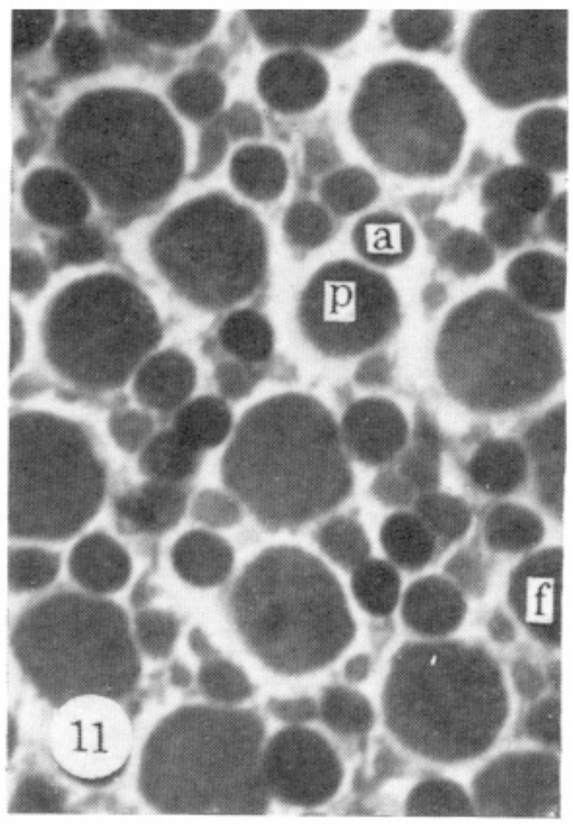

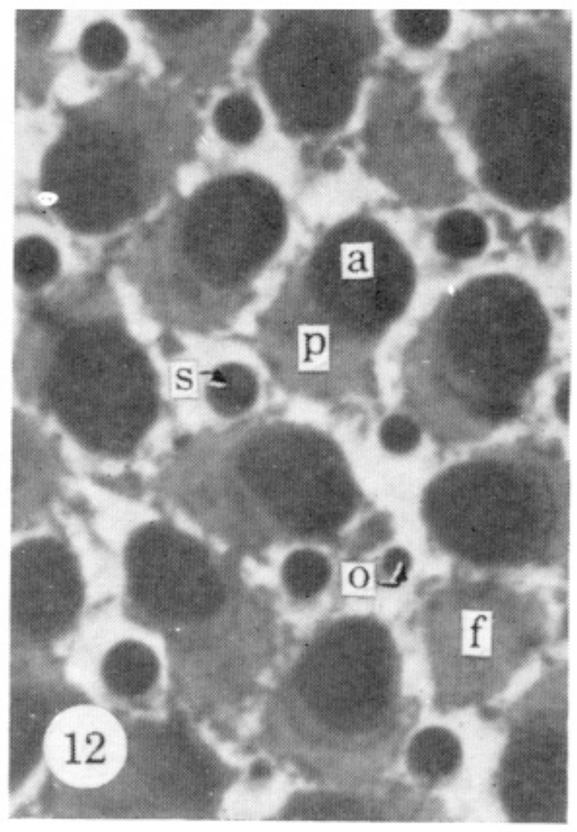

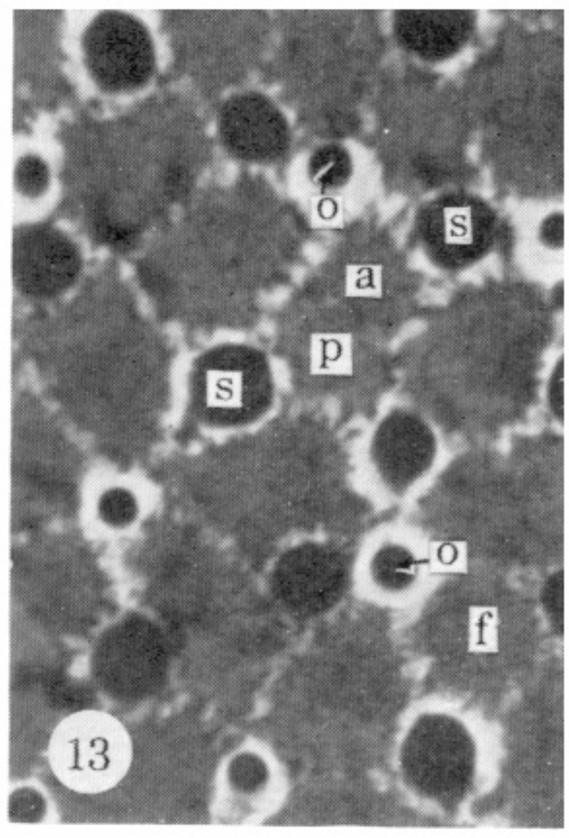

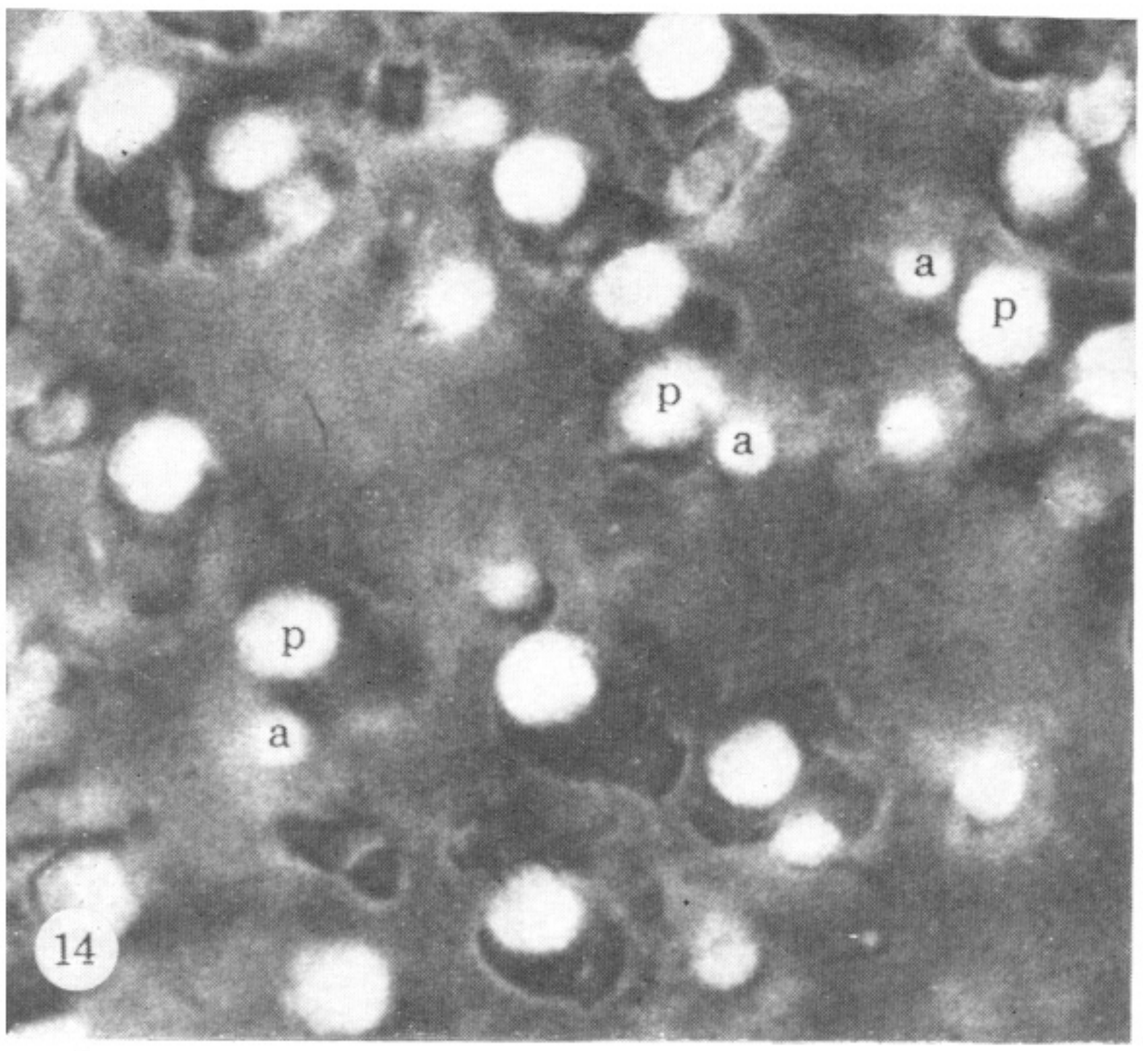

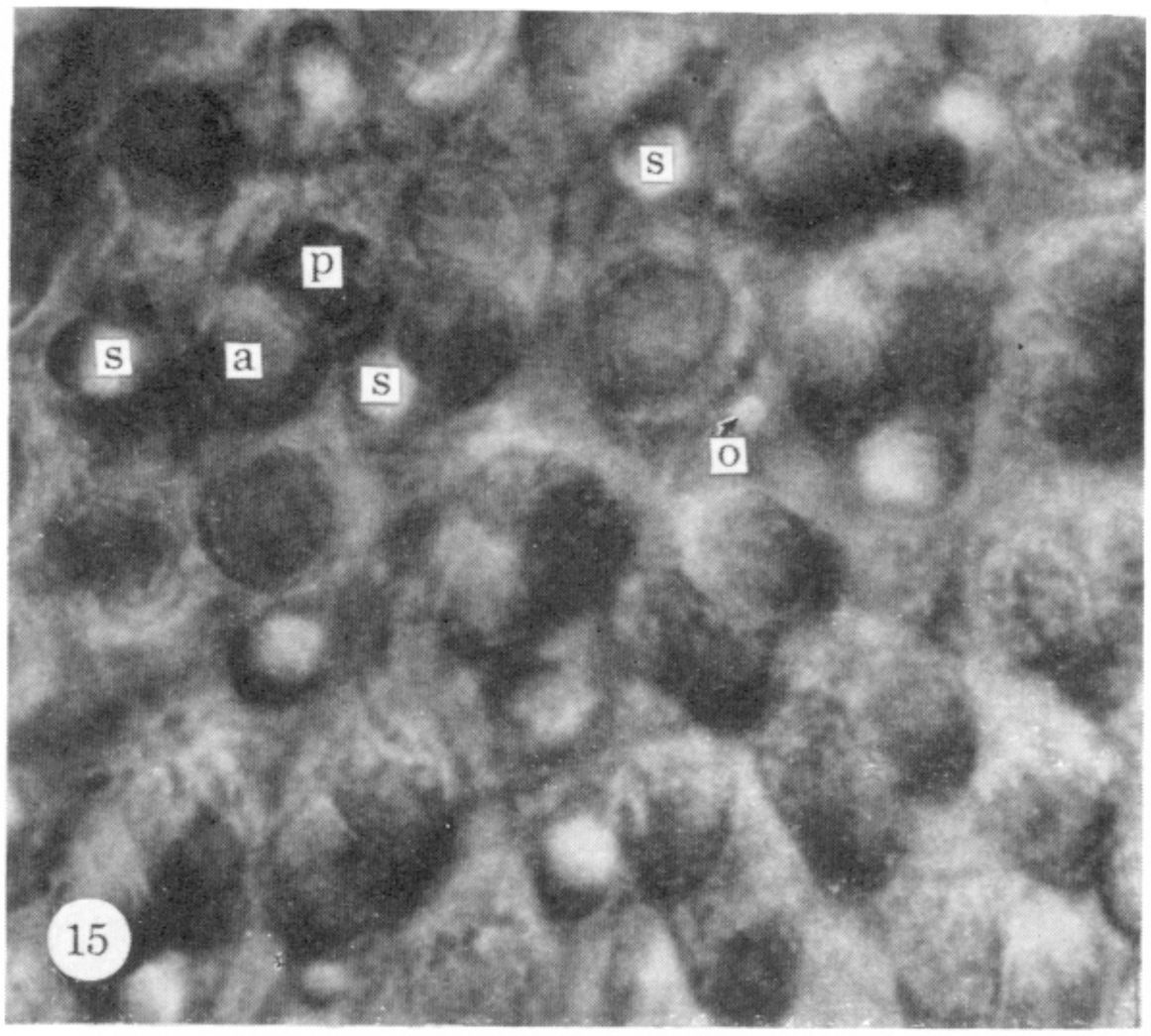

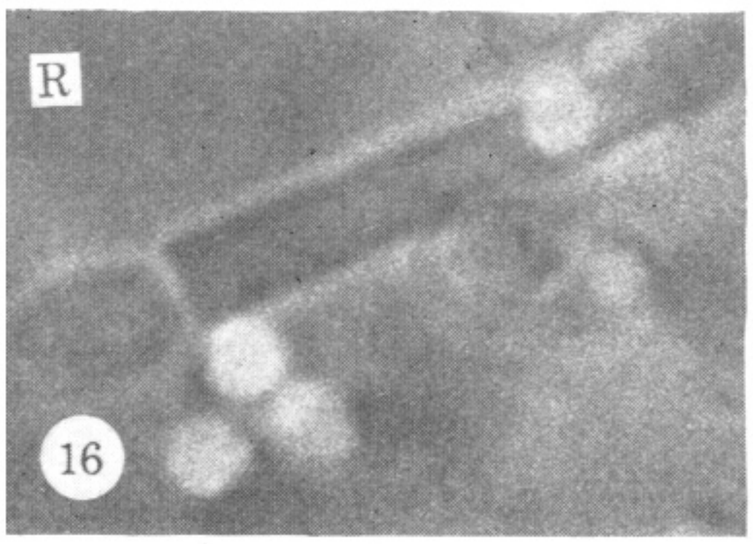

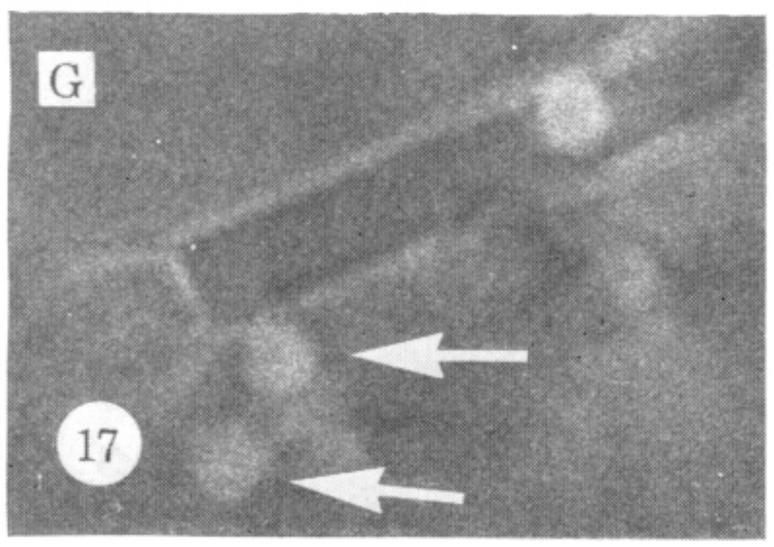

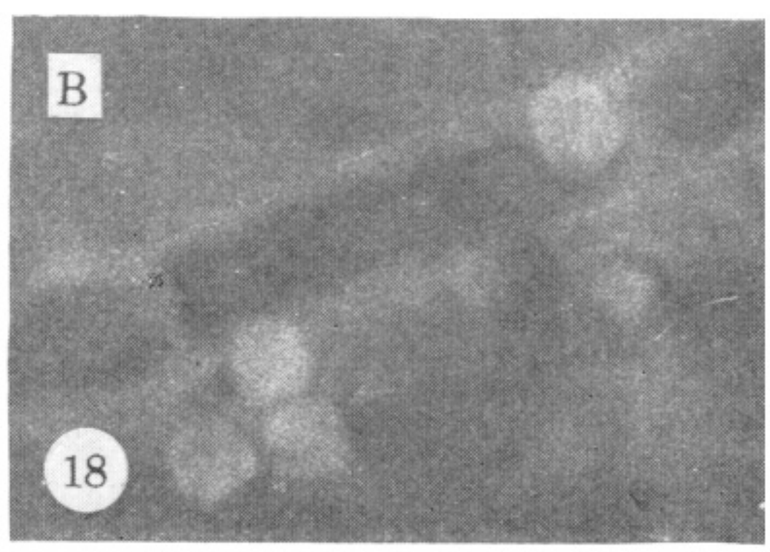

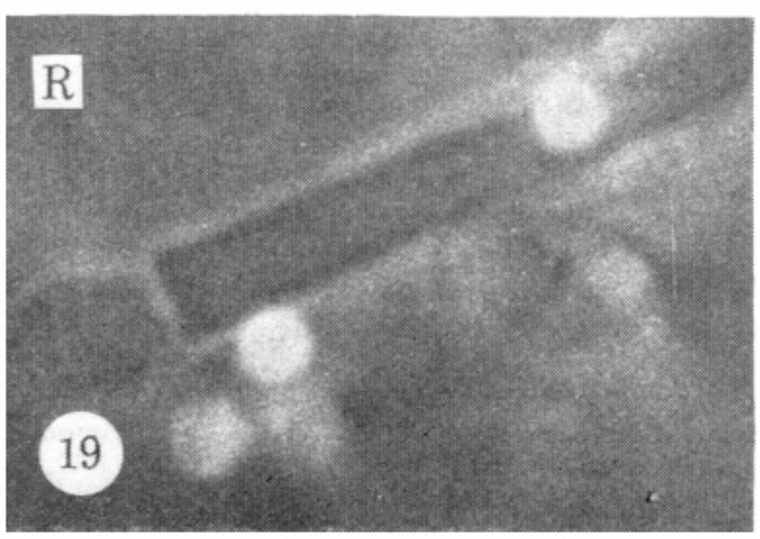

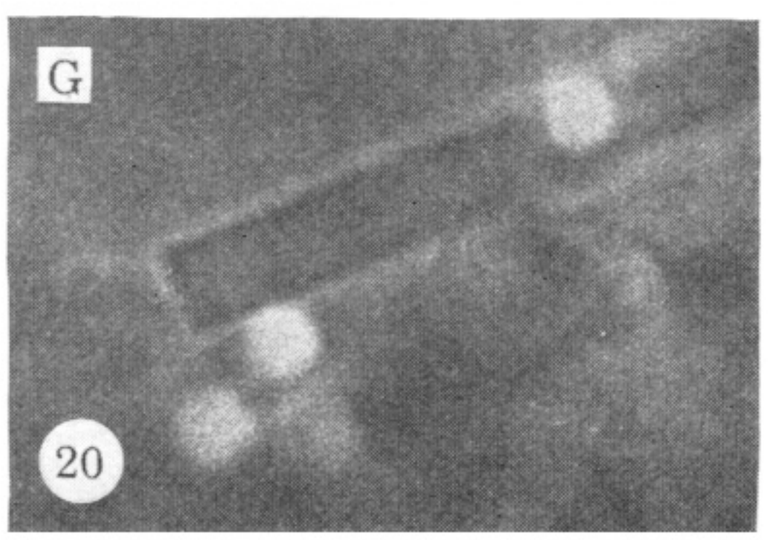

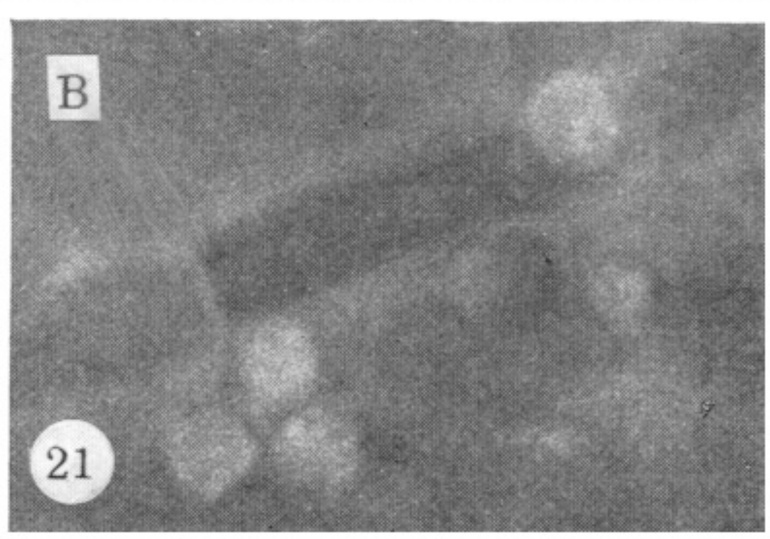

FIGURES 10–21. For description see opposite.

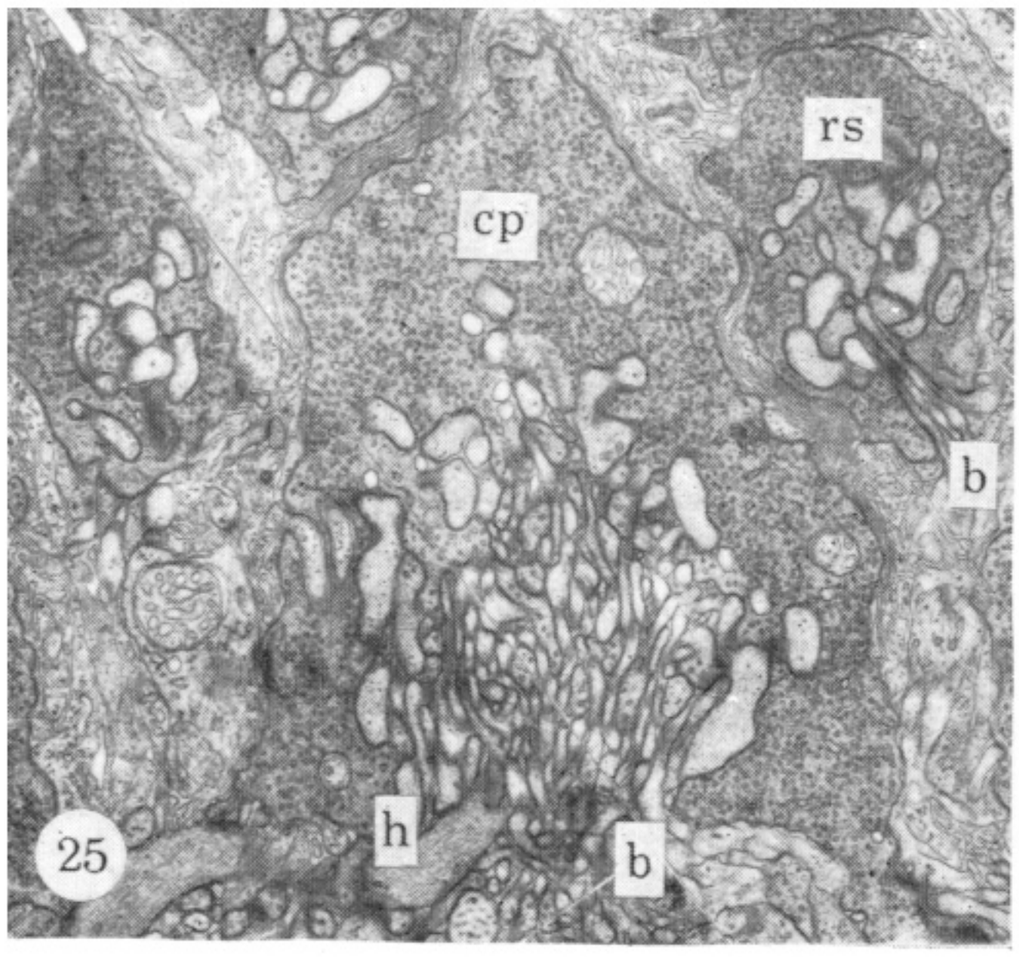

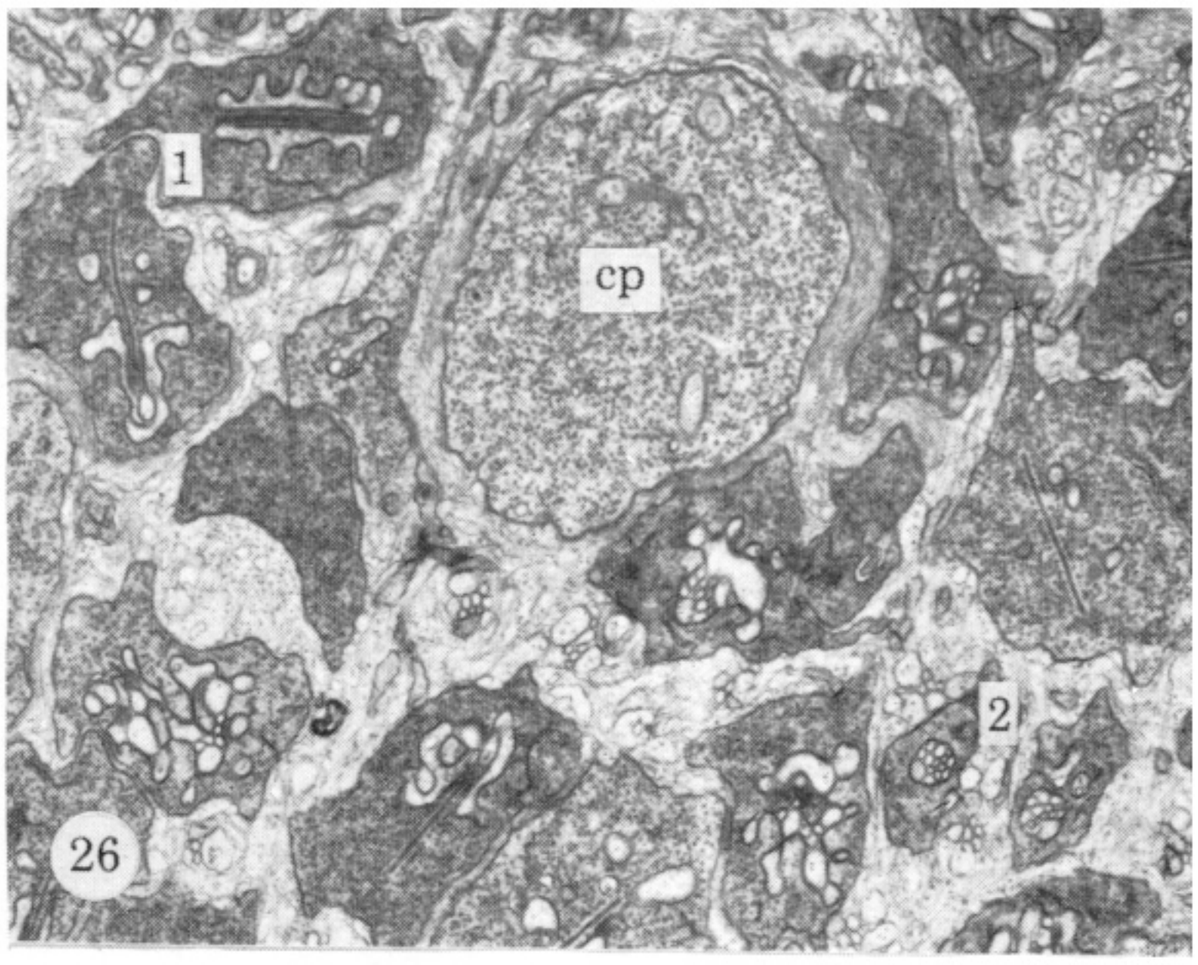

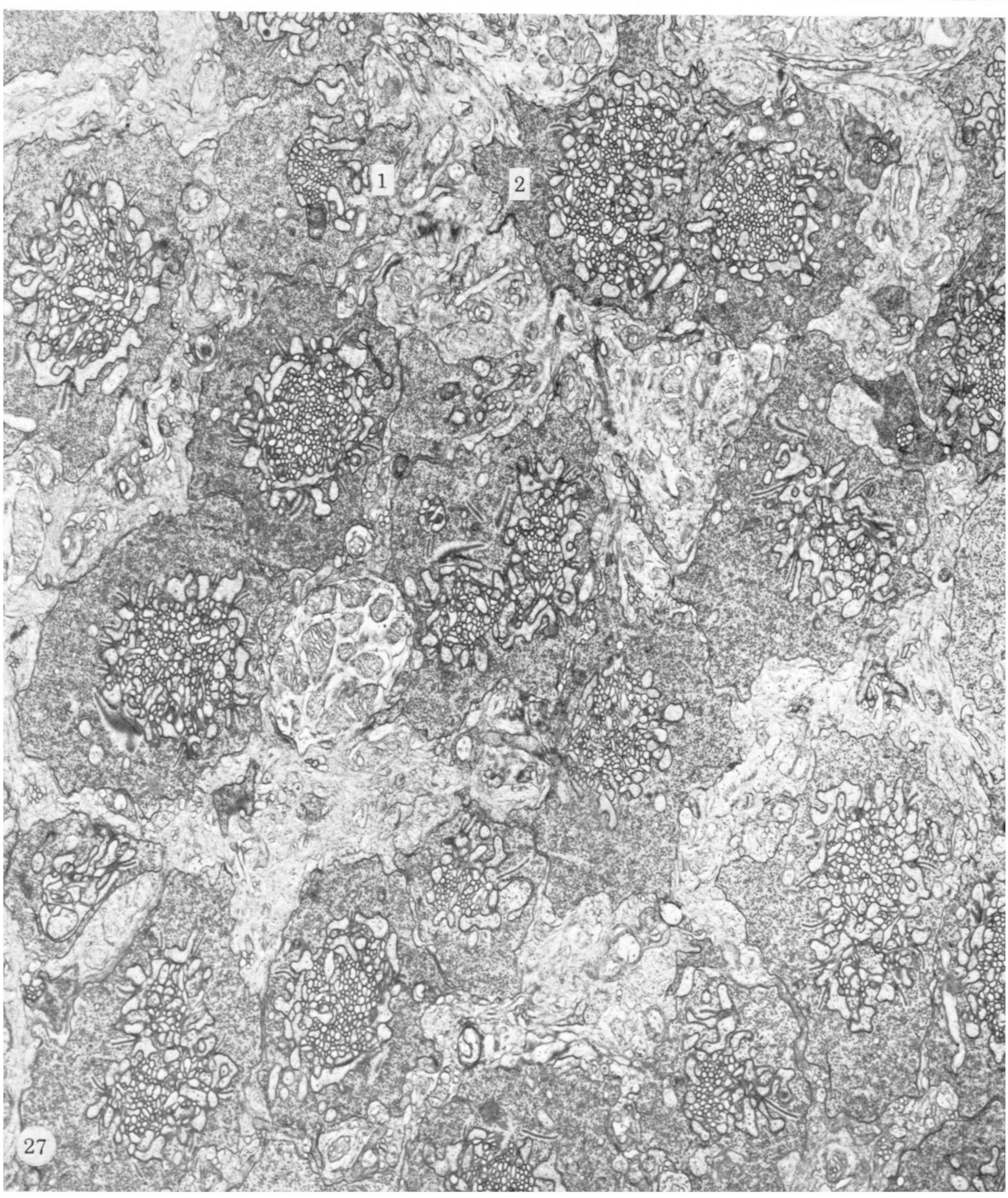

FIGURES 25–27. For description see opposite.

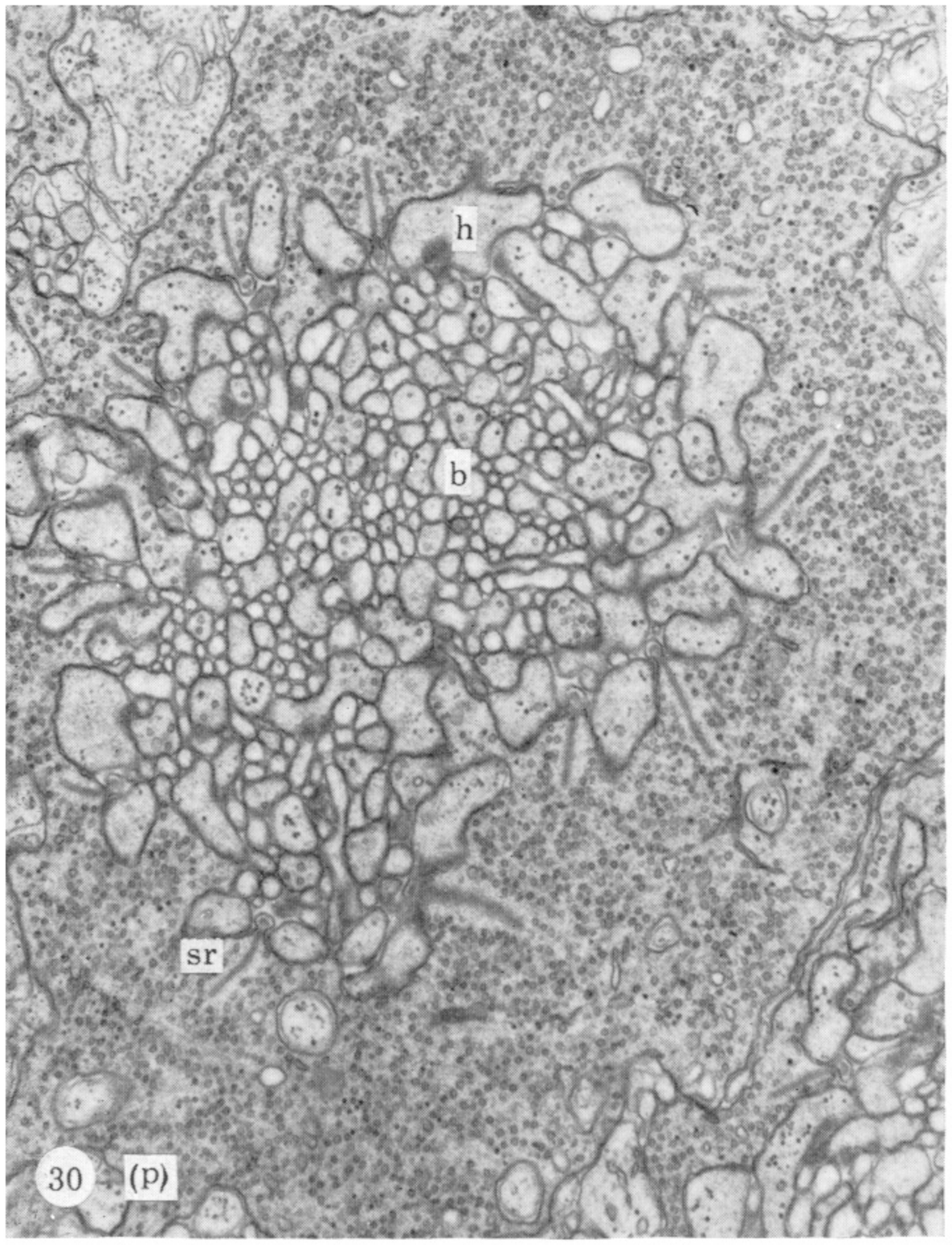

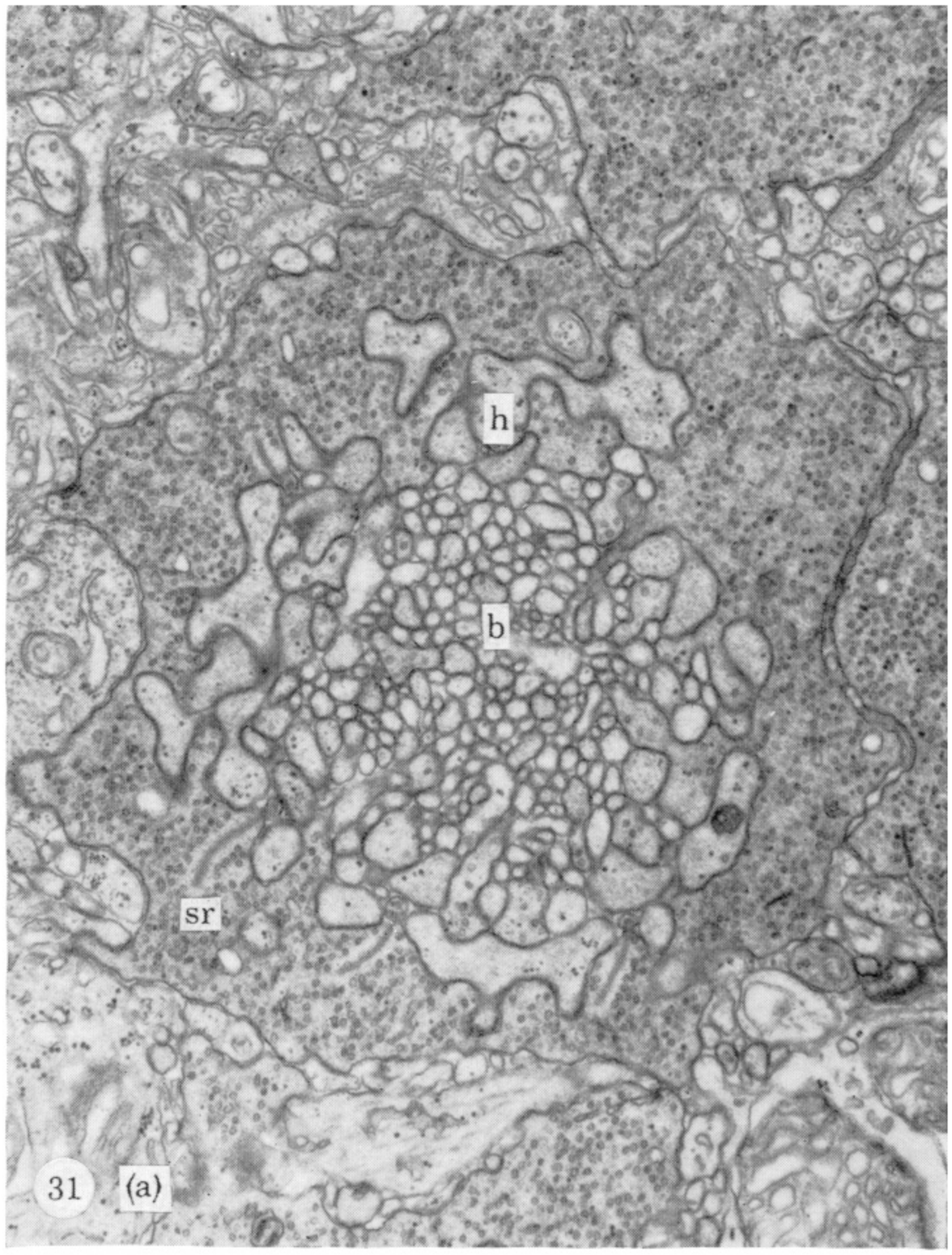

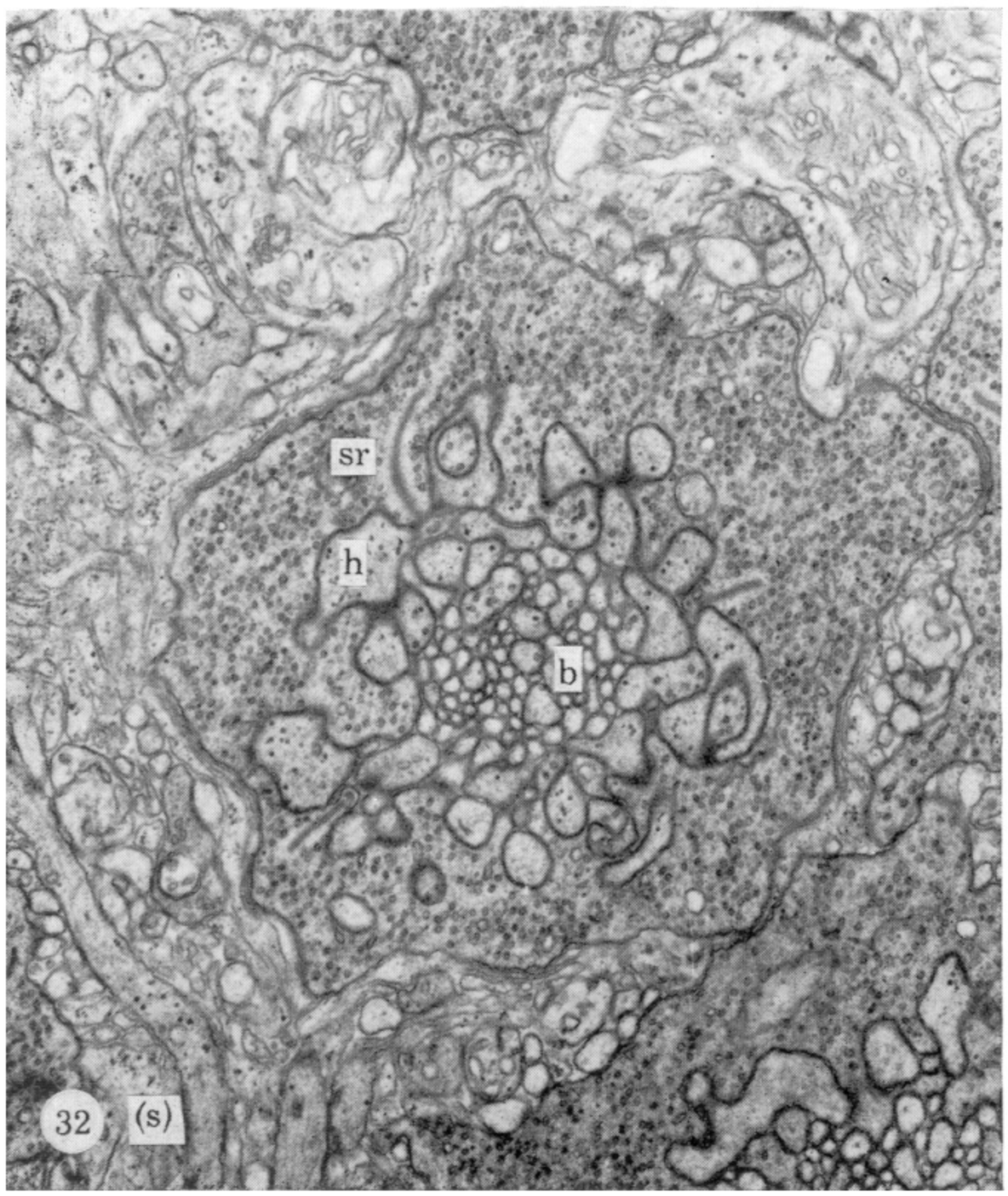

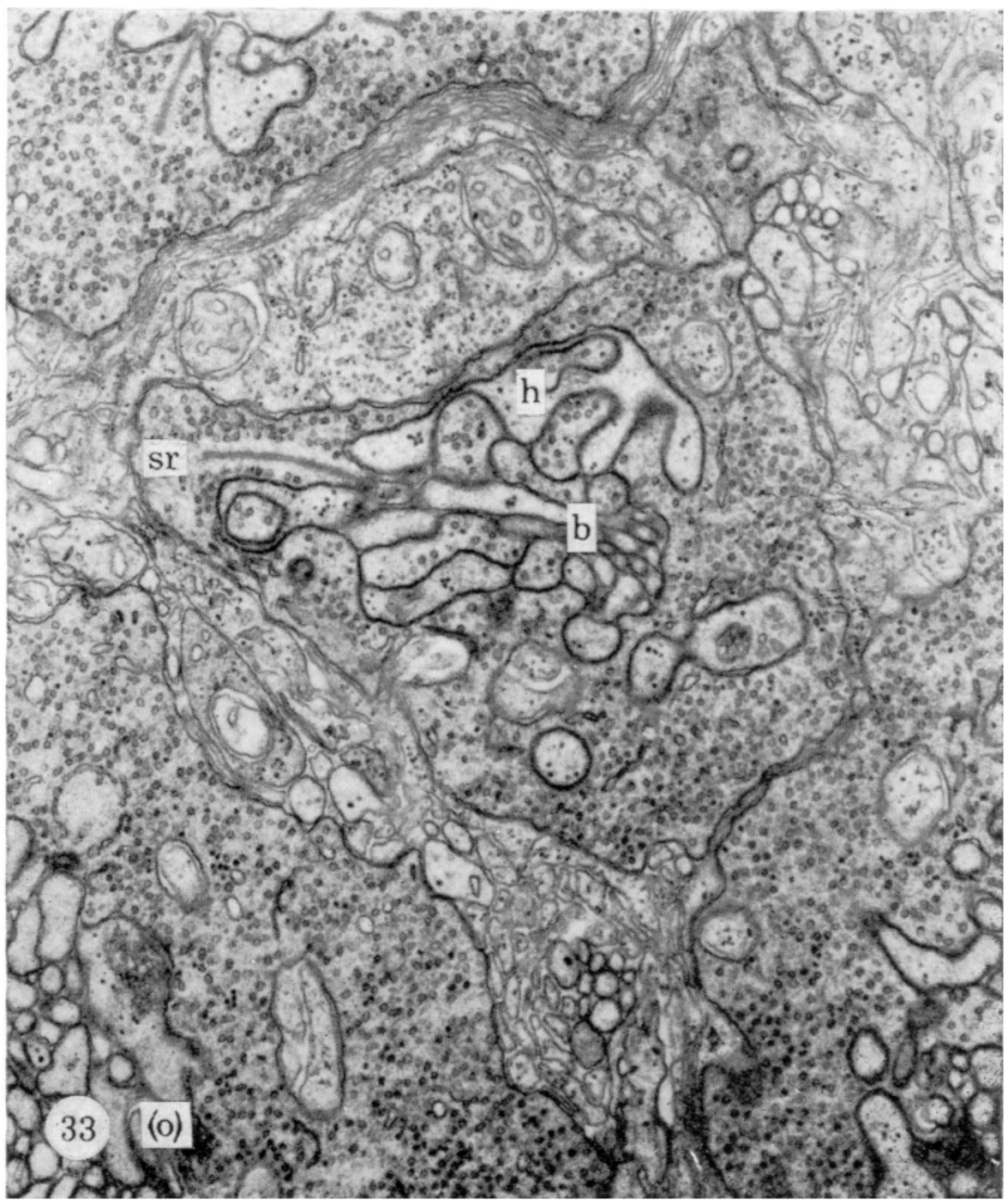

FIGURES 30–33. For description see opposite.

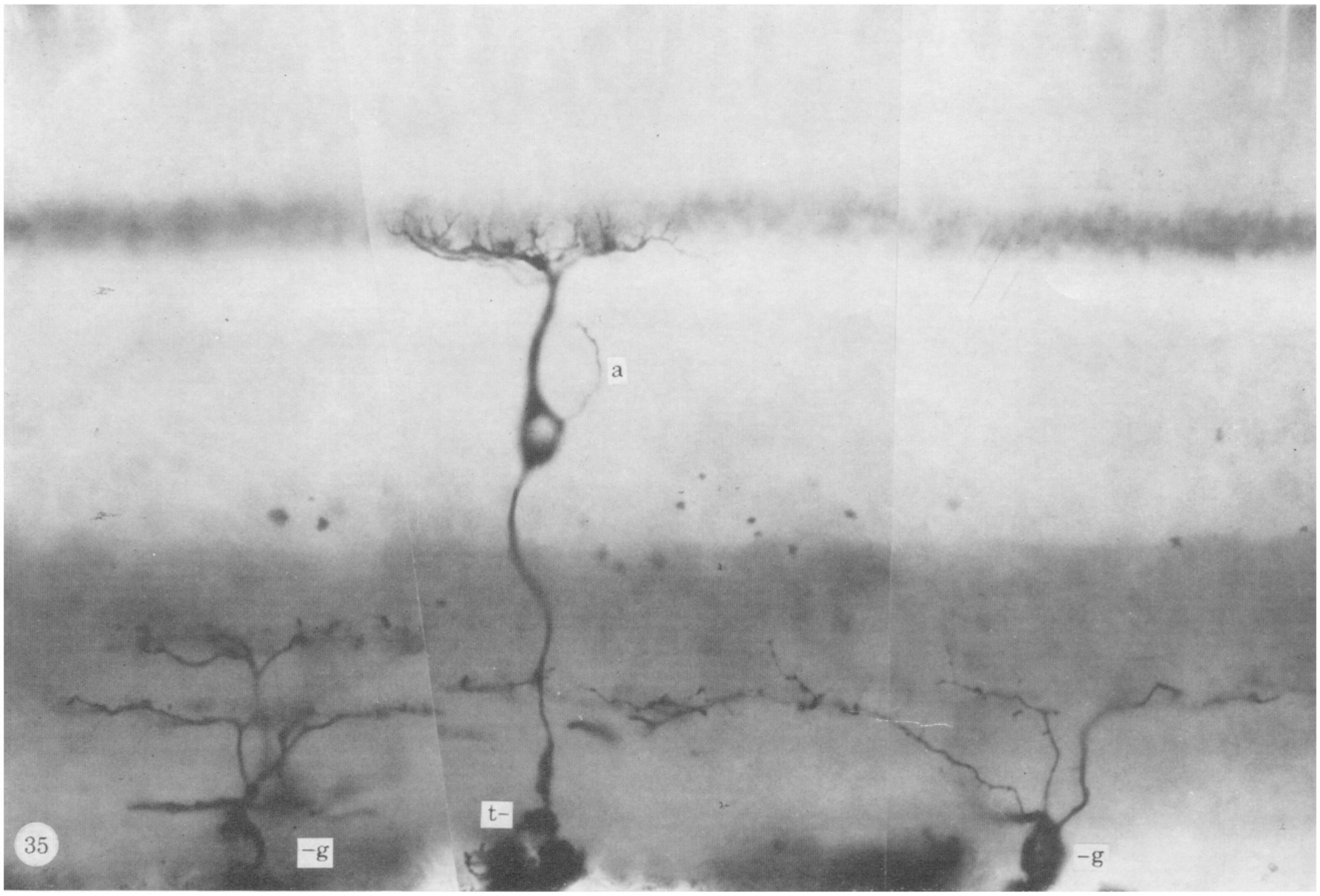

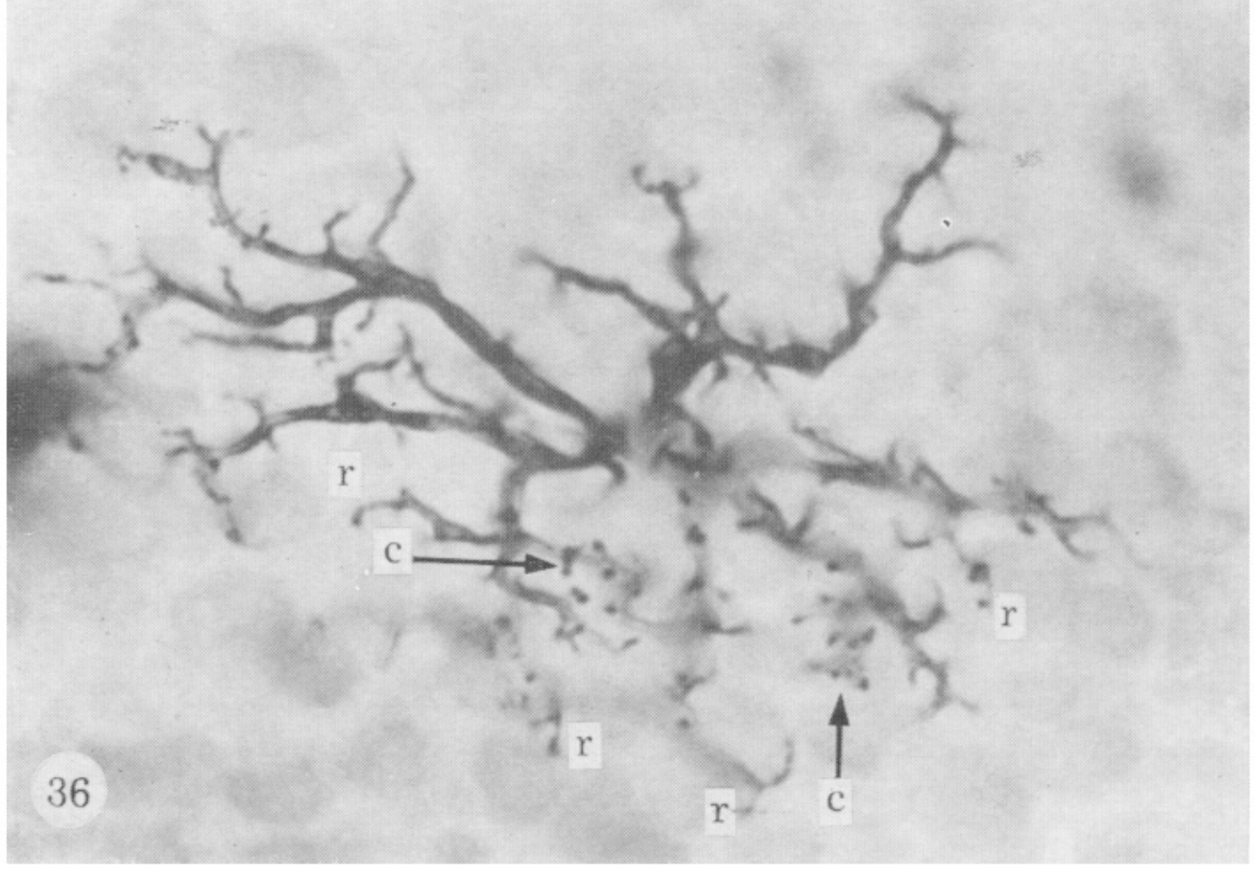

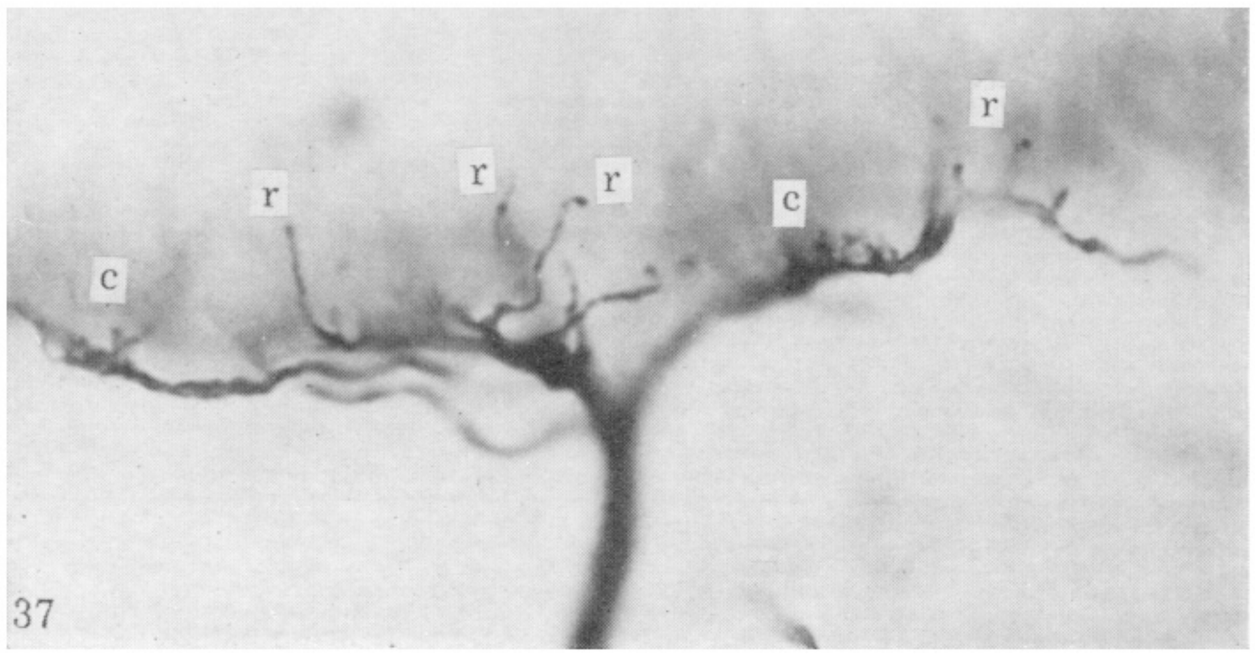

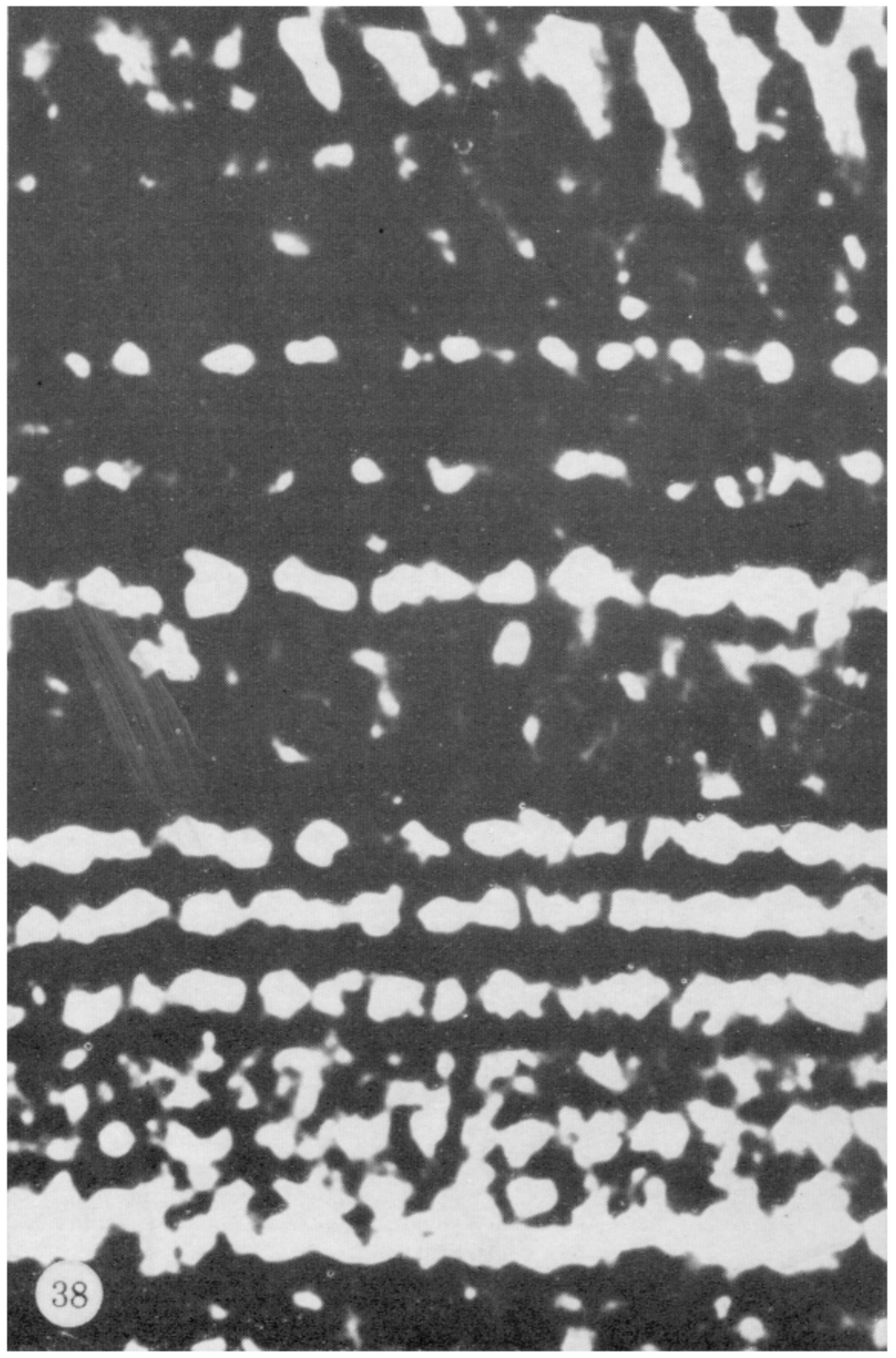

FIGURES 35–38. For description see opposite.

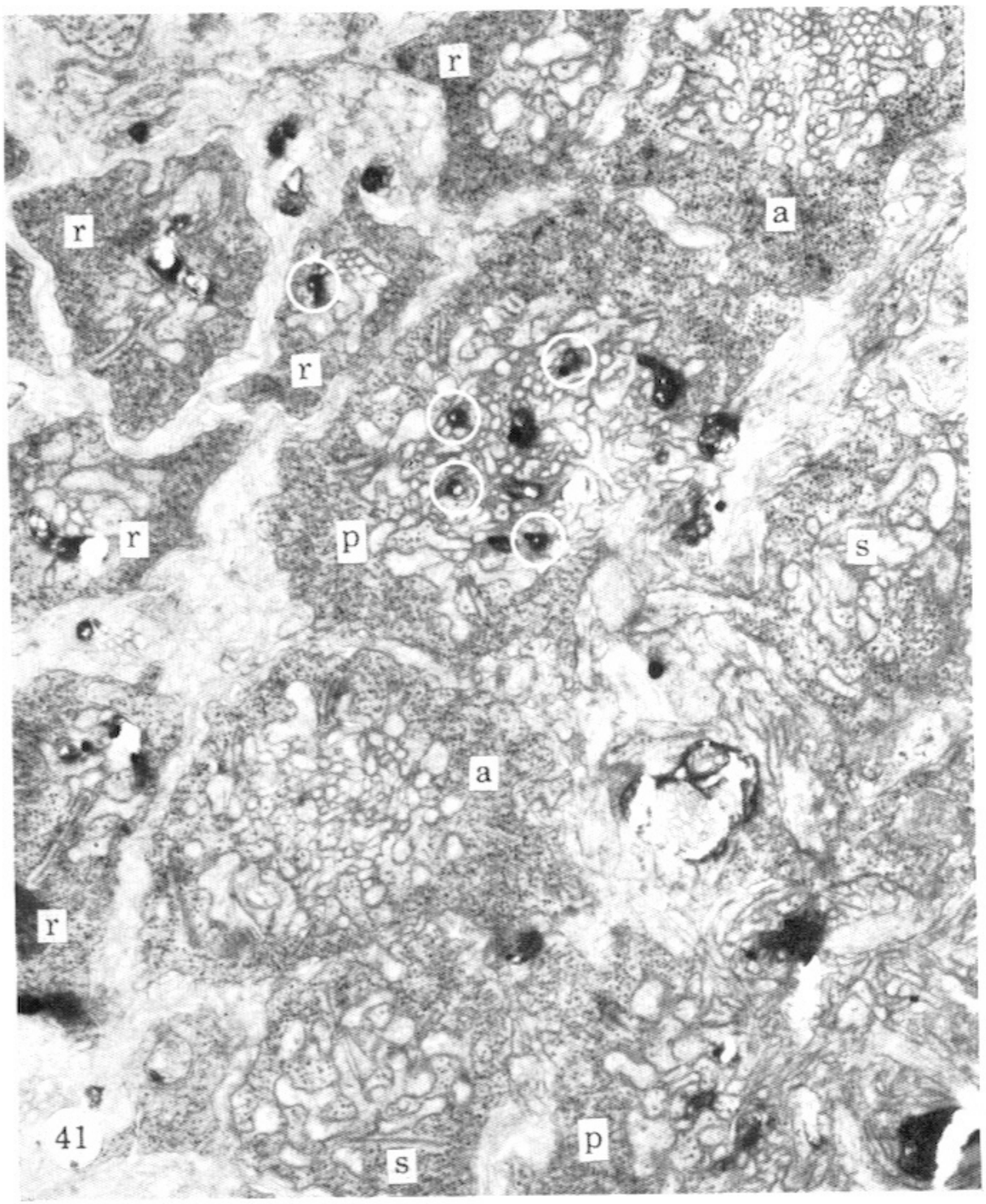

41

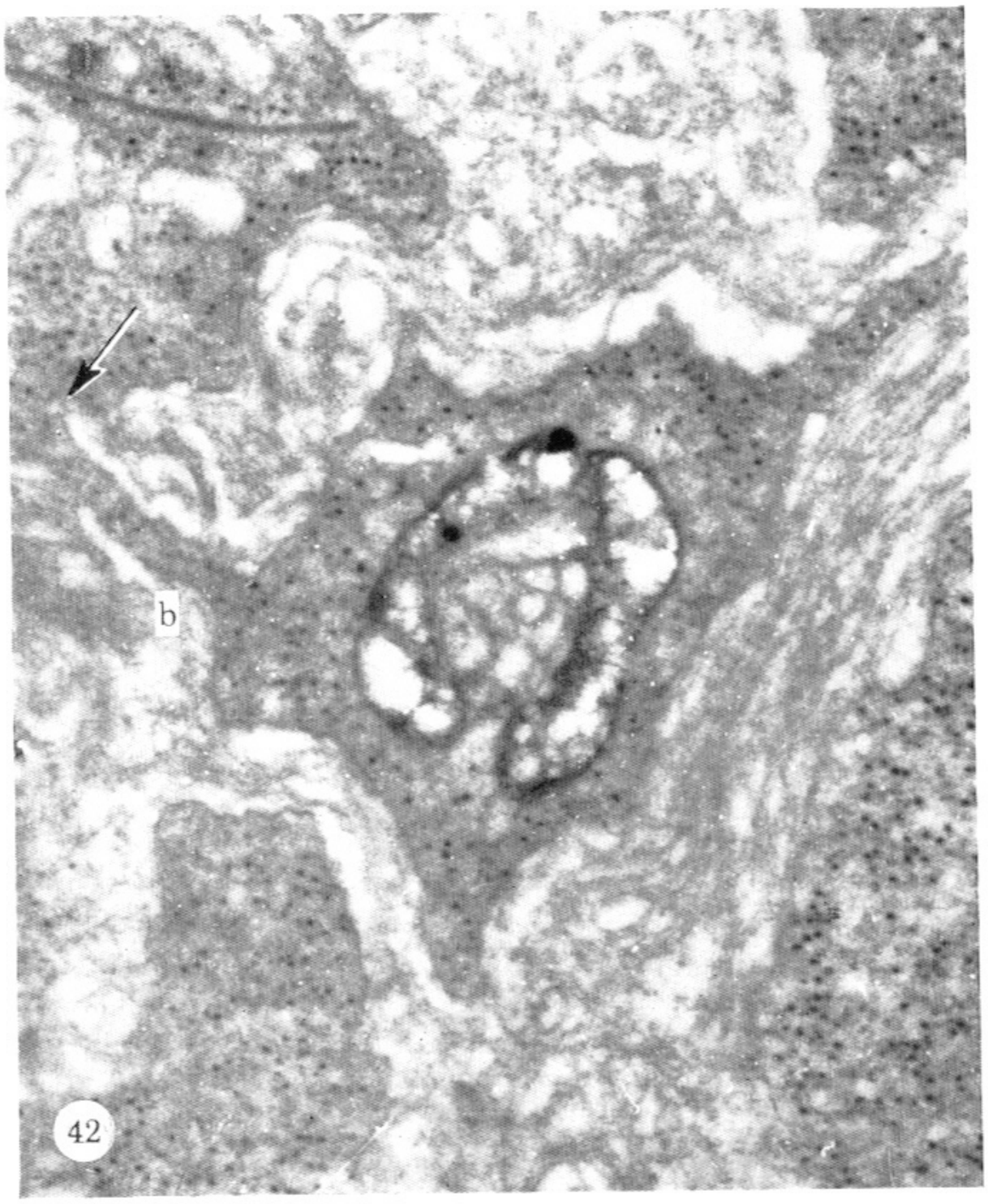

42

43

44

45

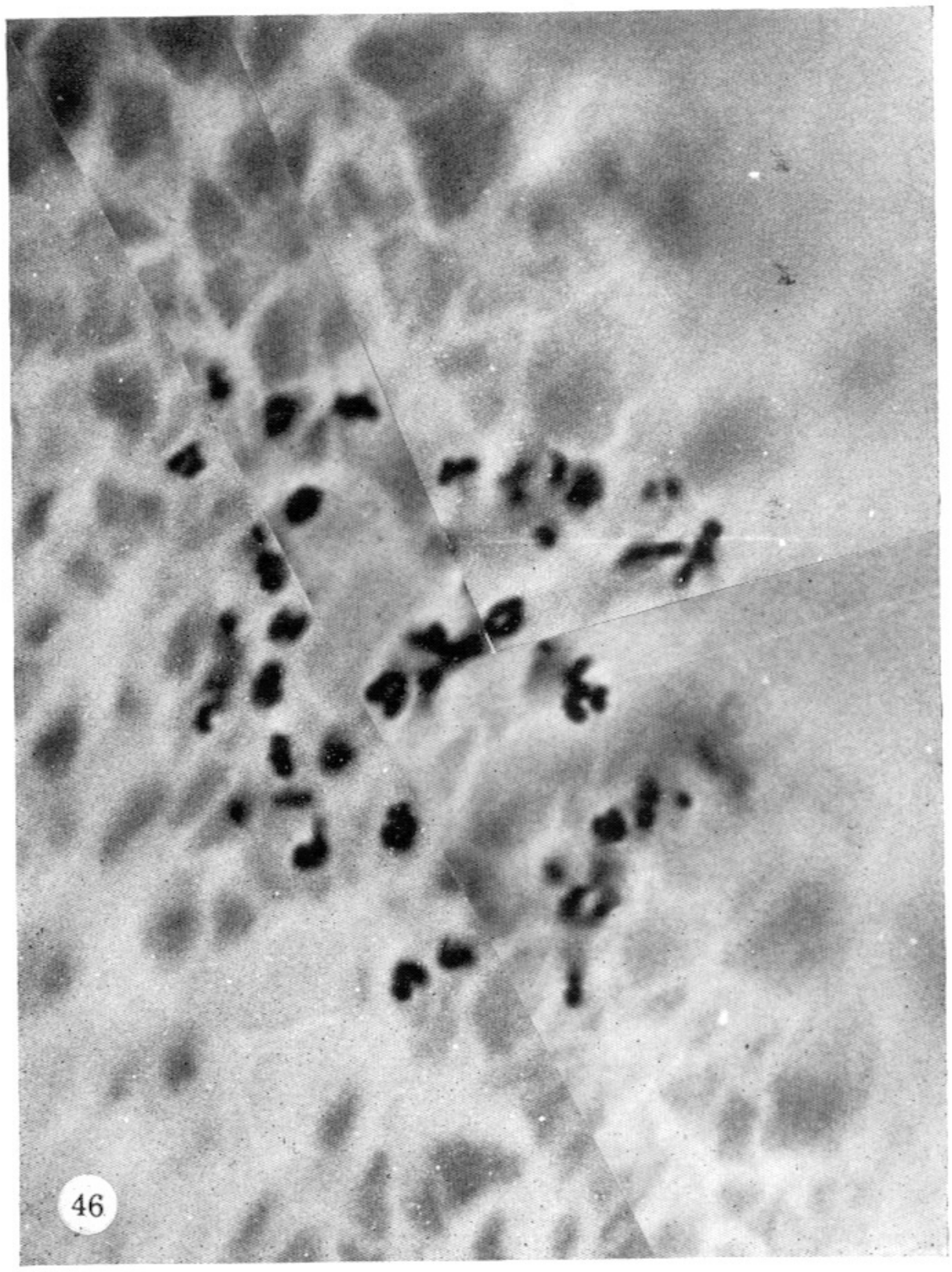

46

FIGURES 41–46. For description see opposite.

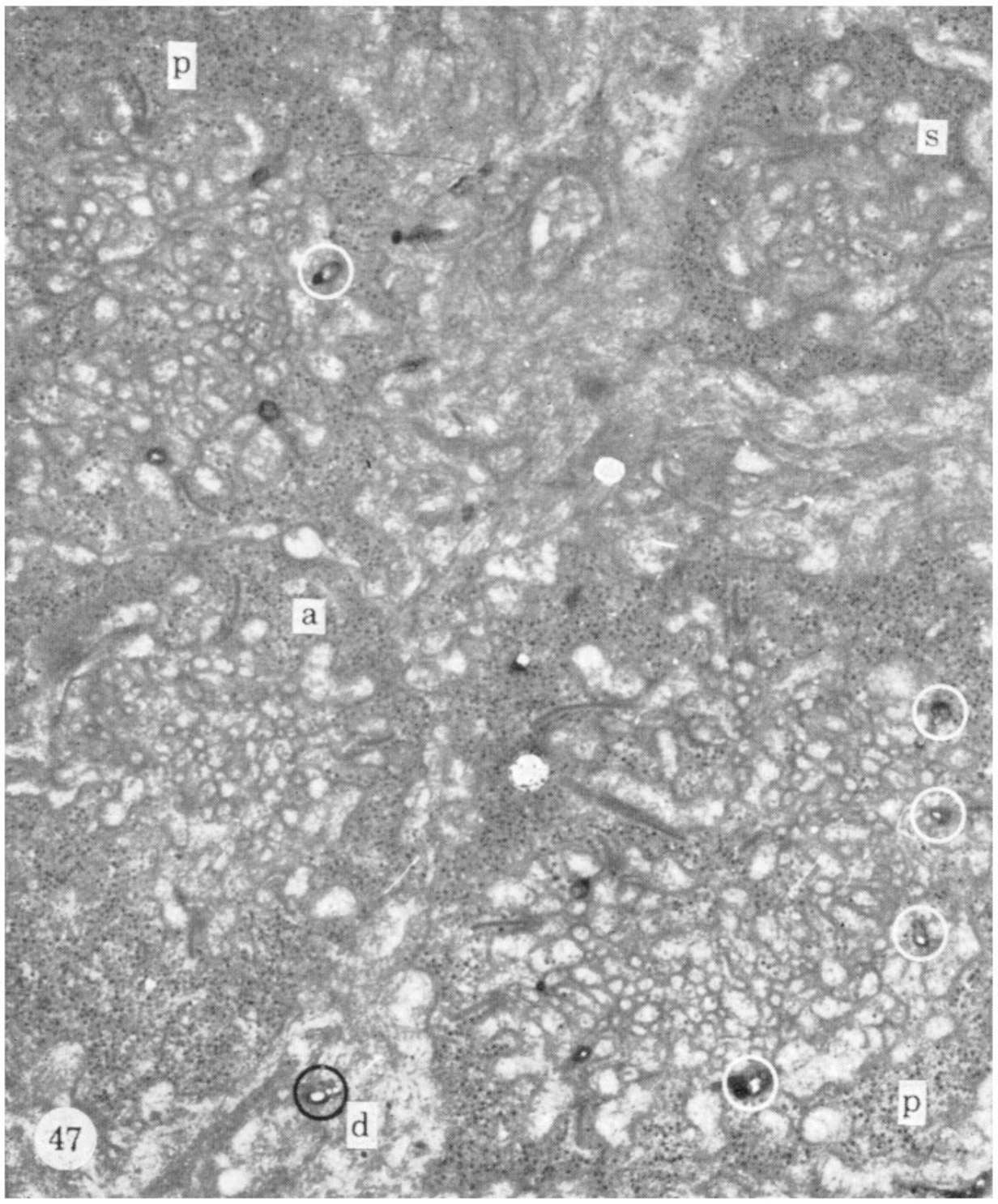

47

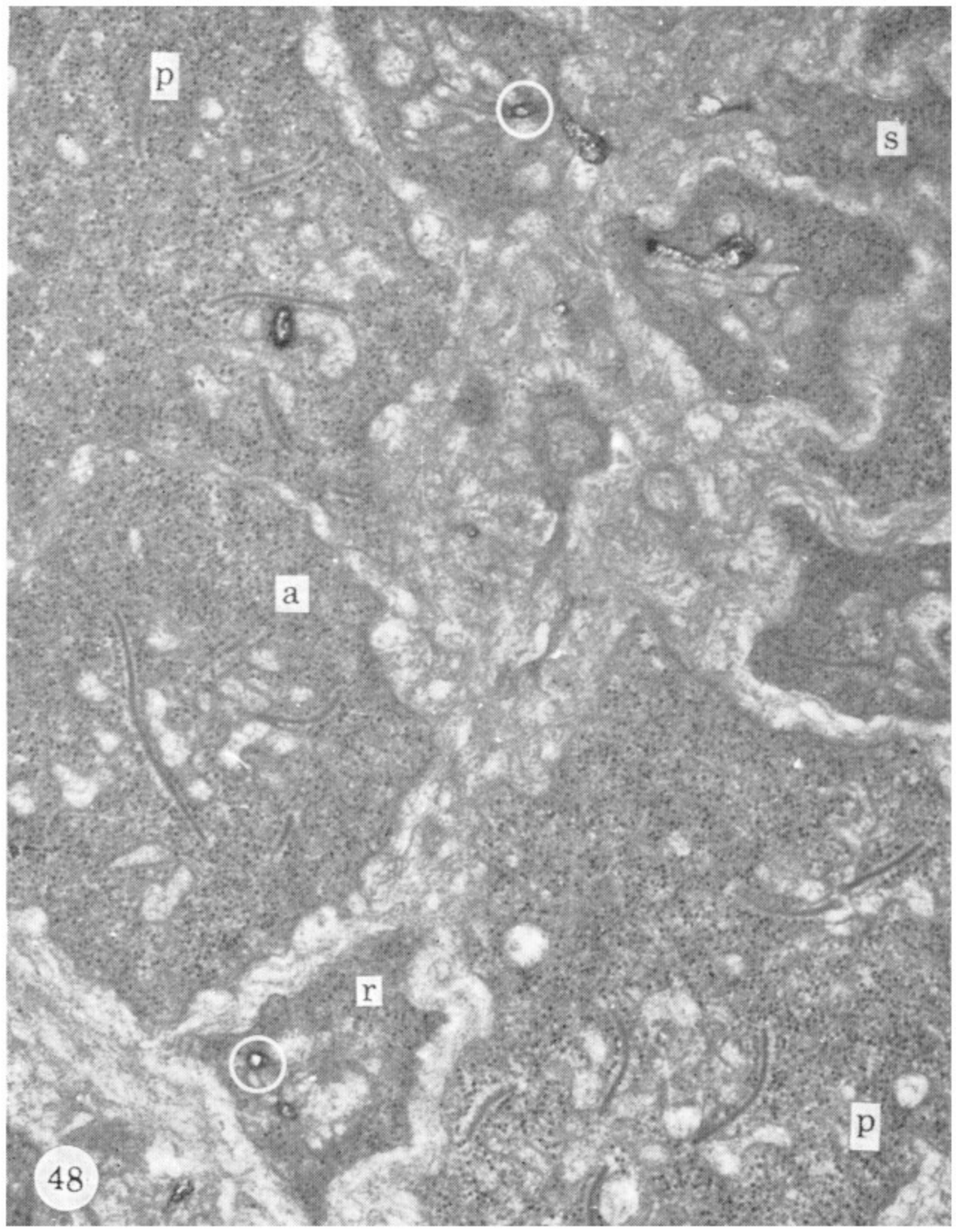

48

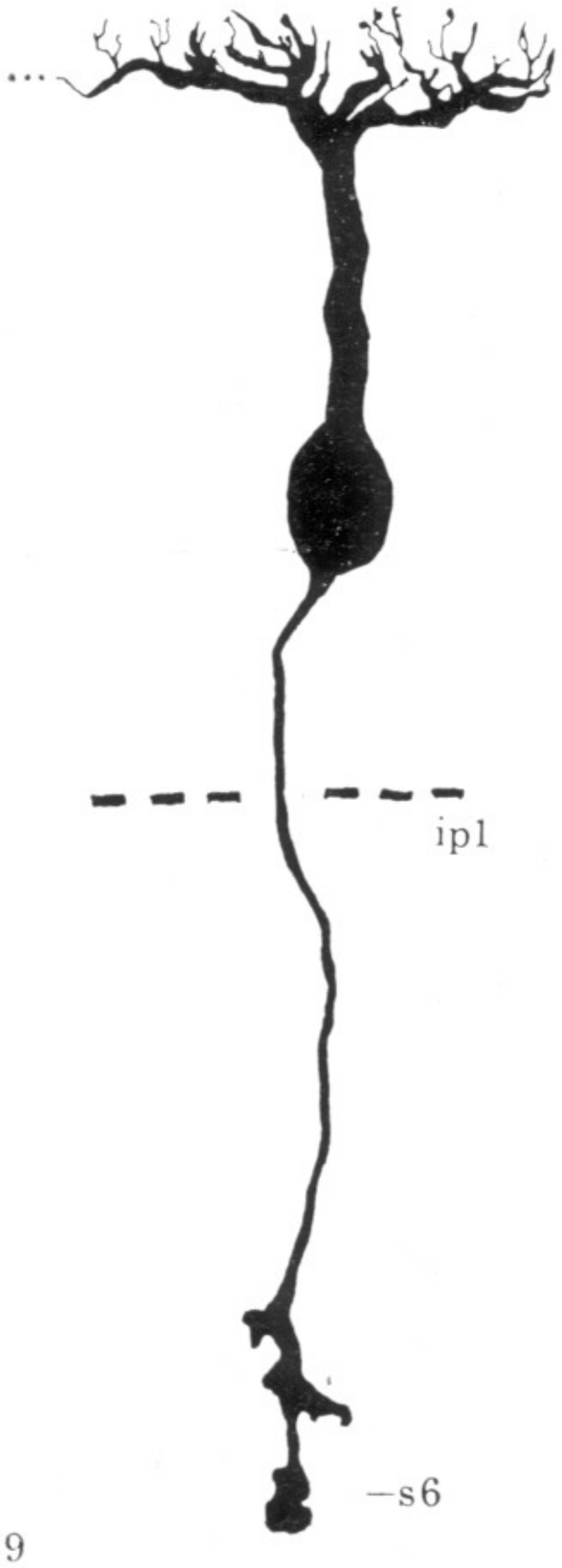

49

50

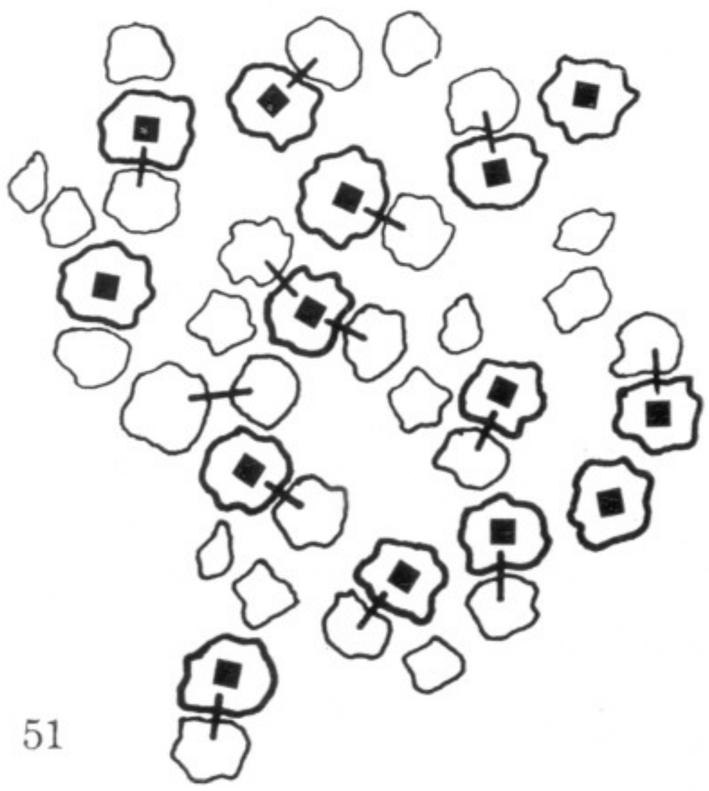

51

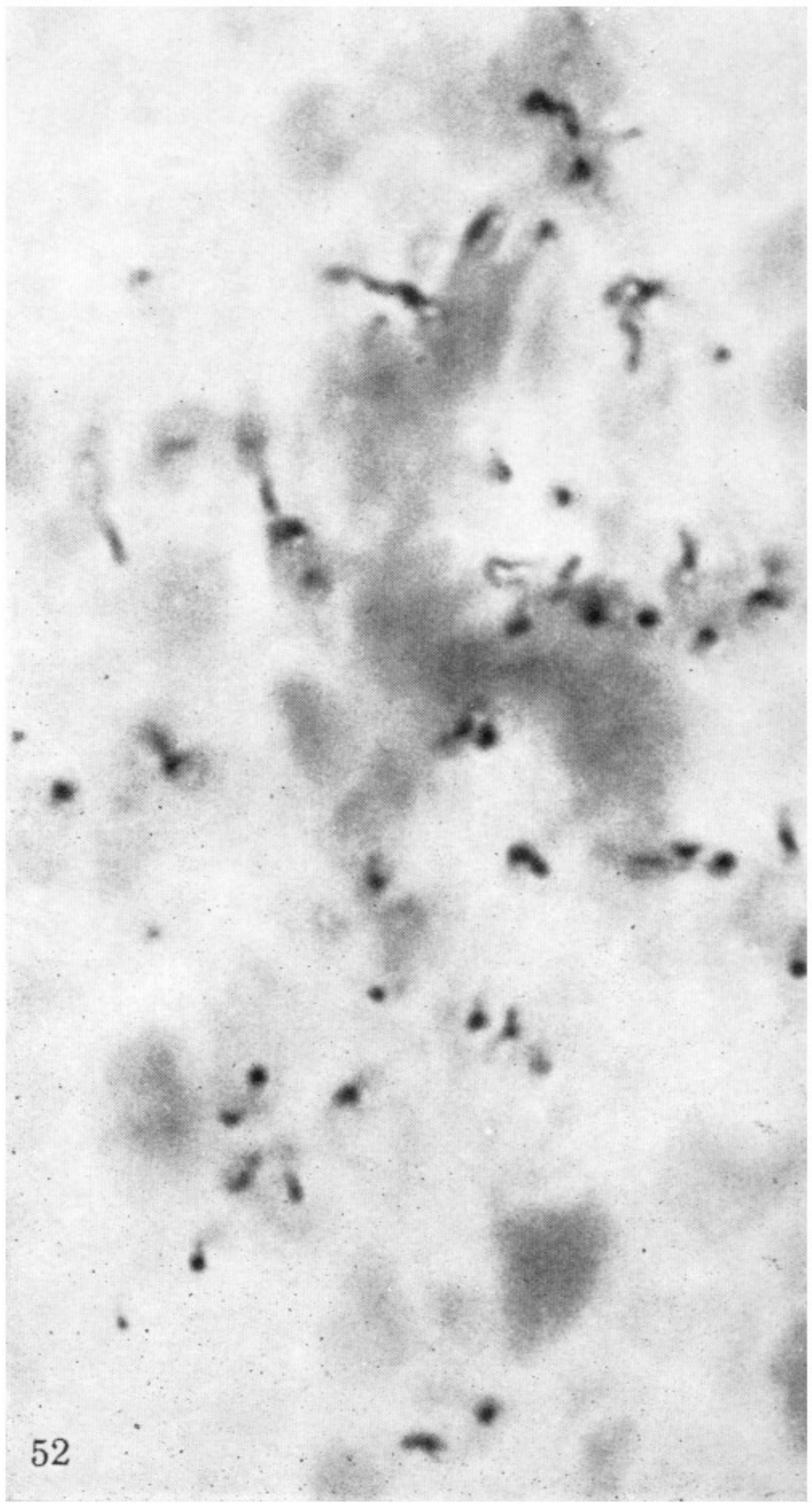

52

FIGURES 47–52. For description see opposite.

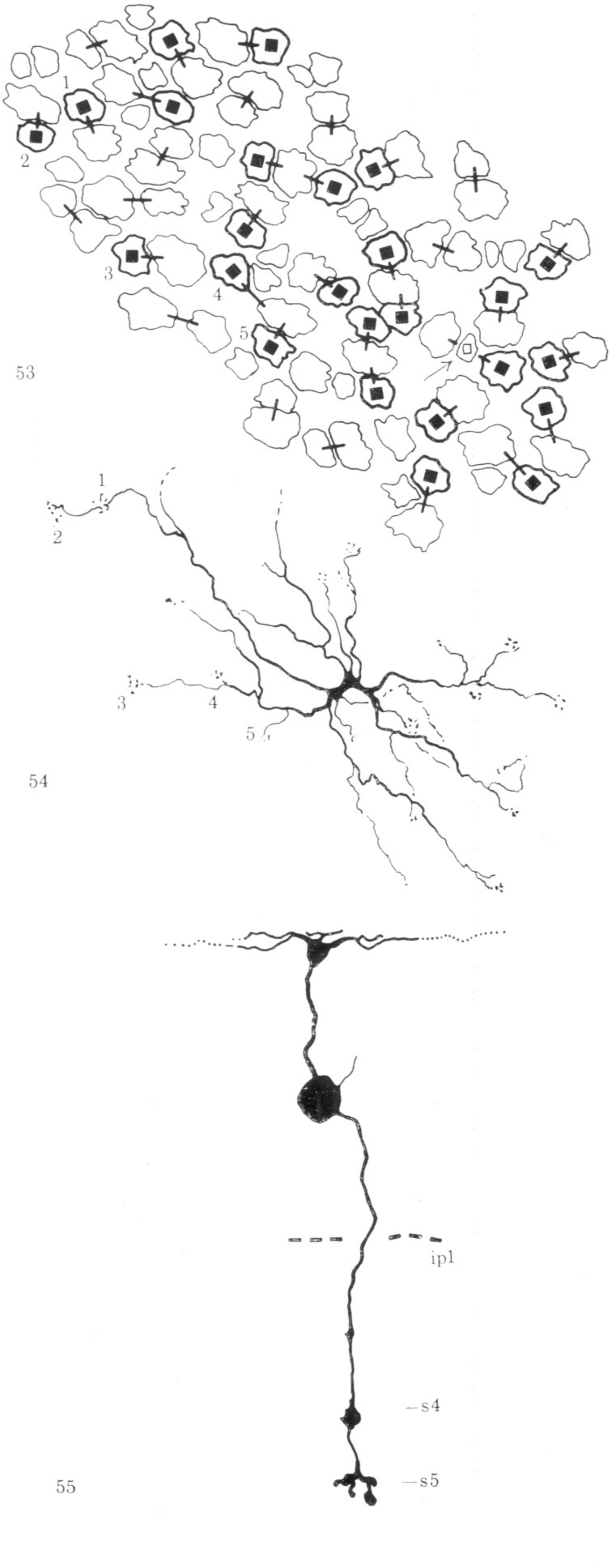

53

54

55

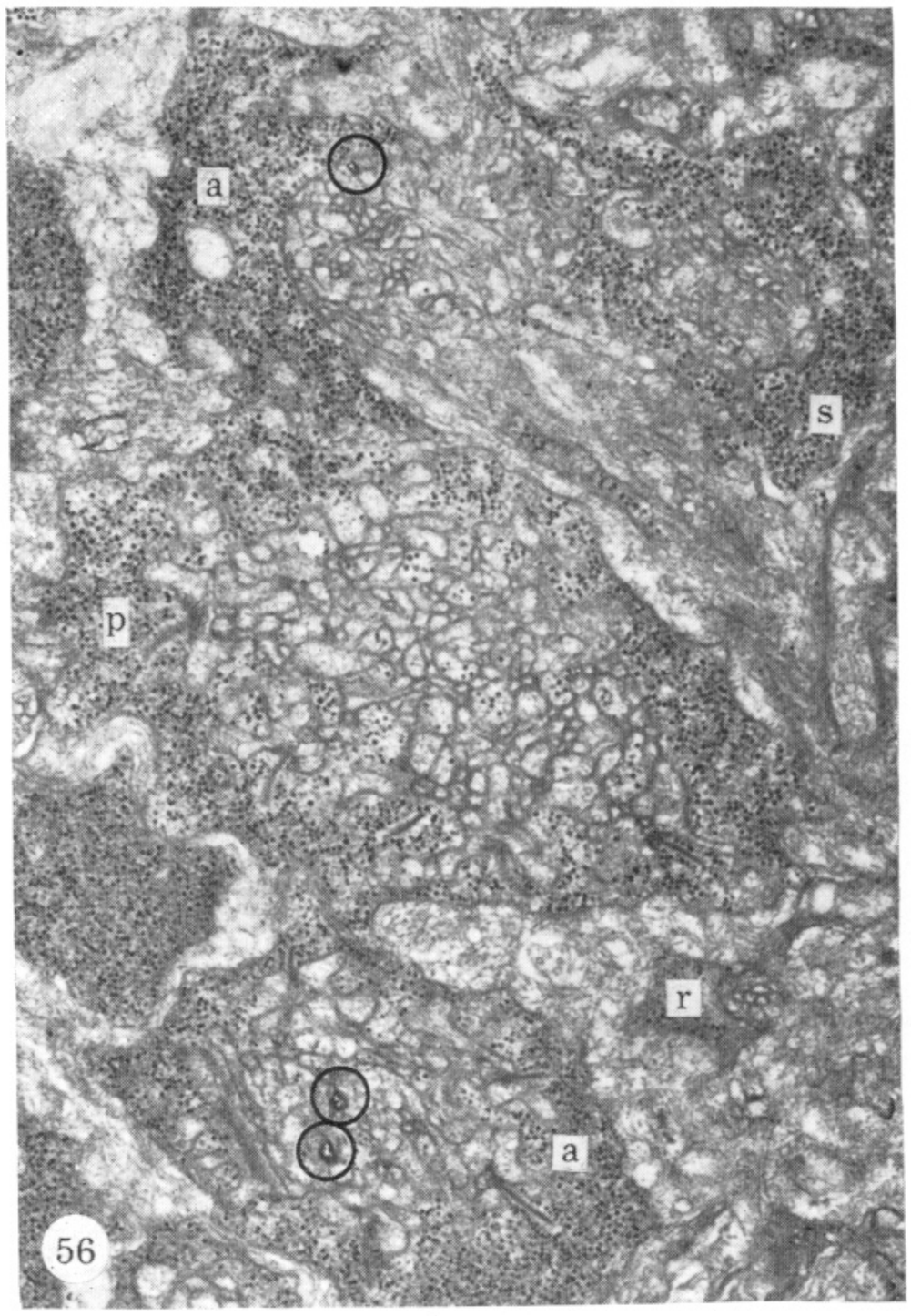

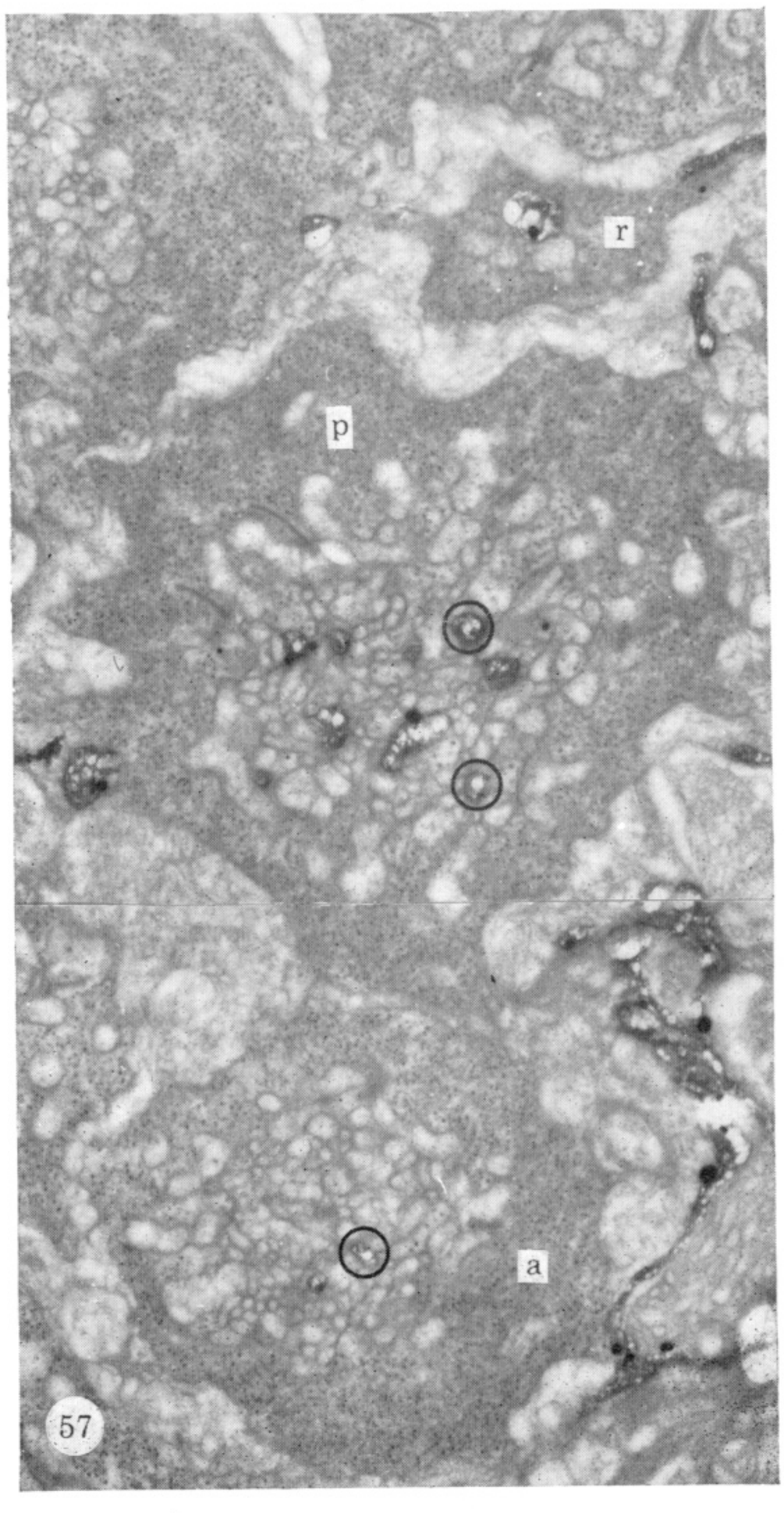

FIGURES 53–57. For description see opposite.

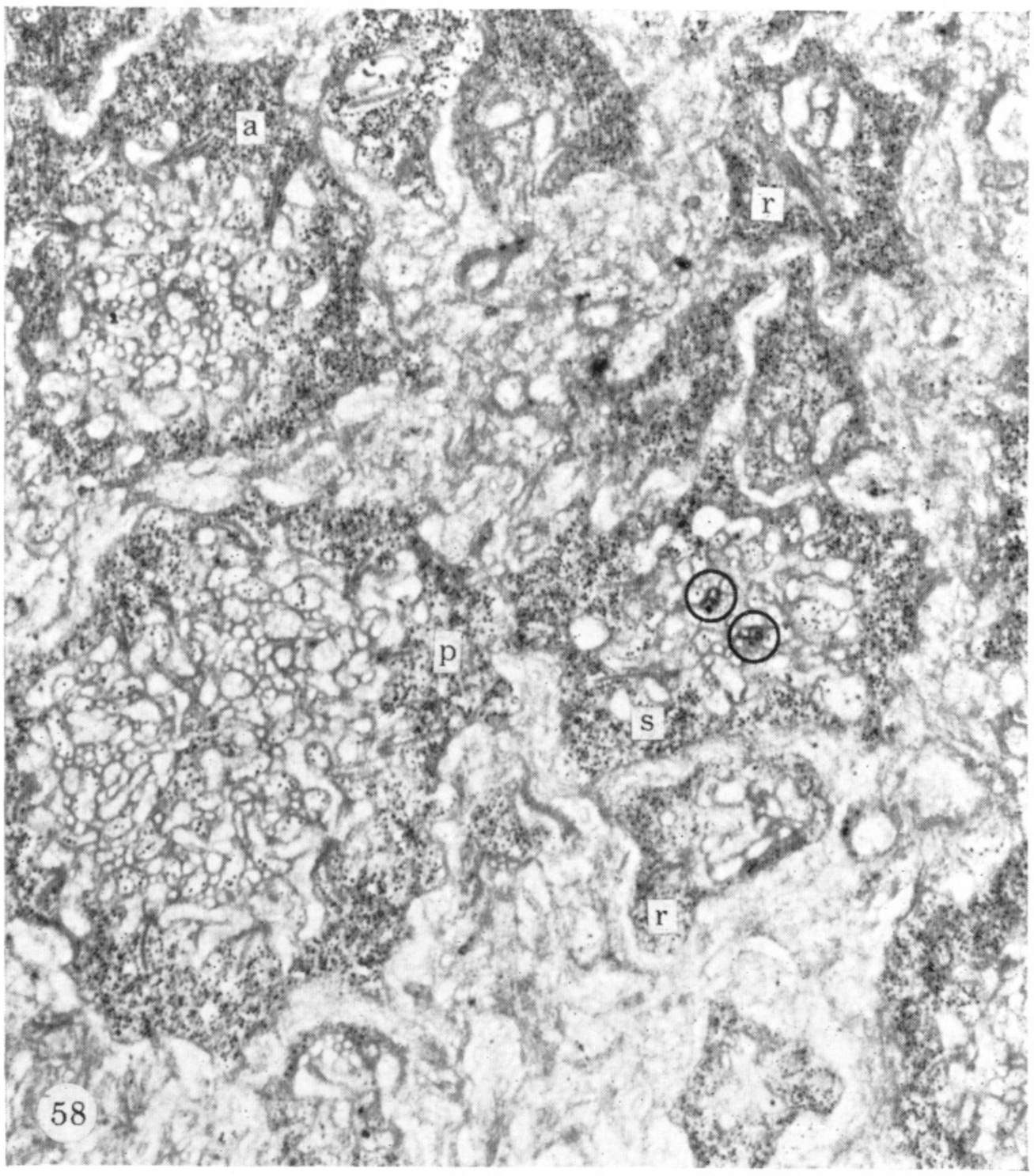

58

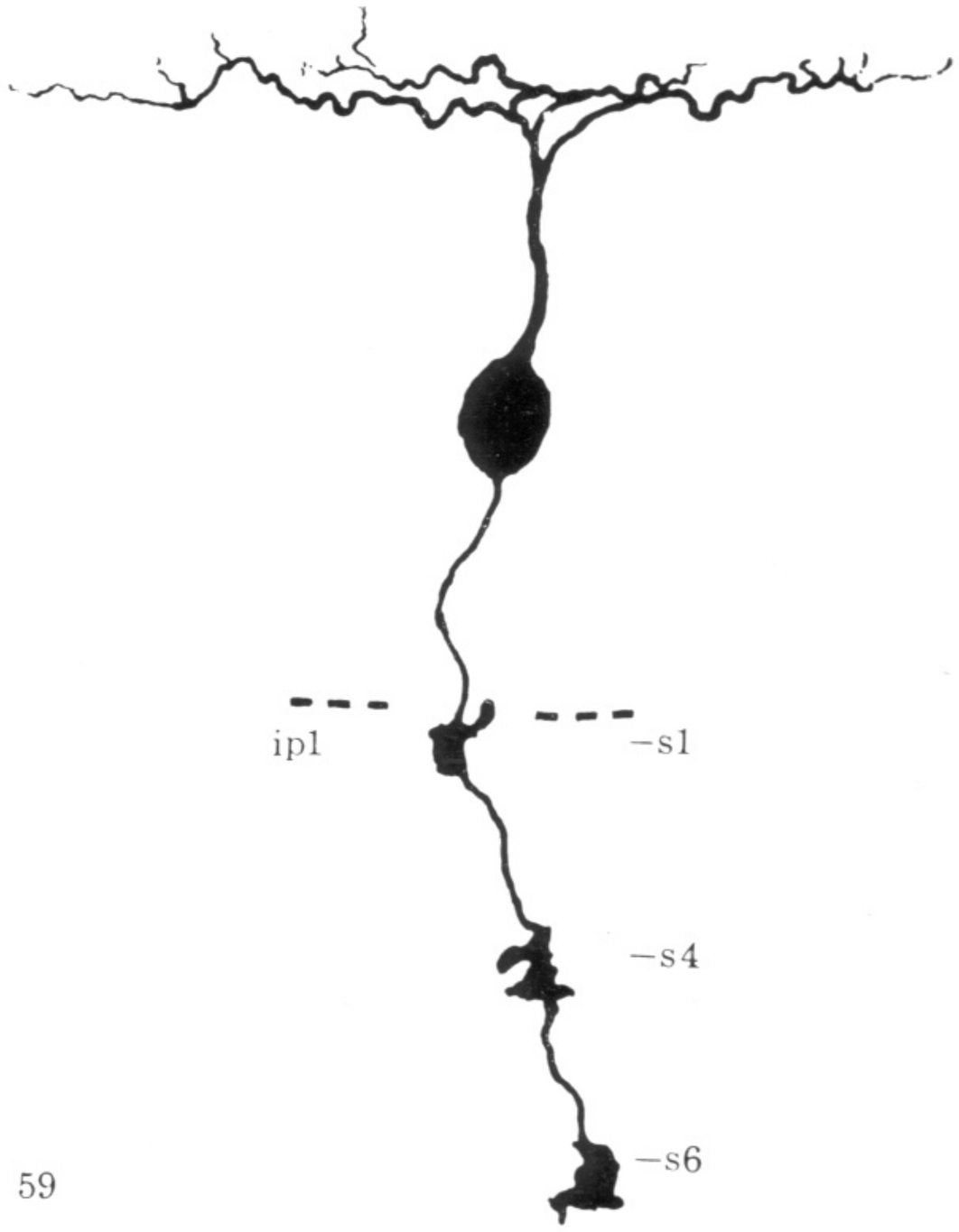

59

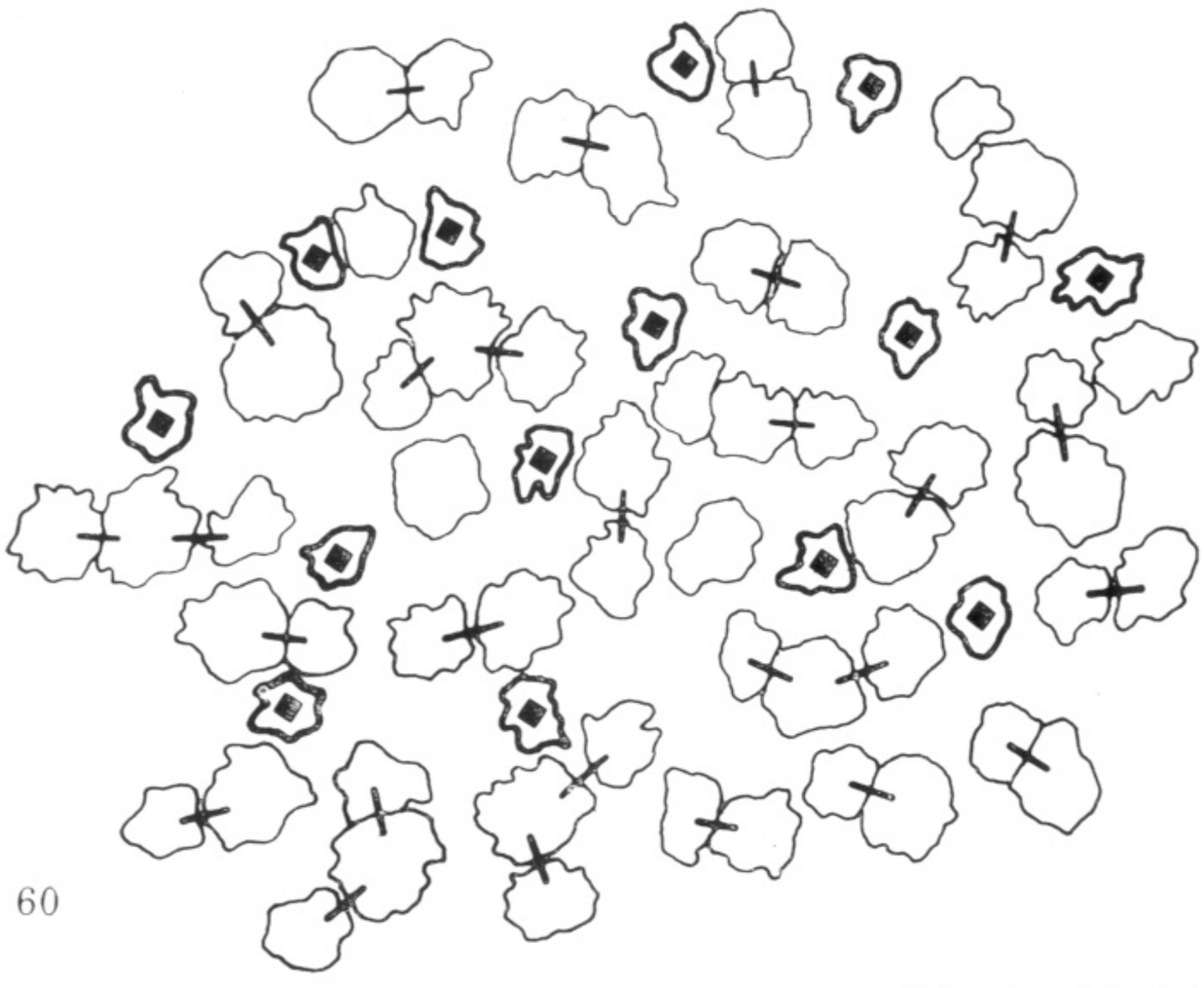

60

61

Selective (single) cone bipolars.

FIGURES 58–61. Analysis of the morphology and connexions of a bipolar specific for single cones; the scale and notation is the same as that used in comparable figures in plates 6–10. Figure 58 shows part of the array of pedicles drawn in figure 60, where a single cone (s) pedicle receives silvered processes from the bipolar (circles), but a principal (p) and an accessory (a) do not.

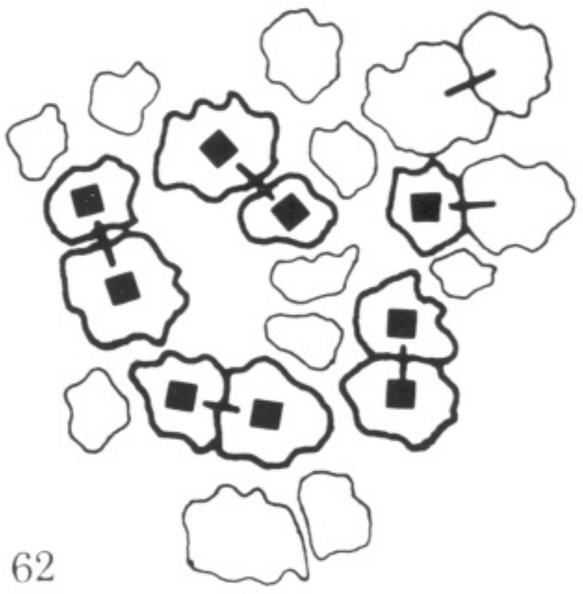

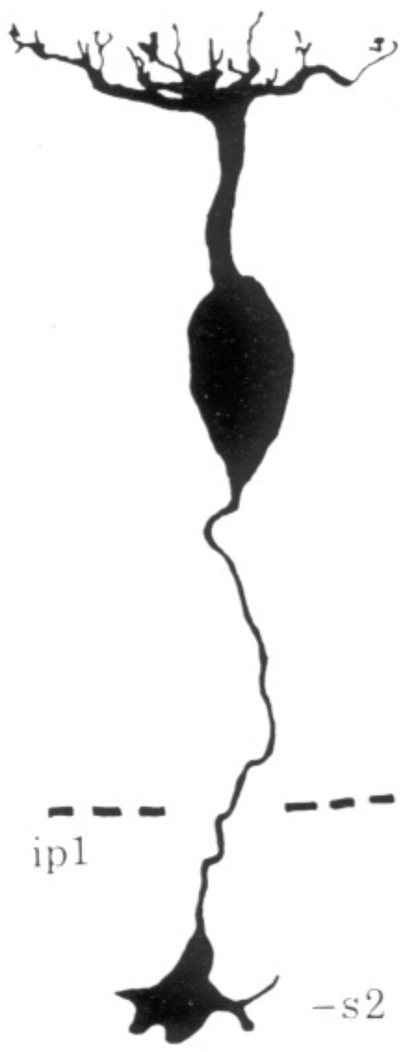

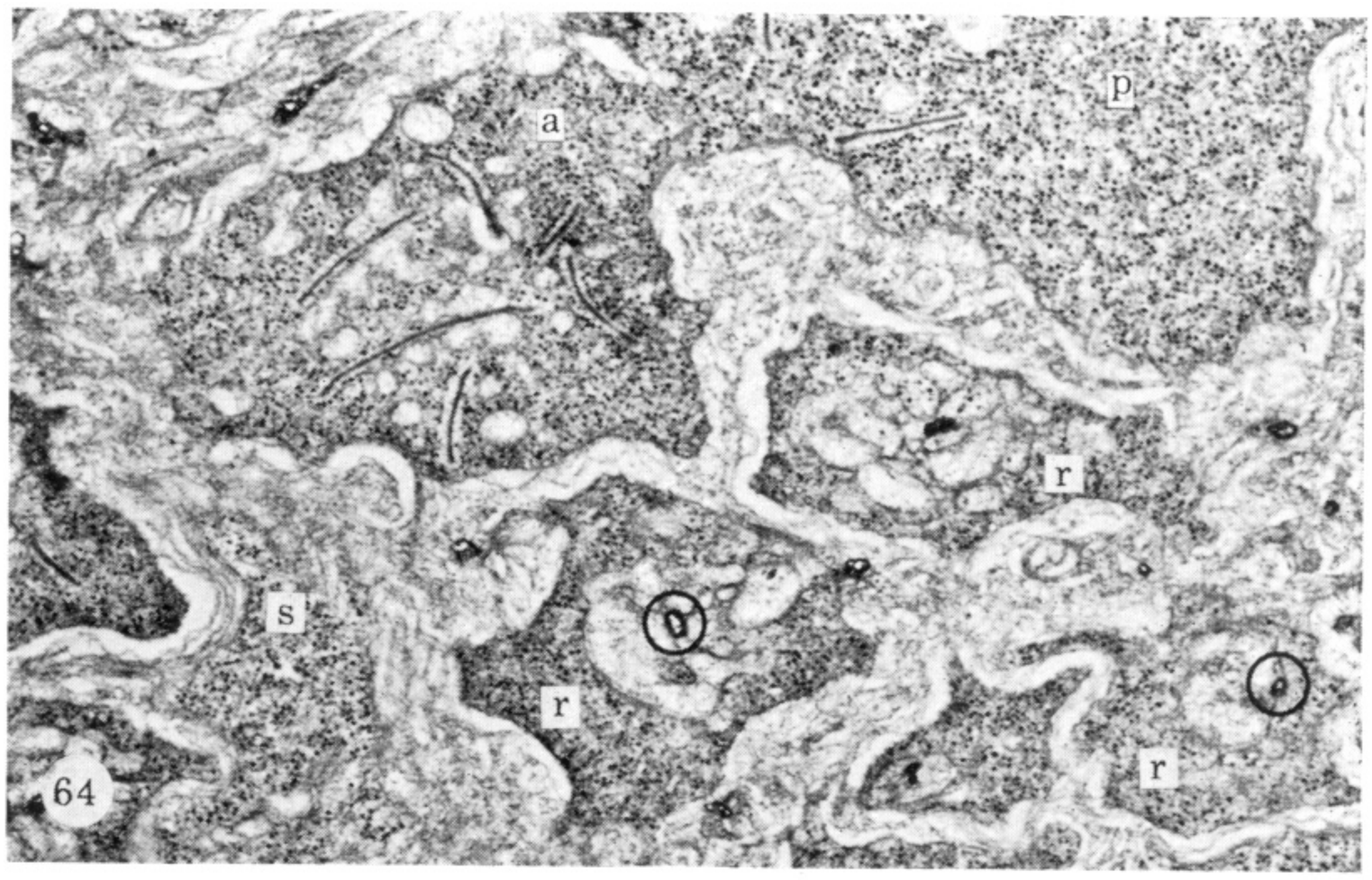

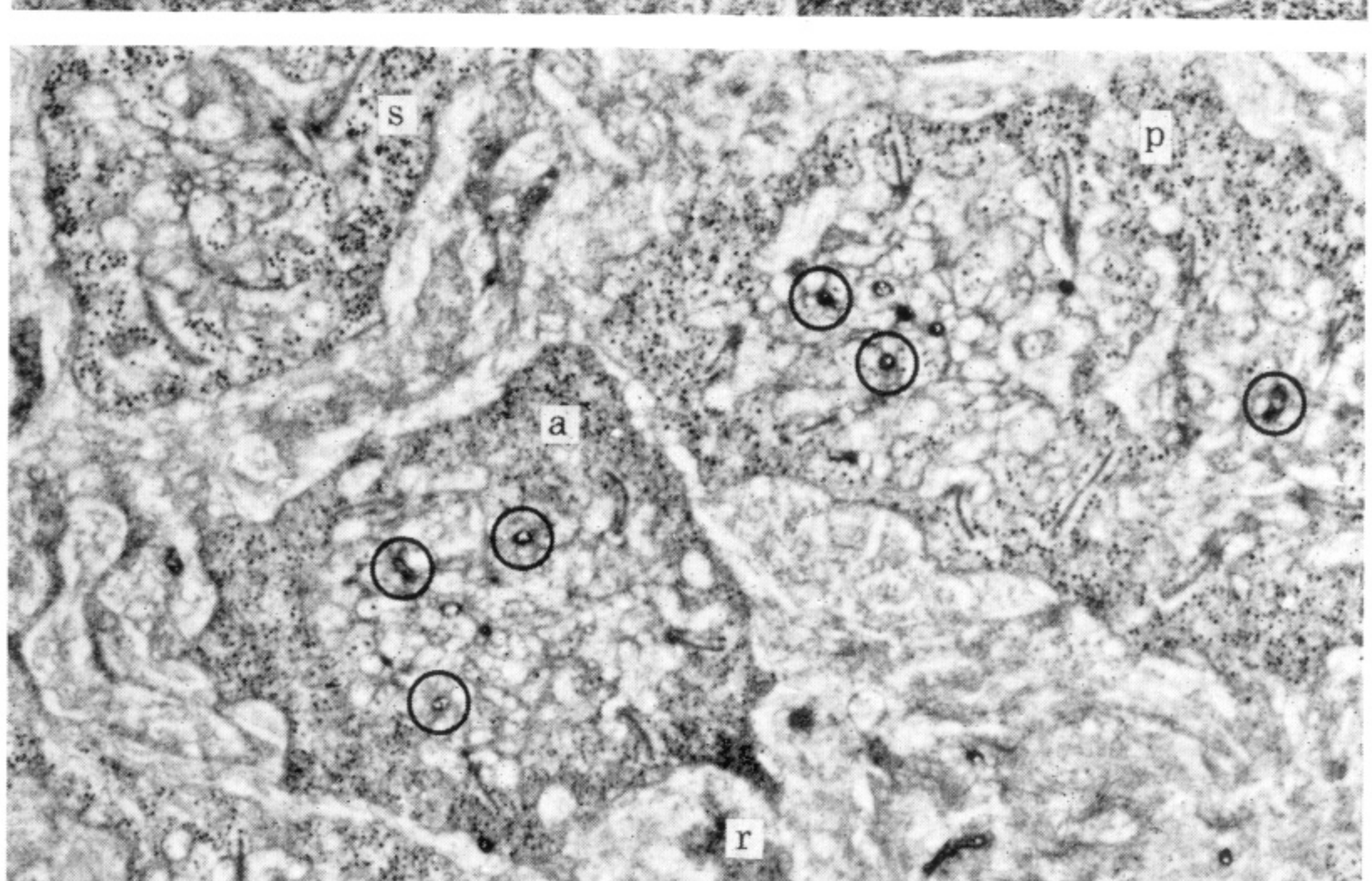

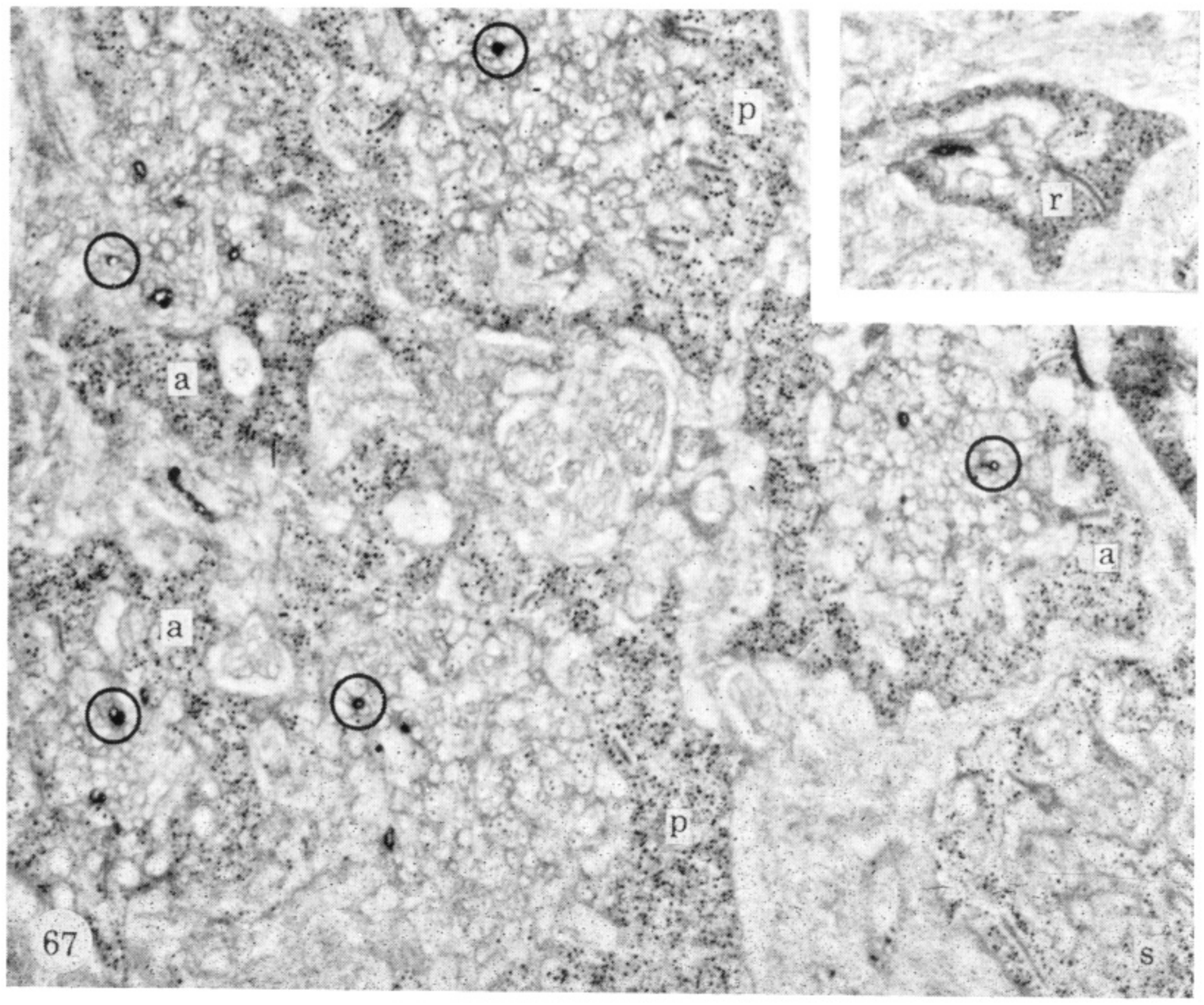

FIGURES 62–67. For description see opposite.

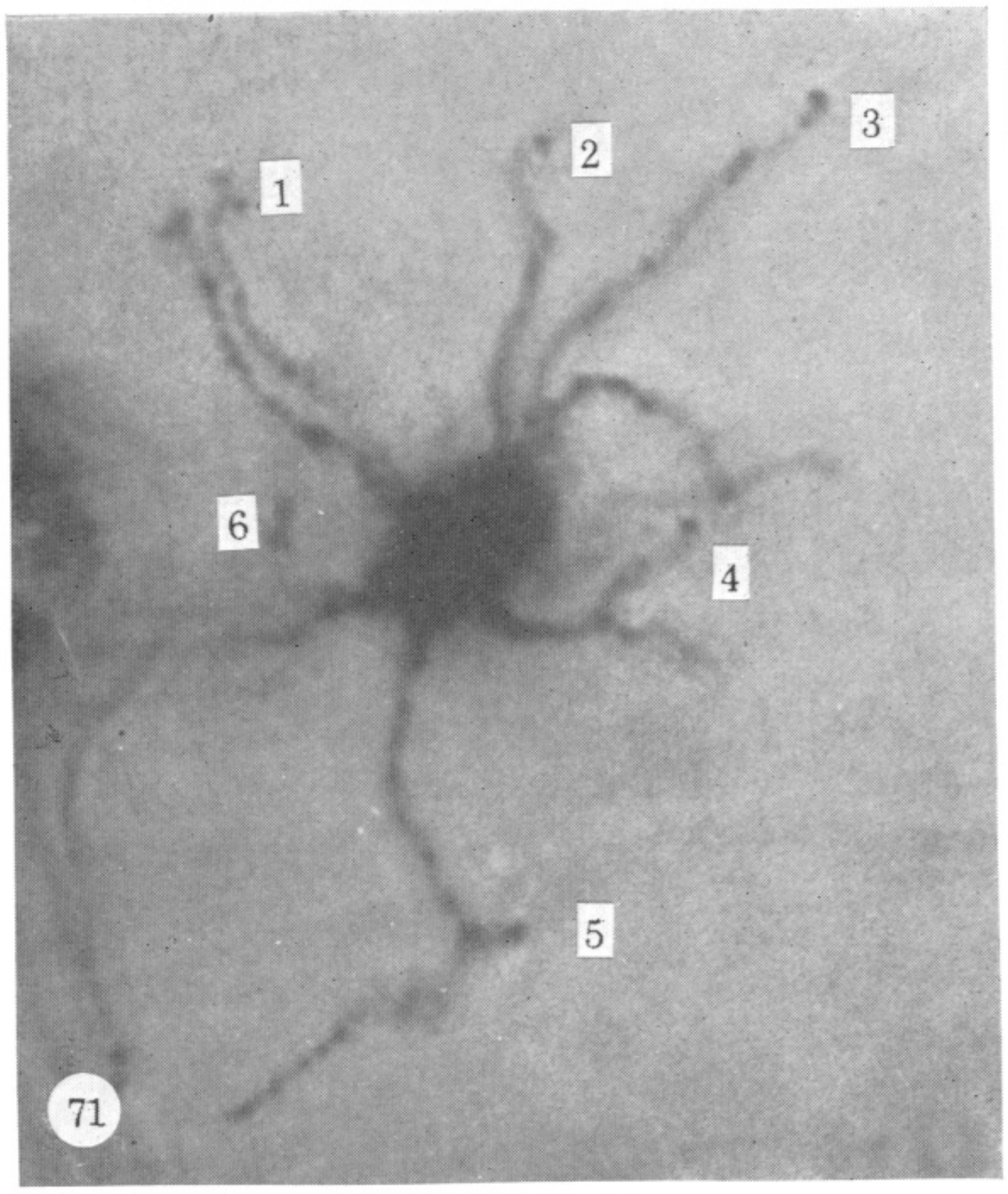

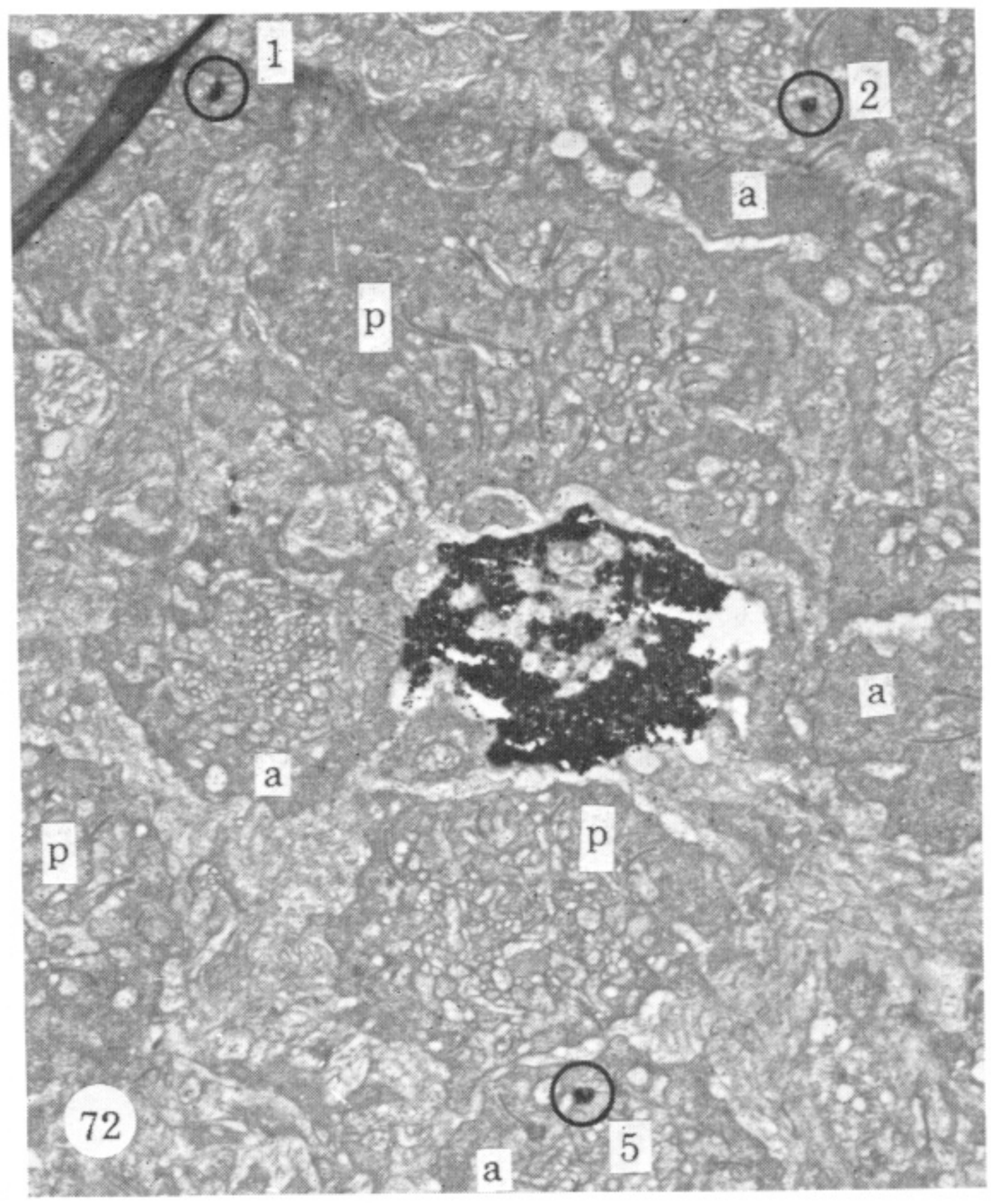

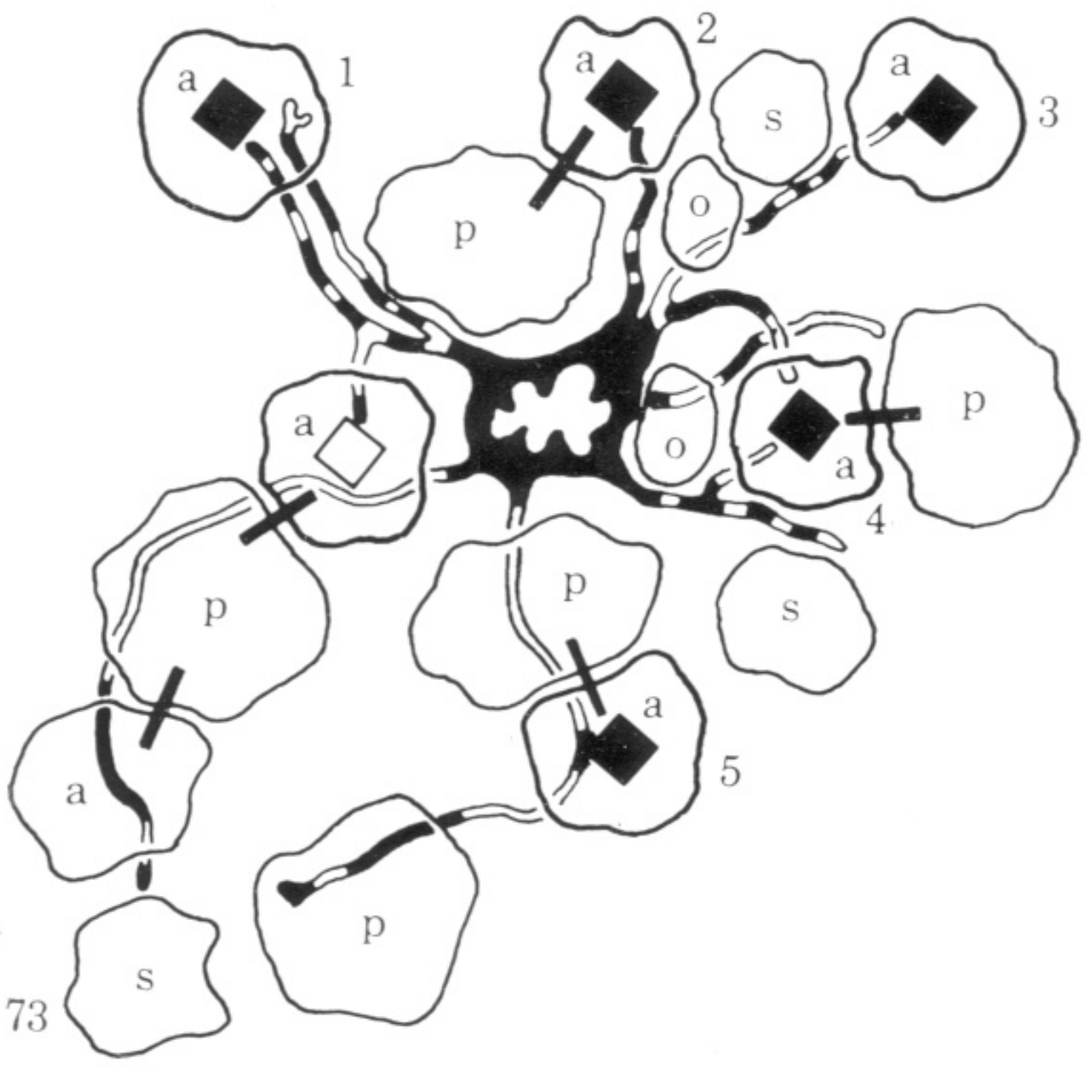

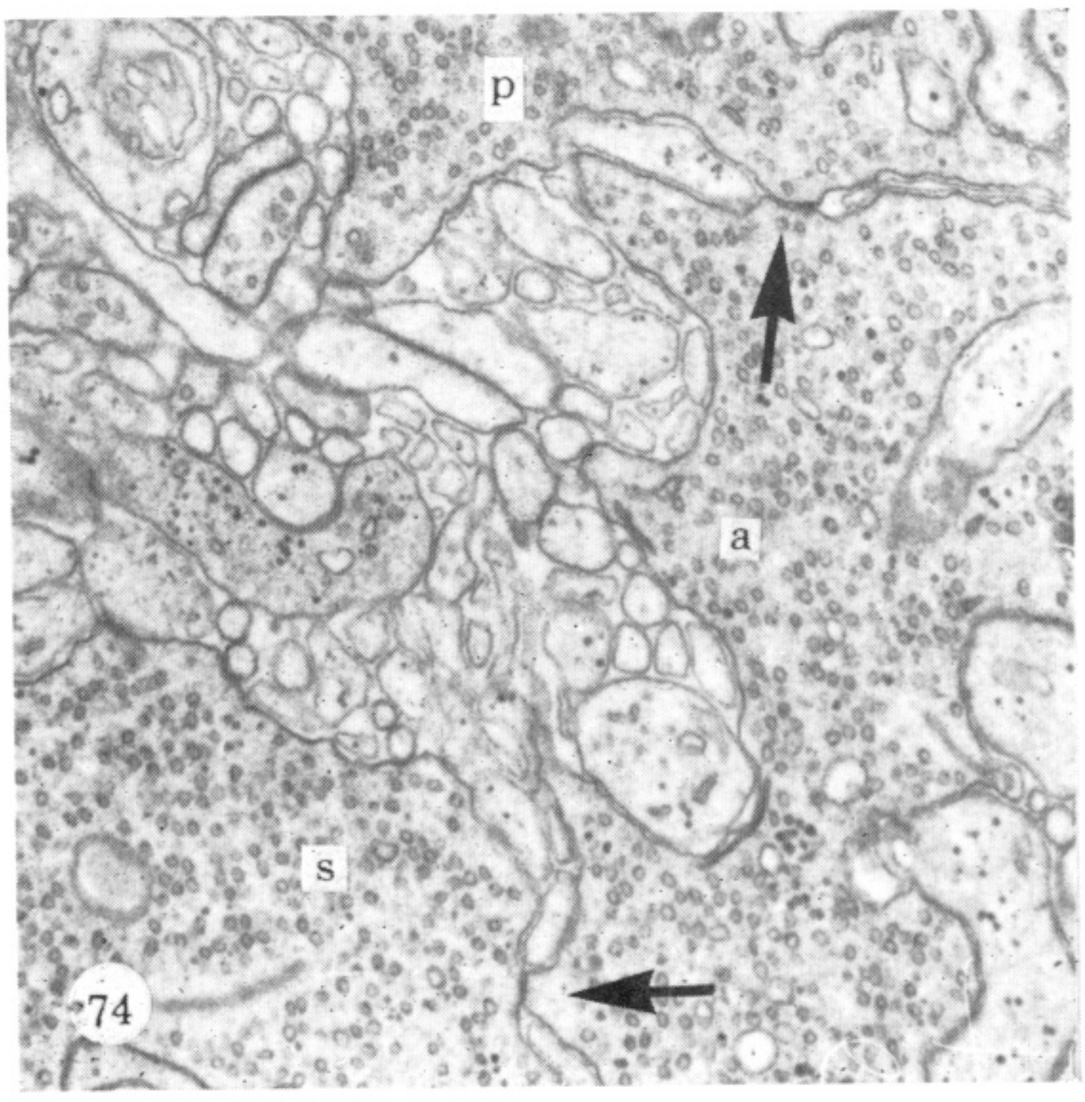

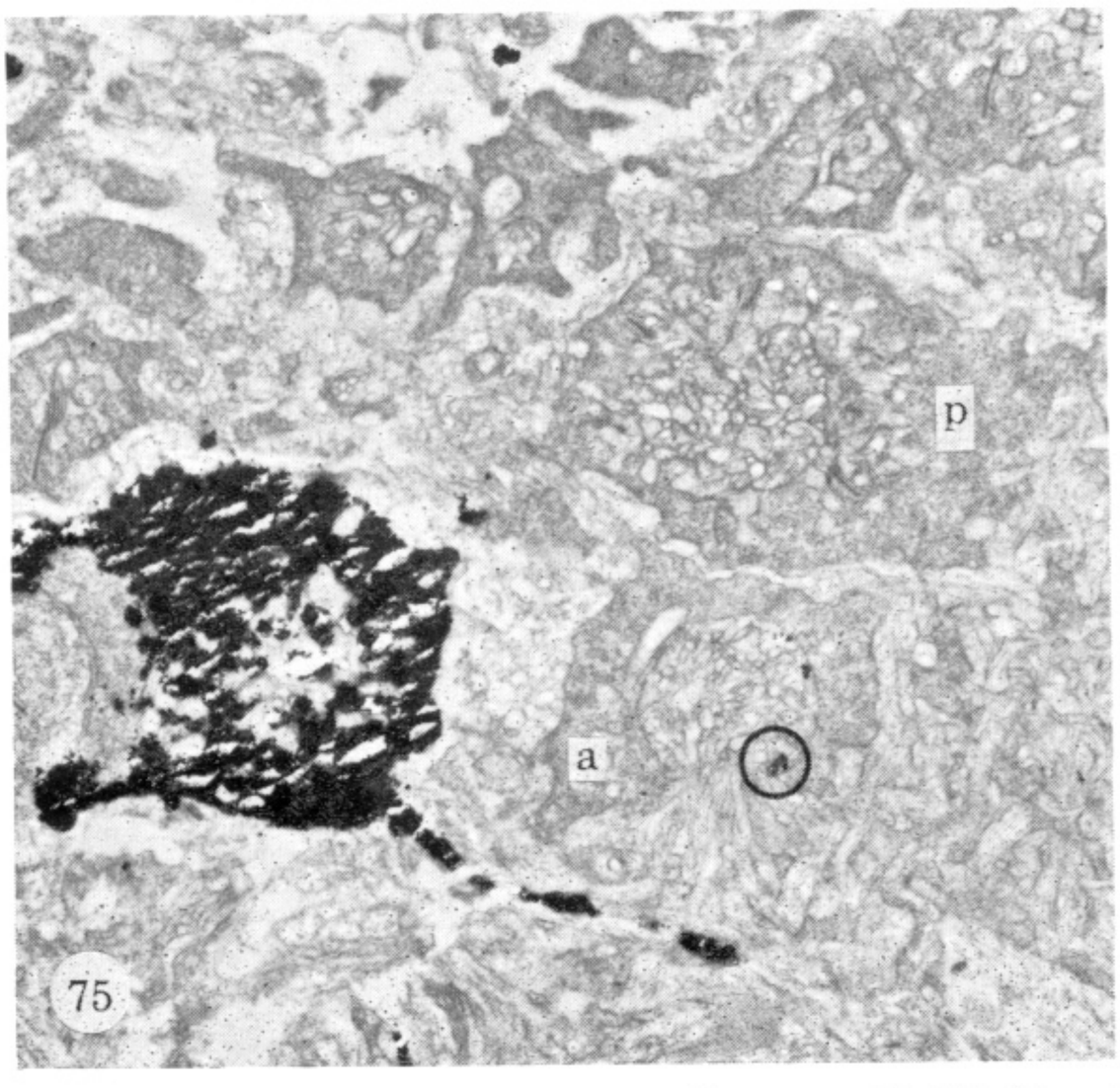

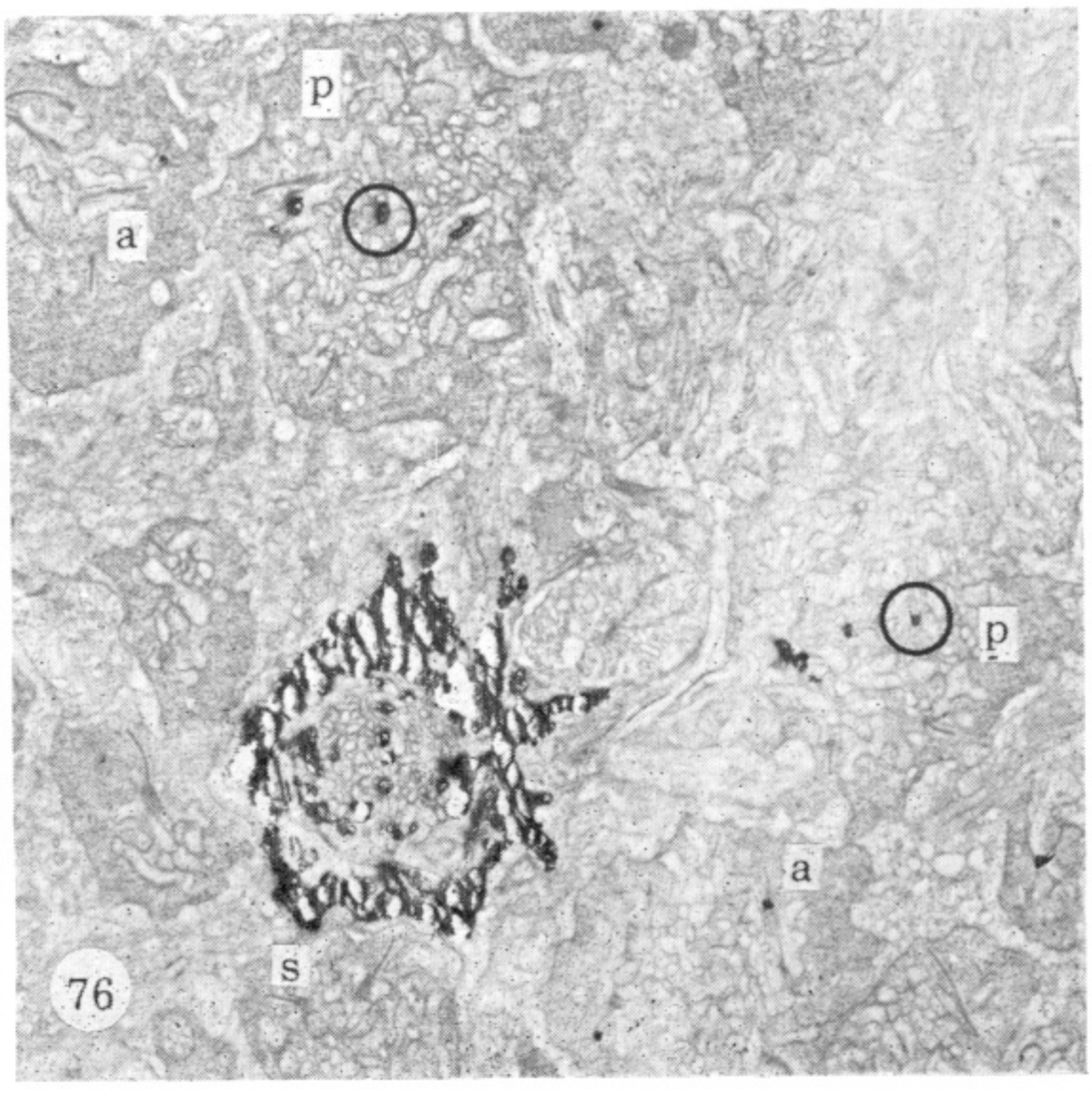

FIGURES 71–76. For description see opposite.